A Tree Algorithm for Helmholtz Potential Wavelets on Non-Smooth Surfaces: Theoretical Background and Application to Seismic Data Postprocessing

Maxim Ilyasov

Vom Fachbereich Mathematik
der Technischen Universität Kaiserslautern
zur Verleihung des akademischen Grades
Doktor der Naturwissenschaften
(Doctor rerum naturalium, Dr. rer. nat.)
genehmigte Dissertation

Erster Gutachter: **Prof. Dr. Willi Freeden**, Kaiserslautern
Zweiter Gutachter: **Prof. Dr. Mikhail M. Popov**, St. Petersburg

Vollzug der Promotion: 8. Juli 2011

D386

Acknowledgments

I gratitude my advisor Prof. Dr. Willi Freeden for giving me opportunity to working on this topic and his support concerning all problems that have come up during my work.

I would like to thank Dr. Franz-Josef Pfreund and Fraunhofer ITWM for making possible my study at University of Kaiserslautern and the financial support.

I want to express my appreciation to Alfred Weber for his helps.

I thank Prof. Dr. Mikhail M. Popov for his suggestions and comments.

Finally, I wish to thank Dr. J. Jegorov, Dr. A. Amirbekyan, Dr. D. Stoyanov, Dr. N. Ettrich, Dr. E. Ivanov, O. Koroleva and N. Kotava for theier continuous support.

Abstract

The interest of the exploration of new hydrocarbon fields as well as deep geothermal reservoirs is permanently growing. The analysis of seismic data specific for such exploration projects is very complex and requires the deep knowledge in geology, geophysics, petrology, etc from interpreters, as well as the ability of advanced tools that are able to recover some particular properties. There again the existing wavelet techniques have a huge success in signal processing, data compression, noise reduction, etc. They enable to break complicate functions into many simple pieces at different scales and positions that makes detection and interpretation of local events significantly easier.

In this thesis mathematical methods and tools are presented which are applicable to the seismic data postprocessing in regions with non-smooth boundaries. We provide wavelet techniques that relate to the solutions of the Helmholtz equation. As application we are interested in seismic data analysis. A similar idea to construct wavelet functions from the limit and jump relations of the layer potentials was first suggested by Freeden and his Geomathematics Group (see, e.g., [32], [36], [48]). The particular difficulty in such approaches is the formulation of limit and jump relations for surfaces used in seismic data processing, i.e., non-smooth surfaces in various topologies (for example, uniform and quadratic). The essential idea is to replace the concept of parallel surfaces known for a smooth regular surface by certain appropriate substitutes for non-smooth surfaces.

By using the jump and limit relations formulated for regular surfaces, Helmholtz wavelets can be introduced that recursively approximate functions on surfaces with edges and corners. The exceptional point is that the construction of wavelets allows the efficient implementation in form of a tree algorithm for the fast numerical computation of functions on the boundary.

In order to demonstrate the applicability of the Helmholtz FWT, we study a seismic image obtained by the reverse time migration (e.g., [2]) which is based on a finite-difference implementation. In fact, regarding the requirements of such migration algorithms in filtering and denoising (e.g., [40], [44], [45], [86]), the wavelet decomposition is successfully applied to this image for the attenuation of low-frequency artifacts and noise. Essential feature is the space localization property of Helmholtz wavelets which numerically enables to discuss the velocity field in pointwise dependence. Moreover, the

multiscale analysis leads us to reveal additional geological information from optical features.

Contents

Introduction

Due to the increasing energy consumption, the exploration of new fields of natural gas and crude oil as well as the exploration of deep geothermal reservoirs as an example of tapping a renewable energy source, are nowadays becoming very important (see, e.g., [42] for more details). The basic and most computationally intensive step in each of such projects is the construction of subsurface images representing the underground structure by use of the seismogram recorded on the surface and in available bore holes. In addition, for the practical applicability the resulting image of such a migration process must be interpreted appropriately from geological point of view. In this respect the multiscale tools as presented in this thesis open new perspectives. In fact, multiscale technique by use of Helmholtz wavelets offer the possibility to relate migration data to certain wavelengths and to decorrelate the $\mathcal{L}^2$-energy contained in the data into low-pass and band-pass filtered information. In conclusion, the description of Helmholtz wavelet reflected multiscale analysis become accessible as component for interpretation within seismic postprocessing. In more detail, the efficiency and economical implementation of this approach is performed by means of the tree algorithm as developed in [31], whose numerical realization has been performed for the first time in this work.

In order to record seismic data, an energy source (vibroseis, airgun, etc) is placed on the surface. The receivers (geo-phones, hydro-phones) are placed along one or many parallel lines. The source produces an impulse, which is transmitted through the Earth interior, reflected at the places of impedance contrasts (rapid changes of density/velocity), transmitted back, and recorded by receivers. Then, this configuration is moved into the direction of seismic acquisition and the experiment is repeated (see Figure 0.1), so that each underground point is covered many times and thus is represented from all incidence angles needed for further data analysis. Other seismic acquisition

strategies are described in many textbooks, for example, [6], [19], [85].

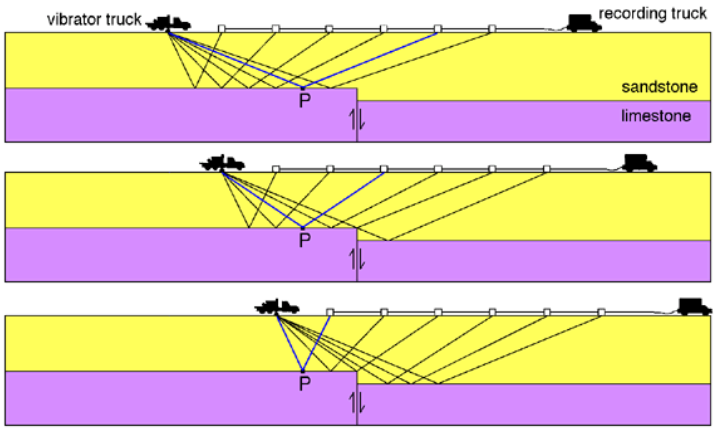

Figure 0.1: Seismic acquisition (source: [83]).

In order to obtain an image of the subsurface structure corresponding to some given parameters, like the wave propagation velocity or the underground density, e.g., the methods of *seismic migration* are used. These methods 'migrate' the seismogram (amplitudes) recorded in time to the 'true' depth position (Figure 0.2), so that the shape, the depth position, and the reflection coefficient can be reconstructed (more details can be found, e.g., in [19], [85] and the references therein).

For the purpose of computation, all migration methods use an approximate velocity model obtained by means of the *migration velocity analysis* (e.g., tomography, full wave inversion, etc.; for more details the reader is referred to [6] and the references therein). In addition, migration methods can be recursively applied in order to refine the given velocity model. For this purpose, the migration is repeated with a velocity differing in a small perturbation in the local area from the initial model. In the end, the velocity model is chosen which yields the obviously 'best' reflector image.

Nowadays a lot of methods are available to migrate seismic data sets, but all of these are based on some approximation of the wave equation or, more generally, on the elastodynamic equation. The strategy of the different migration methods can be roughly divided into the following groups:

- ray based methods which usually model a high-frequency asymptotic solution (see [8]), in terms of Gaussian beams, for example ([60], [66]), or Kirchhoff migration based on the solution of the eikonal equation

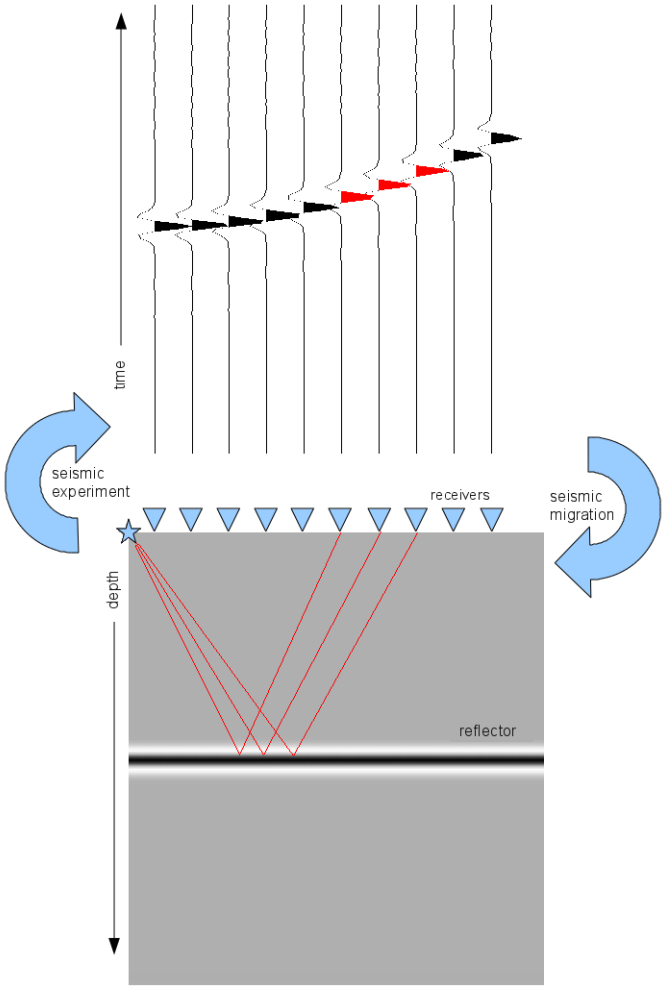

Figure 0.2: Coherence between seismic experiment and migration.

(e.g., [14], [59], [76]);

- depth continuation methods which are usually based on the one way wave equation and compute wave fields from one depth level to the next (e.g., [19], [23], [84]);

- reverse time migration which is based on the full wave equation and follows the recorded seismogram backward in time until the first time is reached (e.g., [2], [11], [41], [70]).

The numerical realizations of all aforementioned methods can be classified according to [85] in tree broad categories:

(i) algorithms based on the integral solution to the scalar wave equation (e.g., [7], [61], [69], [84], etc),

(ii) algorithms based on the finite-difference solutions (e.g., [3], [25], [43], [62], etc),

(iii) algorithms based on the frequency-wavenumber implementations (e.g., [9], [10], [71], etc).

Modern migration methods can combine any number of strategies in order to reach better accuracy and, as a consequence, better resolution in the result image. Such algorithms can compute an initial approximation with the finite difference approximation of the full way wave equation as, for example, in [82] and additionally apply the depth continuation method based on the space frequency implementation.

The further interpretation of such reflector images yields information about available reservoirs, their structures, positions and sizes. Moreover, from the additional analysis of the dependence between the amplitude and the incidence angle (amplitude vs. angle/offset), the information, like density, bulk modulus, etc, can be obtained (more details can be found in, e.g., [85] and the references therein). However, the interpretation of seismic data is a very complicated task and requires the deep knowledge in geology, geophysics, petrology, etc as well as the ability of advanced mathematical and processing tools that are able to recover some specific information in a given seismic data.

Due to the huge success of wavelet techniques in signal processing and noise reduction and their ability to break complicated functions into many small pieces at different scales and positions (e.g., [4], [21], [22], [46], [52]), wavelet approaches are actively applied to seismic data in order to filter (e.g., [17]), compress (e.g., [5], [16], [27]), and even to construct interactive imaging algorithms (e.g., [15], [18], [24]). Such approaches are based, in general, on the geometrical decomposition of the input seismogram or of the resulting image.

In this thesis we provide another wavelet technique that is based on the solution of the Helmholtz equation and can further be applied to seismic data analysis. A similar idea to construct wavelet functions from the limit and jump relations of the layer potentials and to use them to approximate the solution of the partial differential equation was first suggested by Freeden and

his Geomathematics Group (see, e.g., [32], [36], [48]). For the boundary value problem of the Helmholtz equation, and, consequently, of the scalar wave equation, this approach has been developed by Freeden, Mayer and Schreiner ([31], [55]). All these geomathematically reflected methods are related only to regions with smooth boundaries, i.e., boundary surface without edges and corners.

Throughout this work we are not concerned with generating of seismic data by Helmholtz wavelets. Instead, our essential goal is to decorrelate available seismic data (e.g., migration results) for the purposes of multiscale postprocessing by Helmholtz wavelets. To be more concrete, in order to develop a new technique that can be used for the interpretation of seismic data, decomposition procedures in form of a multiscale analysis are studied by space localizing Helmholtz wavelets corresponding to Helmholtz operators $\Delta + \kappa^2$ involving different wave numbers κ. Moreover, compression and reduction of seismic data by Helmholtz wavelets are studied numerically.

The layout of this thesis is as follows: For convenience of the reader the necessary mathematical tools are summarized in Chapter 1. In addition, because the seismic data postprocessing algorithms usually concern regions possessing edges and corners, we extend the classical definition of regular surfaces as given in [31] to certain surfaces with edges and corners.

With respect to the specified regular surface, we present in Chapter 2 the limit and jump relations of the Laplace potential operator. Then, we extend the formulation of the limit and jumps relations from the uniform topology to the $\mathcal{L}^2$-framework only by use of functional analytic means. Additionally, the limit and jump relations of the Helmholtz potential operator are presented. Based on the constructed limit and jump relations, the (scale continuous) scaling functions will be introduced which regularize the kernel functions of the integral representation in the Helmholtz equation. According to the (scale continuous) scaling functions we define the (scale continuous) wavelet functions. Then, scale discrete scaling and wavelet functions providing an associated multiscale analysis in different nomenclatures (pointwise, uniform, and quadratic) will be given in terms of *Helmholtz wavelets*. Additionally, we use a *tree algorithm* (pyramid scheme) for the fast numerical computation (Helmholtz Fast Wavelet Transform (Helmholtz FWT)). The structure of this tree algorithm has already been proposed in [31] for smooth surfaces. However, the numerical realization has not been performed before

and realized in this work for the first time, even for non-smooth surfaces such as cube, polyhedra, etc.

Before we start with the consideration of the application of the Helmholtz wavelet techniques to seismic data postprocessing, we recapitulate one of the standard migration methods, i.e., *reverse time migration*, developed by Baysal et al. (see [2], [3]), in Chapter 3. Additionally, for the purposes of the efficient and economical numerical implementation of this procedure, we propose to apply the additive scheme introduced by Samarkij and Vabishevich (see [65], [73], [74]).

Chapter 4 is devoted to the pointwise application of the developed wavelet techniques to a priori given seismic data (postprocessing), where the seismic data are understood as a prescribed (continuous) function defined on a surface element of a regular surface such as a cube, so that they can be resolved in terms of the Helmholtz scaling functions and wavelets. In order to demonstrate the efficiency and economy of the tree algorithm (the Helmholtz FWT) as described in Chapter 2, we assume the seismic image to be a priori available, e.g., by the reverse time migration based on an additive scheme. Regarding the specific requirements of such migration algorithms in filtering and denoising (e.g., [40], [44], [45], [86]), the wavelet decomposition is successfully applied to the seismic image for the attenuation of low-frequency artifacts and noise. Moreover, the multiscale analysis (scale and detail illustrations) leads us to reveal additional geological information specific for the selected frequency from the given seismic data ready as appropriate tools for optical interpretation.

Chapter 5 summarizes results presented in the thesis. Furthermore, it gives an outline for the further research.

Chapter 1

Basic Fundamentals

Throughout this work we adopt the nomenclature used in the monograph [33].

1.1 Spherical and Cartesian Nomenclature

In this section we introduce some notation in three-dimensional Euclidean space $\mathbb{R}^3$. The most important differential operators as well as basic theorems are listed.

1.1.1 Scalars and Vectors

The letters $\mathbb{N}$, $\mathbb{N}_0$, $\mathbb{Z}$, $\mathbb{R}$, and $\mathbb{C}$ denote the set of positive, non-negative integers, integers, real numbers, and complex numbers, respectively. For the representation of the elements of Euclidean space $\mathbb{R}^3$ we use the notation $x, y, \ldots$. Moreover, for each $x = (x_1, x_2, x_3)^T \in \mathbb{R}^3$ different from the origin 0, we have

$$x = r\xi,\ r = |x| = \sqrt{x_1^2 + x_2^2 + x_3^2}, \tag{1.1}$$

where $\xi = (\xi_1, \xi_2, \xi_3)^T$ is the uniquely determined unit vector of $x \in \mathbb{R}^3$. By Ω we denote the *unit sphere* in $\mathbb{R}^3$:

$$\Omega = \left\{ \xi \in \mathbb{R}^3 \middle| \, |\xi| = 1 \right\}. \tag{1.2}$$

Suppose that $\epsilon^1, \epsilon^2, \epsilon^3$ form the (canonical) orthonormal basis in $\mathbb{R}^3$:

$$\epsilon^1 = \begin{pmatrix} 1 \\ 0 \\ 0 \end{pmatrix},\ \epsilon^2 = \begin{pmatrix} 0 \\ 1 \\ 0 \end{pmatrix},\ \epsilon^3 = \begin{pmatrix} 0 \\ 0 \\ 1 \end{pmatrix}. \tag{1.3}$$

Then, each point $x \in \mathbb{R}^3$ can be represented in Cartesian coordinates by

$$x = \sum_{i=1}^{3} \left(x\epsilon^i\right) \epsilon^i = \sum_{i=1}^{3} x_i \epsilon^i, \; x_i = \left(x\epsilon^i\right), i = 1, 2, 3. \tag{1.4}$$

The inner (scalar), vector and dyadic (tensor) product of elements $x, y \in \mathbb{R}^3$, are defined by

$$xy = x^T y = \sum_{i=1}^{3} x_i y_i; \tag{1.5}$$

$$x \wedge y = \left(x_2 y_3 - x_3 y_2, x_3 y_1 - x_1 y_3, x_1 y_2 - x_2 y_1\right)^T; \tag{1.6}$$

$$x \otimes y = xy^T = \begin{pmatrix} x_1 y_1 & x_1 y_2 & x_1 y_3 \\ x_2 y_1 & x_2 y_2 & x_2 y_3 \\ x_3 y_1 & x_3 y_2 & x_3 y_3 \end{pmatrix}, \tag{1.7}$$

respectively. It is clear, that $x^2 = |x|^2 = xx = x^T x$, $x \in \mathbb{R}^3$. Additionally, we have the *Cauchy-Schwarz inequality*

$$|xy| \leq |x||y|, \; x, y \in \mathbb{R}^3, \tag{1.8}$$

and the *triangle inequality*

$$||x| - |y|| \leq |x \pm y| \leq |x| + |y|, \; x, y \in \mathbb{R}^3. \tag{1.9}$$

1.1.2 Spherical Notation

As already mentioned, the *unit sphere* in $\mathbb{R}^3$ is denoted by Ω

$$\Omega = \left\{ \xi \in \mathbb{R}^3 \middle| \, |\xi| = 1 \right\}. \tag{1.10}$$

We denote by Ω^{int} the *inner space* of Ω, and by Ω^{ext} the *outer space* of Ω. More explicitly,

$$\Omega^{int} = \left\{ x \in \mathbb{R}^3 \middle| \, |x| < 1 \right\}; \tag{1.11}$$

$$\Omega^{ext} = \left\{ x \in \mathbb{R}^3 \middle| \, |x| > 1 \right\}. \tag{1.12}$$

Furthermore, $\Omega(y)$ defines the unit sphere around y

$$\Omega(y) = \left\{ x \in \mathbb{R}^3 \middle| \, |x - y| = 1 \right\}. \tag{1.13}$$

Analogously, $\Omega^{int}(y)$ and $\Omega^{ext}(y)$ define the *inner space* and the *outer space* of $\Omega(y)$, respectively:

$$\Omega^{int}(y) = \left\{ x \in \mathbb{R}^3 \middle| \, |x-y| < 1 \right\}; \tag{1.14}$$

$$\Omega^{ext}(y) = \left\{ x \in \mathbb{R}^3 \middle| \, |x-y| > 1 \right\}. \tag{1.15}$$

The sphere in $\mathbb{R}^3$ with radius R around the origin is denoted by Ω_R

$$\Omega_R = \left\{ x \in \mathbb{R}^3 \middle| \, |x| = R \right\}. \tag{1.16}$$

We set Ω_R^{int} for the *inner space* of Ω_R, while Ω_R^{ext} denotes the *outer space* of Ω_R

$$\Omega_R^{int} = \left\{ x \in \mathbb{R}^3 \middle| \, |x| < R \right\}; \tag{1.17}$$

$$\Omega_R^{ext} = \left\{ x \in \mathbb{R}^3 \middle| \, |x| > R \right\}. \tag{1.18}$$

In the same manner, we introduce the sphere $\Omega_R(y)$ in $\mathbb{R}^3$ with radius R around y

$$\Omega_R(y) = \left\{ x \in \mathbb{R}^3 \middle| \, |x-y| = R \right\}. \tag{1.19}$$

We set $\Omega_R^{int}(y)$ for the *inner space* of $\Omega_R(y)$, while $\Omega_R^{ext}(y)$ denotes the *outer space* of $\Omega_R(y)$:

$$\Omega_R^{int}(y) = \left\{ x \in \mathbb{R}^3 \middle| \, |x-y| < R \right\}; \tag{1.20}$$

$$\Omega_R^{ext}(y) = \left\{ x \in \mathbb{R}^3 \middle| \, |x-y| > R \right\}. \tag{1.21}$$

For the total surface of Ω_R we have

$$\|\Omega_R\| = \int\limits_{\Omega_R} d\omega(\xi) = 4\pi R^2. \tag{1.22}$$

As is well known, we may represent the points $x \in \mathbb{R}^3$, $x = r\xi$, $\xi \in \Omega$ in polar coordinates as follows

$$\begin{aligned} &x = r\xi, \ r = |x|; \\ &\xi = t\epsilon^3 + \sqrt{1-t^2}\left(\cos\phi\epsilon^1 + \sin\phi\epsilon^2\right); \\ &-1 \le t \le 1, \ 0 \le \phi < 2\pi, \ t = \cos\theta, \end{aligned} \tag{1.23}$$

($\theta \in [0,\pi]$: (co-)latitude, ϕ: longitude, t: polar distance), i.e.,

$$\xi = (\sin\theta \ \cos\phi, \sin\theta \ \sin\phi, \cos\theta)^T. \tag{1.24}$$

1.1.3 Function Spaces

The set of scalar functions $F : \Omega \to \mathbb{R}$, for which

$$\|F\|_{\mathcal{L}^p(\Omega)} = \left(\int_{\Omega} |F(\xi)|^p \, d\omega(\xi) \right)^{\frac{1}{p}} < \infty, \; 1 \leq p < \infty, \tag{1.25}$$

is known as $\mathcal{L}^p(\Omega)$. It is clear, that $\mathcal{L}^p(\Omega) \subset \mathcal{L}^q(\Omega)$ for $1 \leq q < p$. A function F is of class $\mathcal{C}^{(k)}(\Omega)$, $0 \leq k \leq \infty$, if $F : \Omega \to \mathbb{R}$ possesses k continuous derivatives on the unit sphere Ω. The class of continuous scalar-valued functions $\mathcal{C}(\Omega)$ $(= \mathcal{C}^{(0)}(\Omega))$ is a complete normed space endowed with

$$\|F\|_{\mathcal{C}(\Omega)} = \sup_{\xi \in \Omega} |F(\xi)| \, . \tag{1.26}$$

By $\ell_F(\delta)$, we denote the *modulus of continuity* of the function $F \in \mathcal{C}(\Omega)$, i.e.,

$$\ell_F(\delta) = \max_{\substack{\xi, \zeta \in \Omega \\ 1 - \xi\zeta \leq \delta}} |F(\xi) - F(\zeta)| \, , 0 < \delta < 2. \tag{1.27}$$

A function $F : \Omega \to \mathbb{R}$ is *Lipschitz-continuous*, if there exists a (Lipschitz) constant $C_F > 0$ such that the inequality

$$|F(\xi) - F(\zeta)| \leq C_F |\xi - \zeta| = \sqrt{2} C_F \sqrt{1 - \xi\zeta} \tag{1.28}$$

holds for all $\xi, \zeta \in \Omega$. The class of all Lipschitz-continuous functions on Ω is denoted by $\mathrm{Lip}(\Omega)$. Clear $\mathcal{C}^{(1)}(\Omega) \subset \mathrm{Lip}(\Omega)$.

$\mathcal{L}^2(\Omega)$ is a Hilbert space with respect to the inner product $(\cdot, \cdot)_{\mathcal{L}^2(\Omega)}$ defined by

$$(F, G)_{\mathcal{L}^2(\Omega)} = \int_{\Omega} F(\xi) \overline{G(\xi)} d\xi, \; F, G \in \mathcal{L}^2(\Omega), \tag{1.29}$$

where $\overline{G(\xi)}$ means complex-conjugate to $G(\xi)$.

In connection with $(\cdot, \cdot)_{\mathcal{L}^2(\Omega)}$, $\mathcal{C}(\Omega)$ is a pre-Hilbert space. For each $F \in \mathcal{C}(\Omega)$ we have the *norm estimate*

$$\|F\|_{\mathcal{L}^2(\Omega)} \leq \sqrt{4\pi} \, \|F\|_{\mathcal{C}(\Omega)} \, . \tag{1.30}$$

It can be proved that $\mathcal{L}^2(\Omega)$ is the completion of $\mathcal{C}(\Omega)$ with respect to the norm $\|\cdot\|_{\mathcal{L}^2(\Omega)}$, i.e.

$$\mathcal{L}^2(\Omega) = \overline{\mathcal{C}(\Omega)}^{\|\cdot\|_{\mathcal{L}^2(\Omega)}}. \tag{1.31}$$

$l^2(\Omega)$ denotes the space of all square-integrable vector fields on Ω. In connection with the inner product

$$(f,g)_{l^2(\Omega)} = \int_\Omega f(\xi)\overline{g(\xi)}d\omega(\xi),\ \ f,g \in l^2(\Omega), \tag{1.32}$$

$l^2(\Omega)$ is a Hilbert space. The space of all p-times continuously differentiable vector fields on Ω we denote by $c^{(p)}(\Omega)$, $0 \leq p \leq \infty$. The space $c(\Omega)$ $(= c^{(0)}(\Omega))$ is complete with respect to the norm

$$\|f\|_{c(\Omega)} = \sup_{\xi\in\Omega} |f(\xi)|\,,\ \ f \in c(\Omega). \tag{1.33}$$

Furthermore, it can be shown that

$$l^2(\Omega) = \overline{c(\Omega)}^{\|\cdot\|_{l^2(\Omega)}}. \tag{1.34}$$

For all $f \in c(\Omega)$ the *norm estimate*

$$\|f\|_{l^2(\Omega)} \leq \sqrt{4\pi}\,\|f\|_{c(\Omega)}\,. \tag{1.35}$$

1.1.4 Differential Operators

For an arbitrary $\Gamma \subset \mathbb{R}^3$, $\partial\Gamma$ denotes the *boundary* of Γ. The set $\overline{\Gamma} = \Gamma \cup \partial\Gamma$ is called the *closure* of Γ. A set $\Gamma \subset \mathbb{R}^3$ will be called a *region* if and only if it is open and connected.

By a scalar or vector function (field) on a region $\Gamma \subset \mathbb{R}^3$, we assume a function that assigns to each point of Γ, a scalar or vectorial function value, respectively. We will use the following notations: capital letters F, G for scalar functions, lower-case letters f, g for vector fields.

The restriction of a scalar-valued function F or a vector-valued function f to a subset M of its domain is denoted by $F|M$ or $f|M$, respectively. For a set S of functions, we set $S|M = \{\, F|M|\, F \in S\}$.

Let $\Gamma \subset \mathbb{R}^3$ be a region and $F : \Gamma \to \mathbb{R}$ be differentiable.
$\nabla F : x \mapsto (\nabla F)(x)$, $x \in \Gamma$, denotes the *gradient* of F on a region Γ. The *partial derivatives* of F at $x \in \Gamma$, briefly written $F_{|i}, i \in \{1,2,3\}$, are represented by

$$F_{|i}(x) = \frac{\partial F}{\partial x_i}(x) = (\nabla F)(x)\epsilon^i = ((\nabla F)(x))_i\,. \tag{1.36}$$

We say that the scalar function $F : \Gamma \to \mathbb{R}$, the vector function $f : \Gamma \to \mathbb{R}^3$, respectively, is of class $\mathcal{C}^{(1)}$ on Γ, $c^{(1)}$ on Γ, if F, f, respectively, is differentiable at every point of Γ and ∇F, ∇f, respectively, is continuous on Γ. The

gradient of ∇F, ∇f is denoted by $\nabla^{(2)}F$, $\nabla^{(2)}f$. Continuing in this manner, we say that F, f, respectively, is of class $\mathcal{C}^{(n)}$, $c^{(n)}$ on Γ, $n \geq 1$ (briefly, $F \in \mathcal{C}^{(n)}(\Gamma)$, $f \in c^{(n)}(\Gamma)$) if it is of class $\mathcal{C}^{(n-1)}, c^{(n-1)}$ and its $(n-1)$st gradient $\nabla^{(n-1)}F$, $\nabla^{(n-1)}f$, respectively, is continuously differentiable (note that we usually write $\mathcal{C}$, c instead of $\mathcal{C}^{(0)}$, $c^{(0)}$, respectively).

Let $u : \Gamma \to \mathbb{R}^3$ be a vector field, and suppose that u is differentiable at a point $x \in \Gamma$. The partial derivatives of u at $x \in \Gamma$ are given by

$$u_{i|j}(x) = \frac{\partial u_i}{\partial x_j}(x) = \epsilon^i \left(\nabla u\right)(x)\epsilon^j. \tag{1.37}$$

Then, the *divergence* of u at $x \in \Gamma$ is the scalar value

$$\nabla_x u(x) = \operatorname{div}_x u(x) = \sum_{i=1}^{3} u_{i|i}(x). \tag{1.38}$$

Let $F : \Gamma \to \mathbb{R}$ be a differentiable scalar field, and suppose that ∇F is differentiable at $x \in \Gamma$. Then we introduce the *Laplace operator (Laplacian)* of F at $x \in \Gamma$ by

$$\Delta_x F(x) = \operatorname{div}_x \left(\left(\nabla F\right)(x)\right) = \nabla_x \left(\left(\nabla F\right)(x)\right). \tag{1.39}$$

Analogously, the *Laplacian* of a continuously differentiable vector field $f : \Gamma \to \mathbb{R}^3$ is defined by

$$\Delta_x f(x) = \operatorname{div}_x \left(\left(\nabla f\right)(x)\right) = \nabla_x \left(\left(\nabla f\right)(x)\right). \tag{1.40}$$

Clearly, for sufficiently often differentiable functions F, f we have

$$\Delta_x F(x) = \sum_{i=1}^{3} F_{|i|i}(x); \tag{1.41}$$

$$\Delta_x f(x)\epsilon^i = \sum_{j=1}^{3} f_{|i|j|j}(x). \tag{1.42}$$

A region $\Gamma \subset \mathbb{R}^3$ is called *admissible*, if its boundary $\partial\Gamma$ allows the *Gauß theorem*

$$\int_{\Gamma} \nabla f(x)dx = \int_{\partial\Gamma} f(x)\nu(x)d\omega(x),$$

for all continuously differentiable vector fields f on $\overline{\Gamma}$, $\overline{\Gamma} = \Gamma \cup \partial\Gamma$ (ν is the outer (unit) normal field). By letting $f = \nabla F$, $F \in \mathcal{C}^{(2)}(\overline{\Gamma})$, $\Gamma \subset \mathbb{R}^3$ admissible, we obtain from the Gauß theorem

$$\int_{\Gamma} \Delta F(x)dx = \int_{\partial\Gamma} \frac{\partial F}{\partial \nu}(x)d\omega(x),$$

where $\dfrac{\partial}{\partial\nu}$ denotes the derivative in the direction of the outer (unit) normal field ν. Consequently, for all functions $F \in \mathcal{C}^{(2)}(\overline{\Gamma})$ satisfying the Laplace equation $\Delta F = 0$ in Γ, we have

$$\int_{\partial\Gamma} \frac{\partial F}{\partial\nu}(x) d\omega(x) = 0.$$

For all vector fields $f = F\nabla G$, $F \in \mathcal{C}^{(1)}(\overline{\Gamma})$, $G \in \mathcal{C}^{(2)}(\overline{\Gamma})$, we get from the Gauß theorem

Theorem 1.1 *(First Green Theorem) Suppose that $\Gamma \subset \mathbb{R}^3$ is an admissible region. For $F \in \mathcal{C}^{(1)}(\overline{\Gamma})$, $G \in \mathcal{C}^{(2)}(\overline{\Gamma})$ we have*

$$\int_{\Gamma} \left(F(x)\Delta G(x) + \nabla F(x)\nabla G(x)\right) dx = \int_{\partial\Gamma} F(x)\frac{\partial G}{\partial\nu}(x) d\omega(x).$$

Taking $f = F\Delta G - G\Delta F$ with $F, G \in \mathcal{C}^{(2)}(\overline{\Gamma})$ we obtain

Theorem 1.2 *(Second Green Theorem) Suppose that $\Gamma \in \mathbb{R}^3$ is an admissible region. For $F, G \in \mathcal{C}^{(2)}(\overline{\Gamma})$ we have*

$$\int_{\Gamma} \left(G(x)\Delta F(x) - F(x)\Delta G(x)\right) dx = \int_{\partial\Gamma} \left(G(x)\frac{\partial F}{\partial\nu}(x) - F(x)\frac{\partial G}{\partial\nu}(x)\right) d\omega(x).$$

Next we mention an extension of the second Green theorem.

Theorem 1.3 *(Extended Second Green Theorem) For a given number $\kappa \in \mathbb{C}$ and an admissible region $\Gamma \subset \mathbb{R}^3$, and for $F, G \in \mathcal{C}^{(2m)}(\overline{\Gamma})$, $m \in \mathbb{N}$, we have*

$$\begin{aligned}\int_{\Gamma} G(x)(\Delta + \kappa^2)^m F(x) dx &= \int_{\Gamma} F(x)(\Delta + \kappa^2)^m G(x) dx \\ &+ \sum_{r=0}^{m-1} \int_{\partial\Gamma} \left(\frac{\partial}{\partial\nu}(\Delta + \kappa^2)^r F(x)\right) \left((\Delta + \kappa^2)^{m-(r+1)} G(x)\right) d\omega(x) \\ &- \sum_{r=0}^{m-1} \int_{\partial\Gamma} \left((\Delta + \kappa^2)^r F(x)\right) \left(\frac{\partial}{\partial\nu}(\Delta + \kappa^2)^{m-(r+1)} G(x)\right) d\omega(x).\end{aligned} \tag{1.43}$$

Its simplest form is the case with vanishing boundary terms, i.e.,

$$\sum_{r=0}^{m-1} \int_{\partial\Gamma} \left(\frac{\partial}{\partial \nu} (\Delta + \kappa^2)^r F(x) \right) \left((\Delta + \kappa^2)^{m-(r+1)} G(x) \right) d\omega(x)$$
$$- \sum_{r=0}^{m-1} \int_{\partial\Gamma} \left((\Delta + \kappa^2)^r F(x) \right) \left(\frac{\partial}{\partial \nu} (\Delta + \kappa^2)^{m-(r+1)} G(x) \right) d\omega(x) = 0,$$

such that (1.43) reduces to the formula

$$\int_{\Gamma} \left(G(x)(\Delta + \kappa^2)^m F(x) - F(x)(\Delta + \kappa^2)^m G(x) \right) dx = 0.$$

Next we come to the well-known definition of harmonic and metaharmonic functions.

Definition 1.4 *$U \in \mathcal{C}^{(2)}(\Gamma)$ is called a **harmonic function** in a region $\Gamma \in \mathbb{R}^3$, if it satisfies the Laplace equation*

$$\Delta U(x) = \sum_{i=1}^{3} \frac{\partial^2}{\partial x_i^2} U(x_1, x_2, x_3) = 0, \ x = (x_1, x_2, x_3)^T \in \Gamma. \tag{1.44}$$

*$U \in \mathcal{C}^{(2m)}(\Gamma)$, $m \in \mathbb{N}$, is called **polyharmonic function** of degree m in $\Gamma \subset \mathbb{R}^3$, if*

$$\Delta^m U(x) = 0, \ x \in \Gamma. \tag{1.45}$$

*$U \in \mathcal{C}^{(2)}(\Gamma)$ is called **metaharmonic function** with respect to the Helmholtz operator $\Delta + \kappa^2$, $\kappa \in \mathbb{C}$, in a region $\Gamma \subset \mathbb{R}^3$, if it satisfies the Helmholtz equation*

$$\left(\Delta + \kappa^2 \right) U(x) = 0, \ x \in \Gamma. \tag{1.46}$$

*$U \in \mathcal{C}^{(2m)}(\Gamma)$, $m \in \mathbb{N}$, is called a **polymetaharmonic function** of degree m in Γ, if*

$$(\Delta + \kappa^2)^m U(x) = 0, \ x \in \Gamma. \tag{1.47}$$

Let $y \in \Gamma$ be fixed, where Γ is a region in $\mathbb{R}^3$. We are looking for a harmonic function U in $\Gamma \setminus \{y\}$ such that

$$U(x) = S(x, y), \ x \in \Gamma \setminus \{y\},$$

i.e., U depends only on the mutual distance of x and y. From the identities

$$\frac{\partial}{\partial x_i}S(x,y) = S'(x,y)\frac{x_i - y_i}{|x-y|}, \tag{1.48}$$

$$\frac{\partial^2}{\partial x_i^2}S(x,y) = S''(x,y)\frac{(x_i-y_i)^2}{|x-y|^2} + S'(x,y)\left(\frac{1}{|x-y|} - \frac{(x_i-y_i)^2}{|x-y|^3}\right), \tag{1.49}$$

we easily obtain

$$\Delta_x S(x,y) = S''(x,y) + \frac{2}{|x-y|}S'(x,y) = 0.$$

In other words, $S(x,y)$ can be written in the form

$$S(x,y) = \frac{C_1}{|x-y|} + C_2, \tag{1.50}$$

with some constants C_1, C_2. By convention (see, e.g., [80]), the function

$$x \mapsto S(|x-y|) = \frac{1}{4\pi|x-y|} \tag{1.51}$$

is called the *fundamental solution in* $\mathbb{R}^3$ *with respect to the Laplace operator* Δ.

The fundamental solution of the Laplace operator possesses the following property.

Lemma 1.5 *For continuous functions* F, G *in the ball* $\overline{\Omega_R^{int}(y)}$ *with* $R > r > 0$*, we have*

$$\lim_{\substack{r\to 0\\ r>0}} \int\limits_{|x-y|=r} G(x)\frac{\partial}{\partial\nu(x)}S(|x-y|)d\omega(x) = -G(y), \tag{1.52}$$

$$\lim_{\substack{r\to 0\\ r>0}} \int\limits_{|x-y|=r} F(x)S(|x-y|)d\omega(x) = 0, \tag{1.53}$$

where the (unit) normal field ν *is directed to the exterior of* $\Omega_R^{int}(y)$.

Proof Because of the continuity of the function F in each ball $\overline{\Omega_r^{int}(y)}$, $r < R$, we find

$$\begin{aligned}\left|\int\limits_{|x-y|=r} F(x)\frac{1}{4\pi|x-y|}d\omega(x)\right| &\le \frac{C}{4\pi}\int\limits_{|x-y|=r}\frac{1}{|x-y|}d\omega(x)\\ &= \frac{C}{4\pi}4\pi r\\ &= C_r\end{aligned}$$

for some positive constant C. This shows the second limit relation (1.53).

For the first limit relation we observe that the normal derivative can be understood as the radial derivative. From the mean value theorem we therefore obtain

$$\begin{aligned}\int\limits_{|x-y|=r} G(x)\frac{\partial}{\partial\nu(x)}\frac{1}{4\pi|x-y|}d\omega(x) &= -\frac{1}{4\pi r^2}\int\limits_{|x-y|=r} G(x)d\omega(x)\\ &= -\frac{1}{4\pi r^2}4\pi r^2 G(x_r)\end{aligned}$$

for certain points $x_r \in \Omega_r(y)$. The limit $r \to 0$ implies $x_r \to y$, such that the continuity of G yields

$$\lim_{\substack{r\to 0\\ r>0}} G(x_r) = G(y).$$

This is the desired result. ■

Next we want to apply the second Green theorem (for an admissible region Γ with continuously differentiable boundary $\partial\Gamma$) especially to the functions

$$\begin{aligned} F &: x \mapsto F(x) = 1, && x \in \overline{\Gamma},\\ G &: x \mapsto S(|x-y|), && x \in \overline{\Gamma}\setminus\{y\},\end{aligned}$$

where $y \in \mathbb{R}^3$ is positioned in accordance with the following three cases:
Case $y \in \Gamma$: For sufficiently small $\epsilon > 0$ we obtain by integration by parts, i.e., the second Green theorem

$$\begin{aligned}\int\limits_{\substack{x\in\Gamma\\ |x-y|\geq\epsilon}} \underbrace{\Delta_x S(|x-y|)}_{=0}\,dx &= \int\limits_{x\in\partial\Gamma}\frac{\partial}{\partial\nu(x)}S(|x-y|)d\omega(x)\\ &\quad+\int\limits_{\substack{x\in\Gamma\\ |x-y|=\epsilon}}\frac{\partial}{\partial\nu(x)}S(|x-y|)d\omega(x).\end{aligned}$$

In connection with Lemma 1.5 we therefore obtain by letting $\epsilon \to 0$

$$\int\limits_{\partial\Gamma}\frac{\partial}{\partial\nu(x)}S(|x-y|)d\omega(x) = 1. \tag{1.54}$$

Case $y \in \partial\Gamma$: Again, by Green's theorem we obtain for $\epsilon > 0$

$$-\int\limits_{\substack{x\in\Gamma\\ |x-y|=\epsilon}}\frac{\partial}{\partial\nu(x)}S(|x-y|)d\omega(x) = \int\limits_{x\in\partial\Gamma}\frac{\partial}{\partial\nu(x)}S(|x-y|)d\omega(x).$$

By letting $\epsilon \to 0$ we now find in case of a continuously differentiable surface $\partial\Gamma$

$$\int\limits_{\partial\Gamma} \frac{\partial}{\partial\nu(x)} S(|x-y|)d\omega(x) = \frac{1}{2}. \tag{1.55}$$

Case $y \notin \overline{\Gamma}$: The second Green theorem now yields

$$\int\limits_{\Gamma} \underbrace{\Delta_x S(|x-y|)}_{=0} dx = \int\limits_{\partial\Gamma} \frac{\partial}{\partial\nu(x)} S(|x-y|)d\omega(x). \tag{1.56}$$

Summarizing all our results we obtain from (1.54), (1.55) and (1.56)

Lemma 1.6 *Let $\Gamma \subset \mathbb{R}^3$ be an admissible region with continuously differentiable boundary $\partial\Gamma$. Then*

$$-\int\limits_{\partial\Gamma} \frac{\partial}{\partial\nu(x)} S(|x-y|)d\omega(x) = \begin{cases} 1, & y \in \Gamma, \\ \frac{1}{2}, & y \in \partial\Gamma, \\ 0, & y \notin \overline{\Gamma}. \end{cases}$$

In other words, the integral is a measure for the *solid angle* subtended by the boundary $\partial\Gamma$ at the point $y \in \mathbb{R}^3$.

Remark 1.7 *From potential theory (see, e.g., [47]) it is known that Lemma 1.6 may be extended to admissible regions Γ with non-smooth boundaries $\partial\Gamma$ such as cube, simplex, polyhedron, more concretely, to admissible regions with solid angle $\omega(y)$ at $y \in \mathbb{R}^3$ subtended by the surface $\partial\Gamma$.*

Definition 1.8 *The function*

$$\omega : y \mapsto \int\limits_{\partial\Gamma} \frac{\partial}{\partial\nu(x)} \frac{1}{|x-y|} d\omega(x), \ y \in \mathbb{R}^3,$$

*is called the **solid angle** at $y \in \mathbb{R}^3$ subtended by the surface $\partial\Gamma$.*

An example of particular interest in our applications is the cube

$$\Gamma = (-R, R)^3 \subset \mathbb{R}^3, \ R > 0.$$

In this case we have

(i) $\omega(y) = 1$, if y is located in the open cube Γ,

(*ii*) $\omega(y) = \dfrac{1}{2}$, if y is located on one of the six faces of the boundary $\partial\Gamma$ of the cube Γ but not on an edge or in a corner,

(*iii*) $\omega(y) = \dfrac{1}{4}$, if y is located on one of the eight edges of $\partial\Gamma$ but not in a vertex,

(*iv*) $\omega(y) = \dfrac{1}{8}$, if y is located in one of the eight corners of $\partial\Gamma$.

Lemma 1.6 is a special case of the third Green theorem in $\mathbb{R}^3$ (see, e.g., [47]) that will mentioned next.

Theorem 1.9 *(Third Green Theorem)*

(*i*) *Let Γ be an admissible region with continuously differentiable boundary $\partial\Gamma$. Suppose that $U : \overline{\Gamma} \to \mathbb{R}$ is twice continuously differentiable, i.e., $U \in \mathcal{C}^{(2)}(\overline{\Gamma})$. Then we have*

$$\int\limits_{\partial\Gamma} \left(S(|x-y|) \frac{\partial}{\partial\nu(x)} U(x) - U(x) \frac{\partial}{\partial\nu(x)} S(|x-y|) \right) d\omega(x)$$

$$- \int\limits_{\Gamma} S(|x-y|) \Delta U(x) dx = \begin{cases} U(y), & y \in \Gamma, \\ \dfrac{1}{2} U(y), & y \in \partial\Gamma, \\ 0, & y \in \mathbb{R}^3 \setminus \overline{\Gamma}. \end{cases}$$

(*ii*) *Let Γ be an admissible region. Suppose that $U : \overline{\Gamma} \to \mathbb{R}$ is twice continuously differentiable, i.e., $U \in \mathcal{C}^{(2)}(\overline{\Gamma})$. Then we have*

$$\int\limits_{\partial\Gamma} \left(S(|x-y|) \frac{\partial}{\partial\nu(x)} U(x) - U(x) \frac{\partial}{\partial\nu(x)} S(|x-y|) \right) d\omega(x)$$

$$- \int\limits_{\Gamma} S(|x-y|) \Delta U(x) dx = \omega(y) U(y),$$

where $\omega(y)$, $y \in \mathbb{R}^3$, is the solid angle at y subtended by the surface $\partial\Gamma$.

Proof We only consider the case $y \in \Gamma$. For every $\epsilon > 0$, Green's formula

tells us that

$$
\begin{aligned}
&- \int\limits_{\substack{|x-y|\geq\epsilon \\ x\in\Gamma}} S(|x-y|)\Delta U(x)dx \\
&\quad = \int\limits_{\partial\Gamma} \left(U(x)\frac{\partial}{\partial\nu(x)}S(|x-y|) - S(|x-y|)\frac{\partial}{\partial\nu(x)}U(x) \right) d\omega(x) \\
&\qquad + \int\limits_{\substack{|x|=\epsilon \\ x\in\Gamma}} \left(U(x)\frac{\partial}{\partial\nu(x)}S(|x-y|) - S(|x-y|)\frac{\partial}{\partial\nu(x)}U(x) \right) d\omega(x).
\end{aligned}
$$

Letting $\epsilon \to 0$ the theorem follows immediately from Lemma 1.5. ■

Finally we mention the *Poisson differential equation*, which is a classical result in potential theory (see, e.g., [33]).

Theorem 1.10 *Let F be of class $\mathcal{C}^{(0)}(\overline{\Gamma})$, $\overline{\Gamma} = \Gamma \cup \partial\Gamma \subset \mathbb{R}^3$. Then $U : \overline{\Gamma} \to \mathbb{R}$ given by*

$$U(x) = \int\limits_{\Gamma} F(y)\frac{1}{|x-y|}dy$$

is of class $\mathcal{C}^{(1)}(\overline{\Gamma})$, and we have

$$\nabla U(x) = \int\limits_{\Gamma} F(y)\nabla_x \frac{1}{|x-y|}dy.$$

If, in addition, F is assumed to be Lipschitz-continuous in Γ, i.e.,

$$|F(x) - F(y)| \leq C_F\,|x-y|$$

for all $x, y \in \Gamma$, then

$$\Delta U = -4\pi F$$

holds true in Γ.

1.1.5 Differential and Integral Calculus

We consider a vector function $\Phi : [0,\infty) \times [0,2\pi) \times [-1,1] \to \mathbb{R}^3$ defined by

$$\Phi(r,\phi,t) = \begin{pmatrix} r\sqrt{1-t^2}\cos\phi \\ r\sqrt{1-t^2}\sin\phi \\ rt \end{pmatrix}. \tag{1.57}$$

If we set $r = 1$, we obtain a local coordinate system on the unit sphere. That means, instead of denoting any element of Ω by its vectorial representation ξ, we may also use its coordinates (ϕ, t) in accordance with Equation (1.23). Calculating the derivatives of Φ and setting $r = 1$, the corresponding set of orthonormal unit vectors in the directions r, ϕ, and t is easily determined to be

$$\epsilon^r(\phi,t) = \begin{pmatrix} \sqrt{1-t^2}\cos\phi \\ \sqrt{1-t^2}\sin\phi \\ t \end{pmatrix}, \epsilon^\phi(\phi,t) = \begin{pmatrix} -\sin\phi \\ \cos\phi \\ 0 \end{pmatrix}, \epsilon^t(\phi,t) = \begin{pmatrix} -t\cos\phi \\ -t\sin\phi \\ \sqrt{1-t^2} \end{pmatrix}. \tag{1.58}$$

It is clear, that $\epsilon^t(\phi,t) = \epsilon^r(\phi,t) \wedge \epsilon^\phi(\phi,t)$.

From Equations (1.58), we immediately obtain a representation of the Cartesian unit vectors in terms of the spherical ones:

$$\epsilon^1 = \sqrt{1-t^2}\cos\phi\epsilon^r(\phi,t) - \sin\phi\epsilon^\phi(\phi,t) - t\cos\phi\epsilon^t(\phi,t); \tag{1.59}$$

$$\epsilon^2 = \sqrt{1-t^2}\sin\phi\epsilon^r(\phi,t) + \cos\phi\epsilon^\phi(\phi,t) - t\sin\phi\epsilon^t(\phi,t); \tag{1.60}$$

$$\epsilon^3 = t\epsilon^r(\phi,t) + \sqrt{1-t^2}\epsilon^t(\phi,t). \tag{1.61}$$

The system $\left\{\epsilon^\phi, \epsilon^t\right\}$ enables us to formulate a *vector differential calculus.*

Gradient fields ∇F can be decomposed into a radial and a tangential component. The *surface gradient* ∇^* contains the tangential derivatives of the gradient ∇ as follows:

$$\nabla = \epsilon^r\frac{\partial}{\partial r} + \frac{1}{r}\nabla^*. \tag{1.62}$$

For any $x = r\xi$, $r = |x|$, $\xi \in \Omega$ there exists $\eta \in \Omega$

$$\nabla_x(x\eta) = \eta = \epsilon^r(\xi\eta) + \nabla^*_\xi(\xi\eta), \tag{1.63}$$

such that

$$\nabla^*_\xi(\xi\eta) = \eta - (\xi\eta)\xi. \tag{1.64}$$

In addition, we denote the *surface divergence* given by

$$\nabla^*_\xi f(\xi) = \sum_{i=1}^{3} \nabla^*_\xi F_i(\xi)\epsilon^i. \tag{1.65}$$

The aforementioned relations can be understood from the well-known role of the Beltrami operator Δ^* in the representation of the *Laplace operator* Δ

$$\Delta_x = \left(\frac{\partial}{\partial r}\right)^2 + \frac{2}{r}\frac{\partial}{\partial r} + \frac{1}{r^2}\Delta^*_\xi. \tag{1.66}$$

In spherical coordinates, the operator Δ^* is represented as follows

$$\Delta^*_\xi = \frac{\partial}{\partial t}\left(1-t^2\right)\frac{\partial}{\partial t} + \frac{1}{1-t^2}\left(\frac{\partial}{\partial \phi}\right)^2. \tag{1.67}$$

Equation (1.58) implies

$$\begin{aligned}\nabla^*_\xi = \frac{1}{\sqrt{1-t^2}}\left(-\sin\phi\epsilon^1 + \cos\phi\epsilon^2\right)\frac{\partial}{\partial\phi} \\ + \sqrt{1-t^2}\left(-t\cos\phi\epsilon^1 - t\sin\phi\epsilon^2 + \sqrt{1-t^2}\epsilon^3\right)\frac{\partial}{\partial\phi}.\end{aligned} \tag{1.68}$$

In the same way as for Euclidean space $\mathbb{R}^3$, a region $\Gamma \subset \Omega$ is called *admissible*, if its boundary $\partial\Gamma$ allows the *surface theorem of Gauß*

$$\int_\Gamma \nabla^*_\xi f(\xi)d\omega(\xi) = \int_{\partial\Gamma} \nu_\xi f(\xi)d\sigma(\xi), \tag{1.69}$$

provided that f is a continuously differentiable field on $\overline{\Gamma} = \Gamma \cup \partial\Gamma$ such that $f(\xi)\xi = 0$, $\xi \in \overline{\Gamma}$. ($\nu$ and τ denotes surface normal vector (outward of Γ) and tangential to $\partial\Gamma$ normal vector, respectively. σ is the arc length along $\partial\Gamma$.)

Applying the Gauß formula (1.69) to $f = F\nabla^* G$ with suitable F, G we obtain the *First Green Theorem*

$$\int_\Gamma \nabla^*_\xi G(\xi)\nabla^*_\xi F(\xi)d\omega(\xi) + \int_\Gamma F(\xi)\Delta^*_\xi G(\xi)d\omega(\xi) = \int_{\partial\Gamma} F(\xi)\frac{\partial}{\partial\nu_\xi}G(\xi)d\sigma(\xi). \tag{1.70}$$

Analogously, we obtain the *Second Green Theorem*

$$\begin{aligned}\int_\Gamma \left(F(\xi)\Delta^*_\xi G(\xi) - G(\xi)\Delta^*_\xi F(\xi)\right)d\omega(\xi) \\ = \int_{\partial\Gamma}\left(F(\xi)\frac{\partial}{\partial\nu_\xi}G(\xi) - G(\xi)\frac{\partial}{\partial\nu_\xi}F(\xi)\right)d\sigma(\xi) \\ = \int_{\partial\Gamma}\left(F(\xi)\frac{\partial}{\partial\tau_\xi}G(\xi) - G(\xi)\frac{\partial}{\partial\tau_\xi}F(\xi)\right)d\sigma(\xi).\end{aligned} \tag{1.71}$$

There are immediate consequences of the above formulas due to the fact that the integral identities also hold true on $\Omega \setminus \overline{\Gamma}$ (under suitable assumptions on

the integrands). For the whole sphere this leads to

$$\int_{\Omega} f(\xi)\nabla_{\xi}^{*}F(\xi)d\omega(\xi) = -\int_{\Omega} F(\xi)\nabla_{\xi}^{*}f(\xi)d\omega(\xi); \tag{1.72}$$

$$\int_{\Omega} \nabla_{\xi}^{*}F(\xi)\nabla_{\xi}^{*}G(\xi)d\omega(\xi) = -\int_{\Omega} F(\xi)\Delta_{\xi}^{*}G(\xi)d\omega(\xi) \tag{1.73}$$

$$\int_{\Omega} \nabla_{\xi}^{*}F(\xi)\nabla_{\xi}^{*}G(\xi)d\omega(\xi) = -\int_{\Omega} G(\xi)\Delta_{\xi}^{*}F(\xi)d\omega(\xi). \tag{1.74}$$

Furthermore,

$$\int_{\Omega} \nabla_{\xi}^{*}f(\xi)d\omega(\xi) = 0; \tag{1.75}$$

$$\int_{\Omega} \nabla_{\xi}^{*}\left(f(\xi)\wedge\xi\right)d\omega(\xi) = 0, \tag{1.76}$$

provided that $F:\Omega\to\mathbb{R}$ (resp. $f:\Omega\to\mathbb{R}^3$) are sufficiently often continuously differentiable.

By virtue of the isomorphism $\Omega\ni\xi\mapsto R\xi\in\Omega_R$, $R>0$, we can assume functions $F:\Omega\to\mathbb{R}$ to be defined on Ω_R. With the surface measure $d\omega_R$ of Ω_R, $d\omega_R = R^2 d\omega$, we are able to introduce the $\mathcal{L}^2(\Omega_R)$-inner product $(\cdot,\cdot)_{\mathcal{L}^2(\Omega_R)}$ and the associated norm $\|\cdot\|_{\mathcal{L}^2(\Omega_R)}$, as usual. With the relationship $\xi\leftrightarrow R\xi$, the *surface gradient* $\nabla^{*;R}$ and the *Beltrami operator* $\Delta^{*;R}$ on Ω_R, respectively, have the representation $\nabla^{*;R}=(1/R)\nabla^{*}$ and $\Delta^{*;R}=(1/R^2)\Delta^{*}$. It is clear that the function spaces defined on Ω admit their natural generalization as spaces of functions defined on Ω_R. We have for example, $\mathcal{C}^{(\infty)}(\Omega_R)$, $\mathcal{L}^p(\Omega_R)$, etc.

1.2 Analytical and Geometrical Prerequisites

Based on the analytical and geometrical constructions as, e.g., introduced in [72], [79] in this section we give some analytical and geometrical basics for the 'regularization' of regions with non-smooth boundaries.

Definition 1.11 *A non-degenerate, compact surface element $\Xi\subset\mathbb{R}^3$ free of double points, is called* ***regular****, if it satisfies the properties:*

(i) Ξ is twice continuously differentiable.

(ii) *There exist constants $\tilde{M}, d > 0$, such that for each surface point $x \in \Sigma$ $\Omega_d^{int}(x) \cap \Xi$ can be represented in a Cartesian coordinate system (tangential-normal-system) in the form*

$$x_3 = \tilde{H}(x_1, x_2),\ (x_1, x_2) \in \tilde{T} \subset \mathbb{R}^2,$$

where the function $\tilde{H}(x_1, x_2)$ is twice continuously differentiable on the parameter domain $\tilde{T} \subset \mathbb{R}^2$. Additionally, on $\tilde{T} \subset \mathbb{R}^2$ the following estimates are satisfied

$$\left|\tilde{H}(x_1, x_2)\right| \leq \tilde{M}\left(x_1^2 + x_2^2\right),$$
$$\left|\nabla\tilde{H}(x_1, x_2)\right| \leq \tilde{M}\sqrt{x_1^2 + x_2^2}.$$

(iii) *The boundary $\partial\Xi$ of Ξ is a continuous and piecewise twice continuously differentiable curve.*

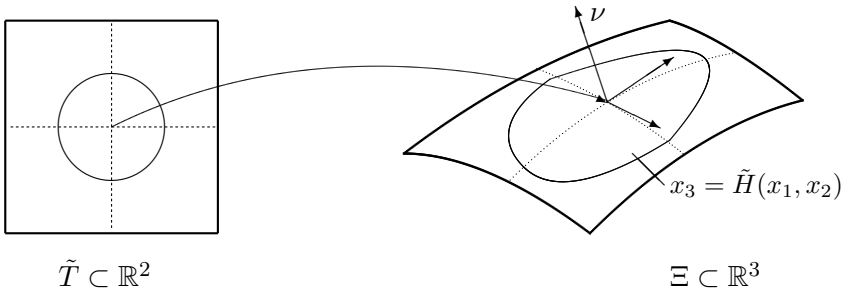

Figure 1.1: Parameterization of regular surface element $\Xi \subset \mathbb{R}^3$

An example of the surface element $\Xi \subset \mathbb{R}^3$ with its parameter space $\tilde{T} \subset \mathbb{R}^2$ is adumbrated in Figure 1.1.

In what follows we consider regions $\mathfrak{G}$ in $\mathbb{R}^3$ with a boundary $\partial\mathfrak{G}$ being not necessary smooth. We use Definition 1.11 specify the boundary $\Sigma = \partial\mathfrak{G}$ of an admissible region $\mathfrak{G}$ as a finite union of regular surface elements Ξ^l, $l = 1, \ldots, n$. An example of a such region $\mathfrak{G}$ is roughly illustrated in Figure 1.2.

Definition 1.12 *Let $\mathfrak{G}$ be a bounded, simply-connected region in $\mathbb{R}^3$. We say that its boundary $\Sigma = \partial\mathfrak{G}$ is* ***regular****, if it satisfies the following properties:*

(i) *Σ can be divided into a finite number of regular surface elements, i.e., $\Sigma = \bigcup_{i=1}^{n} \overline{\Xi^l}$, $\overline{\Xi^l} = \Xi^l \cup \partial\Xi^l$, $l = 1, \ldots, n$, that are pairwise disjoint, except for common boundary points.*

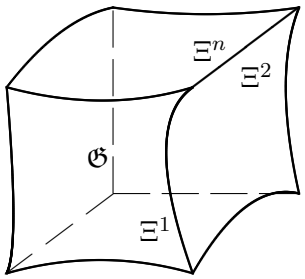

$$\Sigma = \bigcup_{i=1}^{n} \overline{\Xi^l}$$

Figure 1.2: Regular surface Σ of an admissible region $\mathfrak{G} \subset \mathbb{R}^3$

(ii) *For each $x \in \Sigma$ the solid angle $\omega(x)$ satisfies the relation*

$$\sup_{x \in \Sigma} \left| \frac{\omega(x)}{2\pi} - 1 \right| < 1.$$

(iii) *Σ has a continuous directional unit field μ pointing into the outer space Σ^{ext}. The directional unit field μ is twice continuously differentiable on each regular surface element $\Xi^l, l = 1, \ldots, n$, and pointing into the outer space Σ^{ext}, such that there exist constants $M, \delta > 0$ that for each boundary point x $\Omega_\delta^{int}(x) \cap \Sigma$ can be represented in a Cartesian coordinate system ($\epsilon^3 = \mu(x)$) by*

$$x_3 = H(x_1, x_2), \ (x_1, x_2) \in T \subset R^2,$$

where the function H is continuous, piecewise twice continuously differentiable on the parameter domain $T \subset \mathbb{R}^2$. Additionally, on $T \subset \mathbb{R}^2$ the following relations are satisfied

$$|H(x_1, x_2)| \leq M \sqrt{x_1^2 + x_2^2}; \tag{1.77}$$

$$|\nabla H(x_1, x_2)| \leq M. \tag{1.78}$$

(The parameter domain T is decomposed in the neighborhood of edges and corners into a finite number of subdomains, so that the estimate (1.78) *is satisfied in each subdomain.)*

(iv) *The inner space $\mathfrak{G}$ contains the origin.*

The directional unit field μ can be understood as a regularization of the normal field ν, as illustrated in Figure 1.3. In addition, if the regular surface Σ contains no edges and corners, the field μ equals to the field ν.

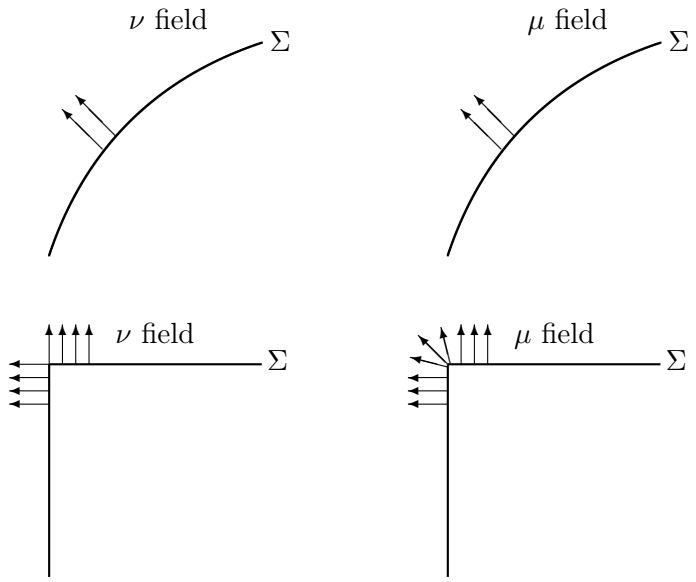

Figure 1.3: The directional unit field μ and the normal unit field ν.

Remark 1.13

(*i*) *As is well known, for each point $x \in \Sigma$, the solid angle $\omega(x)$ can be defined by use of the tangential normal vector*

$$\tau(x) = \lim_{\substack{y \to x \\ y \in \Sigma}} \frac{y - x}{|y - x|}, \tag{1.79}$$

because the set of all $\tau(x)$ defines a cone which intersects a surface $\omega(x)$ out of the unit sphere with the center in x.

(*ii*) *Definition 1.12 $(ii) - (iv)$ guarantees the validity of the inner and outer cone condition for each boundary point (as, for example, considered in [20], [77]).*

(*iii*) *The existence of the directional unit field μ is shown in [78], [79] that is applied for the local surface representation in Definition 1.12 $(iii), (iv)$. The basic concept is the extension theorem according to [49], which guarantees the extension of regular surface elements to a closed regular surface.*

Lemma 1.14 *If $\Sigma = \partial\mathfrak{G}$ is the boundary of a region $\mathfrak{G}$ as defined by Definition 1.12, then there exists a constant $\alpha < 1$, such that*

$$|\mu(x)(x - y)| \leq \alpha\,|x - y|$$

uniformly with respect to $x \in \Sigma$ *and* $y \in \Omega_\delta^{int}(x) \cap \Sigma$, $\Sigma = \partial\mathfrak{G}$.

Proof According to the condition (*iii*) of Definition 1.12, we are able to set x to the origin of a local coordinate system and $\mu(x) = \epsilon^3$, so that

$$|\mu(x)(x-y)| = |H(y_1, y_2)| \leq M\sqrt{y_1^2 + y_2^2}$$

for all $y = y_1\epsilon^1 + y_2\epsilon^2 + H(y_1, y_2)\epsilon^3 \in \Omega_\delta^{int}(x) \cap \Sigma$.

Additionally, we are able to introduce a constant α satisfying the relation

$$\alpha = \sqrt{\frac{M^2}{M^2+1}} < 1. \tag{1.80}$$

Observing the value α satisfying (1.80), we are led to

$$|H(y_1, y_2)| \leq M\sqrt{y_1^2 + y_2^2} = \sqrt{\frac{\alpha^2}{1-\alpha^2}\left(y_1^2 + y_2^2\right)}.$$

Hence, after an obvious manipulation, we obtain

$$\left(1-\alpha^2\right)|H(y_1, y_2)|^2 \leq \alpha^2\left(y_1^2 + y_2^2\right).$$

Altogether this yields

$$|H(y_1, y_2)| \leq \alpha\sqrt{y_1^2 + y_2^2 + H(y_1, y_2)^2} = \alpha\,|x-y|$$

■

Lemma 1.15 *Let* Σ *be a regular surface as introduced by Definition 1.12. Assume that the constant* α *is given as defined by Equation* (1.80)*. Then, for constants* τ, σ *satisfying* $|\sigma| \leq \dfrac{1-\alpha}{4}|\tau| \leq \dfrac{1-\alpha}{5-\alpha}\dfrac{\delta}{2}$, $\tau \neq 0$, *the integral*

$$\int_\Sigma \frac{1}{|x + \tau\mu(x) - (y + \sigma\nu(y))|} d\omega(y) \tag{1.81}$$

exists for all $x \in \Sigma$ *(The integral* (1.81) *has to be understood as the sum of surface integrals over the occurring regular surface elements* Ξ^l, $l = 1, \ldots, n$*).*

Proof Let x be a point of the boundary Σ and δ be given as in Definition 1.12. We split the integral (1.81) into a sum of two integrals in the form

$$\int_{\Sigma\setminus\Omega_\delta^{int}(x)} \frac{d\omega(y)}{|x + \tau\mu(x) - (y + \sigma\nu(y))|} + \int_{\Sigma\cap\Omega_\delta^{int}(x)} \frac{d\omega(y)}{|x + \tau\mu(x) - (y + \sigma\nu(y))|}. \tag{1.82}$$

Our purpose is to estimate each integral of (1.82), separately.

For all $y \in \Sigma \setminus \Omega_\delta^{int}(x)$ it follows by use of triangle inequality that

$$\begin{aligned} |\tau\mu(x) - \sigma\nu(y)| &\leq |\tau||\mu(x)| + |\sigma||\nu(y)| \leq |\tau| + |\sigma| \\ &\leq |\tau| + \frac{1-\alpha}{4}|\tau| = \frac{5-\alpha}{4}|\tau| \leq \frac{\delta}{2}. \end{aligned}$$

From the last inequality, we are able to deduce that

$$\begin{aligned} |x + \tau\mu(x) - (y + \sigma\nu(y))| &\geq ||x-y| - |\tau\mu(x) - \sigma\nu(y)|| \\ &\geq \delta - \frac{\delta}{2} = \frac{\delta}{2} > 0. \end{aligned} \tag{1.83}$$

Now, for all $y \in \Sigma \cap \Omega_\delta^{int}(x)$ we have

$$\begin{aligned} |x + \tau\mu(x) - (y + \sigma\nu(y))|^2 &= |(x-y) + \tau\mu(x) - \sigma\nu(y)|^2 \\ &= (x-y)^2 + \tau^2 + \sigma^2 + [2\tau\mu(x)(x-y)] \\ &\quad - [2\sigma\nu(y)(x-y)] - [2\tau\sigma\mu(x)\nu(y)]\,. \end{aligned} \tag{1.84}$$

In connection with Lemma 1.14 we are able to give estimates for each term on the right side in the squared brackets of Equation (1.84). More concretely,

$$2\,|\tau|\,|\mu(x)(x-y)| \leq 2\alpha\,|\tau|\,|x-y| \leq \alpha\,|\tau|^2 + \alpha\,|x-y|^2\,, \tag{1.85}$$

where the second part of the inequality can be evaluated by virtue of Binomial's rule

$$|\tau|^2 - 2\,|\tau|\,|x-y| + |x-y|^2 = (|\tau| - |x-y|)^2 \geq 0.$$

From the inequality (1.85), we obtain the estimate for the first expression in the squared brackets in Equation (1.84) on the right side

$$2\tau\mu(x)\,(x-y) \geq -\alpha\left(|\tau|^2 + |x-y|^2\right). \tag{1.86}$$

Analogously, according to our assumptions, we find

$$2\,|\sigma|\,|\mu(y)\,(x-y)| \leq \frac{1-\alpha}{4} 2\,|\tau|\,|x-y| \leq \frac{1-\alpha}{4}\left(|\tau|^2 + |x-y|^2\right).$$

The last inequality gives us the estimate for the second expression in the squared brackets in Equation (1.84).

$$-2\sigma\mu(y)\,(x-y) \geq -\frac{1-\alpha}{4}\left(|\tau|^2 + |x-y|^2\right). \tag{1.87}$$

By observing the inequality

$$2\,|\tau|\,|\sigma|\,|\mu(x)\nu(y)| \leq 2\,|\tau|\,\frac{1-\alpha}{4}\,|\tau| = \frac{1-\alpha}{2}\,|\tau|^2\,,$$

we obtain the estimate of the third expression in the squared brackets in Equation (1.84) on the right side

$$-2\tau\sigma\mu(x)\nu(y) \geq -\frac{1-\alpha}{2}\,|\tau|^2\,. \tag{1.88}$$

Collecting (1.86), (1.87), and (1.88) we obtain the estimate of Equation (1.84) and, as a consequence, we arrive at

$$\begin{aligned}|x+\tau\mu(x)-(y+\sigma\nu(y))|^2 &\geq |x-y|^2\left(1-\alpha-\frac{1-\alpha}{4}\right)\\ &+|\tau|^2\left(1-\alpha-\frac{1-\alpha}{4}-\frac{1-\alpha}{2}\right)+|\tau|^2 \geq |\tau|^2\,\frac{1-\alpha}{4} > 0.\end{aligned} \tag{1.89}$$

Summarizing all our results, i.e., Equations (1.83), (1.89), we obtain

$$|x+\tau\mu(x)-(y+\sigma\nu(y))| > 0,\ x,y \in \Sigma$$

and, as a consequence, the integral (1.81) exists for all $x \in \Sigma$ ■

Remark 1.16 *In the case of $\sigma = 0$, Equation* (1.84) *implies the following estimate*

$$|x \pm \tau\mu(x) - y|^2 \geq (1-\alpha)\left(|\tau|^2 + |x-y|^2\right).$$

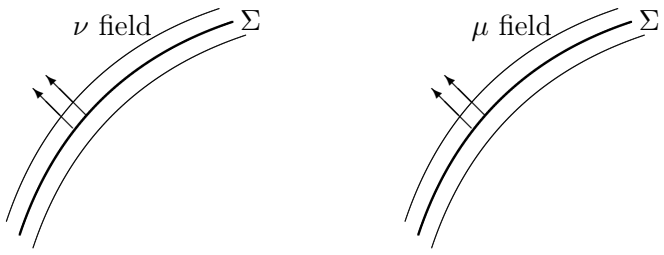

Figure 1.4: The construction of (smoothed) parallel surfaces for a regular surface Σ without edges and corners.

For regular surfaces corresponding to regions $\Sigma = \mathfrak{S}$ in $\mathbb{R}^3$ with smooth boundaries $\partial\mathfrak{S}$, the concept of parallel surfaces as introduced, e.g., in [28],

[31], [48] can be handled appropriately. In this case the parallel surfaces are defined as the set

$$\left\{ x \in \mathbb{R}^3 \middle| \, x = y + \tau\nu(y), y \in \partial\mathfrak{S} \right\}, \tag{1.90}$$

which are exterior to $\partial\mathfrak{S}$ for $\tau > 0$ and interior for $\tau < 0$, as illustrated in Figure 1.4. It is well known from the differential geometry (e.g., [58]) that if $|\tau|$ sufficiently small, then the parallel surfaces to a smooth surface are regular, and the normal to one parallel surface is a normal to the other.

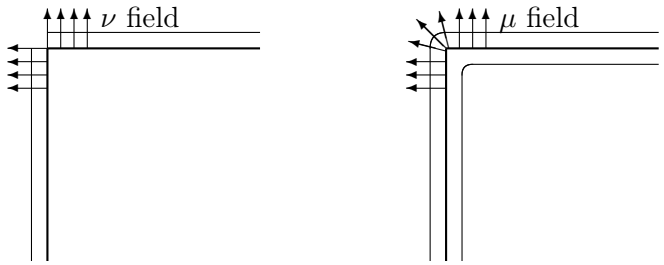

Figure 1.5: The construction of smoothed parallel surfaces for a regular surface Σ with edges and corners.

For a non-smooth surface the concept of parallel surfaces as described above is not applicable, since the surfaces as defined by (1.90) are not necessarily closed. In consequence, for a region $\mathfrak{G}$ in $\mathbb{R}^3$ with a non-smooth boundary $\partial\mathfrak{G}$ we have to find a different approach. As a matter of fact, in order to build a sequence of surfaces converging to $\partial\mathfrak{G}$ from the outer and inner space, we use the advantage of the local representation by application of the directional unit field μ. The sequence of such local 'parallel' surfaces converge to the surface Σ from the outer and inner space (see Figure 1.5).

Definition 1.17 *For a sufficiently small $\tau_0 > 0$ and for all $|\tau| < \tau_0$, and the directional unit field μ from Definition 1.12, the set*

$$\Sigma(\tau) = \left\{ x \in \mathbb{R}^3 \middle| \, x = y + \tau\mu(y), y \in \Sigma \right\}$$

is called a ***smoothed parallel surface*** *which is exterior to Σ for $\tau > 0$ and interior for $\tau < 0$.*

Clearly, if Σ is a smooth boundary (without edges and corners), a smoothed parallel surface is a parallel surface.

Remark 1.18 *Because the directional unit field μ is continuous and piecewise continuously differentiable on each regular surface $\Xi^l, l = 1, \ldots, n$, a smoothed parallel surface $\Sigma(\tau)$ can be understood to satisfy all properties in Definition 1.12. Furthermore, $\Sigma(\tau)$ can be verified to converge to Σ as $|\tau| \to 0$.*

In this respect, a result due to [56] based on [78] and [49] is of particular interest for the later proof of double layer potentials: it uses the fact that the surfaces $\Sigma(\tau)$ converge to Σ for $|\tau| \to 0$ „with bounded relation“. In consequence, the next result become obvious.

Lemma 1.19 *For each regular surface Σ and corresponding smoothed local parallel surfaces $\Sigma(\tau)$ as defined by Definition 1.17, a constant $M > 0$ exists, such that*

$$\int\limits_{\Sigma(\tau)} \left| \frac{\partial}{\partial \nu(y)} \frac{1}{|x-y|} \right| d\omega(y) \leq M,$$

is uniformly satisfied for all $x \in \mathbb{R}^3$ and all $|\tau| < \tau_0$.

Chapter 2

Helmholtz Potential Wavelets

This chapter is the main part of the thesis. It is concerned with the introduction and construction of *Helmholtz potential wavelets*. The preparatory settings are listed in Section 2.1. Then, as an introductory case, we study the Laplace case in Section 2.2. The Laplace concept later on serves as a tool for further consideration. In accordance with the classical approach in potential theory (see, e.g., [47]), we consider limit and jump relations in the Banach space for continuous functions on Σ in uniform metric. Then, following [28], [31], [55], we extend the limit and jump relations to the Hilbert space topology of $\mathcal{L}^2(\Sigma)$. Section 2.3 is devoted to the framework of Helmholtz potential operators for regular surfaces Σ (as defined in Chapter 1). Moreover, it contain the formulation of limit and jump relations for the Helmholtz operator in $\mathcal{L}^2(\Sigma)$. The so constructed kernel functions can be used to regularize singular integral representations of the Helmholtz potential operators. In fact, these kernel functions are understood as scaling functions, where the scale parameter is determined by the 'distance' τ of the smoothed parallel surface $\Sigma(\tau)$ to surface Σ. The scaling functions enable us to construct wavelet functions in usual way (see, e.g., [52]) in Section 2.4. Scale continuous and scale discretized reconstruction formulas can be developed in straightforward manner. Furthermore, we show that the expansion of the scaling and wavelet functions provides a multiscale analysis of the Hilbert space $\mathcal{L}^2(\Sigma)$. Finally, an efficient and economical multiscale implementation in form of a *tree algorithm* (pyramid scheme) for the fast wavelet transform (FWT) by means of Helmholtz wavelets is presented in Section 2.5.

2.1 Preliminaries

In this section we recapitulate some settings and structures of function spaces, scalar products and norms that are used throughout this chapter.

Let Σ be a regular surface as defined by Definition 1.12. $\mathcal{C}(\Sigma)$ denotes the class of all complex continuous functions on Σ. As usual, the supremum norm on Σ is given by

$$\|F\|_{\mathcal{C}(\Sigma)} = \sup_{x\in\Sigma} |F(x)|\,,\ F \in \mathcal{C}(\Sigma).$$

Equipped with the norm $\|.\|_{\mathcal{C}(\Sigma)}$ the space $\left(\mathcal{C}(\Sigma), \|.\|_{\mathcal{C}(\Sigma)}\right)$ is a Banach space and with scalar product defined for all functions $F, G \in \mathcal{C}(\Sigma)$ by

$$(F,G)_{\mathcal{L}^2(\Sigma)} = \int_\Sigma F(x)\overline{G(x)}d\omega(x), \tag{2.1}$$

$\left(\mathcal{C}(\Sigma), (.,.)_{\mathcal{L}^2(\Sigma)}\right)$ is a pre-Hilbert space. The scalar product (2.1) implies the norm

$$\|F\|_{\mathcal{L}^2(\Sigma)} = \left((F,F)_{\mathcal{L}^2(\Sigma)}\right)^{1/2}. \tag{2.2}$$

As usual, we let

$$\mathcal{L}^2(\Sigma) = \left\{ f | f : \Sigma \to \mathbb{R} \text{ measurable}, \int_\Sigma |f(x)|^2 d\omega(x) < \infty \right\}$$

to be the *space of (Lebesgue) square-integrable functions* on the regular surface Σ. With respect to the scalar product (2.1), $\mathcal{L}^2(\Sigma)$ is a Hilbert space, and a Banach space according to the norm (2.2). Moreover, $\mathcal{L}^2(\Sigma)$ is the completion of $\mathcal{C}(\Sigma)$ with respect to the norm $\|\cdot\|_{\mathcal{L}^2(\Sigma)}$:

$$\overline{\mathcal{C}(\Sigma)}^{\|\cdot\|_{\mathcal{L}^2(\Sigma)}} = \mathcal{L}^2(\Sigma). \tag{2.3}$$

By $\tilde{\mathcal{C}}^{(1)}(\Sigma)$ we denote the space of all continuously differentiable functions F that map Σ into $\mathbb{R}$ and vanish with all its first derivatives at all edges and corners on Σ. As is well known, [72], [79] the space $\tilde{\mathcal{C}}^{(1)}(\Sigma)$ with respect to the supremum norm is a normed space, i.e., $\left(\tilde{\mathcal{C}}^{(1)}, \|.\|_{\mathcal{C}(\Sigma)}\right)$, and it is a dense subspace in $\mathcal{L}^2(\Sigma)$ corresponding to the scalar product (2.1), i.e., $\left(\tilde{\mathcal{C}}^{(1)}, (.,.)_{\mathcal{L}^2(\Sigma)}\right)$.

By $\hat{\mathcal{C}}(\Sigma)$ we denote the space of all piecewise differentiable and bounded functions F on Σ that map Σ into $\mathbb{R}$.

As before, μ denotes the directional unit field defined on Σ. Canonically, the directional derivative of F at point $x \in \Sigma$ in the direction $\mu(x)$ is given canonically by

$$\frac{\partial}{\partial \mu} F(x) = \lim_{\substack{\tau \to 0 \\ \tau \neq 0}} \frac{F(x + \tau\mu(x)) - F(x)}{\tau}. \tag{2.4}$$

For later use we introduce the identity operator $\mathcal{I} : \mathcal{C}(\Sigma) \to \mathcal{C}(\Sigma)$

$$\mathcal{I}F(x) = F(x), \ x \in \Sigma$$

and the operator $\tilde{\mathcal{I}} : \tilde{\mathcal{C}}^{(1)}(\Sigma) \to \mathcal{C}(\Sigma)$ defined by

$$\tilde{\mathcal{I}}F(x) = \begin{cases} 0, & \text{at edges and corners,} \\ (\mu(x)\nu(x))\, F(x), & \text{outside edges and corners.} \end{cases} \tag{2.5}$$

By convention, the operator norm will be designated with the same symbol as the norm of the corresponding reference space.

2.2 Limit and Jump Relation for the Laplace Operator

The construction of scaling and wavelet functions (cf. [31]) is based on the formulation of limit and jump relations. Our purpose is to formulate these relations first in the framework of the space $\mathcal{C}(\Sigma)$ for Σ being a regular surface. Later on we go over to the $\mathcal{L}^2$-topology.

We start with the study of the limit and jump relations for the Laplace operator Δ.

Definition 2.1 *Let $\tau, \sigma \in \mathbb{R}$, $\tau \neq 0$, satisfy the assumptions known from Lemma 1.15 and Definition 1.17, i.e.,*

$$|\sigma| \leq \frac{1-\alpha}{4}|\tau| \leq \frac{1-\alpha}{5-\alpha}\frac{\delta}{2}, \ |\tau| \leq \tau_0.$$

Then, for a regular surface Σ as defined by Definition 1.12, the operator $Q^{\Sigma}(\tau, \sigma) : \mathcal{L}^2(\Sigma) \to \mathcal{C}(\Sigma)$ represented by

$$Q^{\Sigma}(\tau, \sigma)F(x) = \int_{\Sigma} F(y) \frac{1}{|x + \tau\mu(x) - (y + \sigma\nu(y))|} d\omega(y), \ F \in \mathcal{L}^2(\Sigma),$$

*is called a **Laplace potential operator** on Σ.*

In the sense of this definition we are able to introduce the Laplace potential operators for a single and a double layer on the regular surface Σ.

The *Laplace potential operator of a single layer* on Σ for values on the smoothed parallel surface $\Sigma(\tau)$: $Q^{\Sigma}(\tau,0) : \mathcal{L}^2(\Sigma) \to \mathcal{C}(\Sigma)$ is given by

$$Q^{\Sigma}(\tau,0)F(x) = \int_{\Sigma} F(y)\frac{1}{|x+\tau\mu(x)-y|}d\omega(y). \tag{2.6}$$

Analogously, we can introduce the *Laplace potential operator of a double layer* on Σ for values on $\Sigma(\tau)$: $Q^{\Sigma}_{|2}(\tau,0) : \mathcal{L}^2(\Sigma) \to \mathcal{C}(\Sigma)$ by

$$\begin{aligned} Q^{\Sigma}_{|2}(\tau,0)F(x) &= \frac{\partial}{\partial\sigma}Q^{\Sigma}(\tau,\sigma)F(x)\Big|_{\sigma=0} \\ &= \int_{\Sigma} F(y)\frac{\nu(y)(x+\tau\mu(x)-y)}{|x+\tau\mu(x)-y|^3}d\omega(y). \end{aligned} \tag{2.7}$$

In the same manner, we are able to introduce the *Laplace potential operator of the directional derivative of a single layer potential* for values on $\Sigma(\tau)$:

$$\begin{aligned} Q^{\Sigma}_{|1}(\tau,0)F(x) &= \frac{\partial}{\partial\tau}Q^{\Sigma}(\tau,\Sigma)F(x)\Big|_{\sigma=0} \\ &= -\int_{\Sigma} F(y)\frac{\mu(x)(x+\tau\mu(x)-y)}{|x+\tau\mu(x)-y|^3}d\omega(y). \end{aligned} \tag{2.8}$$

If $\tau = \sigma = 0$, the kernels of the formally defined potentials have weak singularities. The associated potential operators are given by the weakly singular integral expressions

$$Q^{\Sigma}(0,0)F(x) = \int_{\Sigma} F(y)\frac{1}{|x-y|}d\omega(y), \tag{2.9}$$

$$Q^{\Sigma}_{|2}(0,0)F(x) = \int_{\Sigma} F(y)\frac{\partial}{\partial\nu(y)}\frac{1}{|x-y|}d\omega(y), \tag{2.10}$$

$$Q^{\Sigma}_{|1}(0,0)F(x) = \frac{\partial}{\partial\mu(x)}\int_{\Sigma} F(y)\frac{1}{|x-y|}d\omega(y). \tag{2.11}$$

Remark 2.2 *Let F be a continuous function on a regular surface Σ. Then the functions* (2.9)*,* (2.10)*, and* (2.11) *are infinitely often differentiable and satisfy the Laplace equation in Σ^{int} and Σ^{ext}. In addition, these functions are regular at infinity.*

For $F \in \mathcal{C}(\Sigma)$, these function can be continued continuously to the surface Σ, but the limits depend from which (smoothed) parallel surface (inner or outer) the point x tend to Σ. On the other hand, the functions also are defined on the surface Σ, i.e., all integrals (2.9), (2.10), *and* (2.11) *exist for $x \in \Sigma$. However, it is known (see, e.g., [47], [56]) the integrals do not coincide, in general, with the inner or outer limits of the potentials. This observation, in fact, is the reason for the introduction of potential wavelets as discussed in our approach.*

In order to give concise formulations of the limit formulas and jump relations in the Hilbert space $\mathcal{L}^2(\Sigma)$, the adjoint operators should be introduced.

Definition 2.3 *The operator $Q^{\Sigma}(\tau,\sigma)^* : \mathcal{L}^2(\Sigma) \to \mathcal{C}(\Sigma)$ satisfying*

$$\big(F, Q^{\Sigma}(\tau,\sigma)G\big)_{\mathcal{L}^2(\Sigma)} = \big(Q^{\Sigma}(\tau,\sigma)^* F, G\big)_{\mathcal{L}^2(\Sigma)},$$

*for all functions $F, G \in \mathcal{L}^2(\Sigma)$ is called the **adjoint Laplace operator** of $Q^{\Sigma}(\tau,\sigma)$ with respect to the scalar product $(\cdot,\cdot)_{\mathcal{L}^2(\Sigma)}$.*

According to Fubini's theorem we are able to interchange the order of integration

$$\begin{aligned}
\big(F, Q^{\Sigma}(\tau,\sigma)G\big)_{\mathcal{L}^2(\Sigma)} &= \int_{\Sigma} F(x) \int_{\Sigma} G(y) \frac{1}{|x+\tau\mu(x) - (y+\sigma\nu(y))|} d\omega(y) d\omega(x) \\
&= \int_{\Sigma} G(y) \int_{\Sigma} F(x) \frac{1}{|x+\tau\mu(x) - (y+\sigma\nu(y))|} d\omega(x) d\omega(y) \\
&= \big(Q^{\Sigma}(\tau,\sigma)^* F, G\big)_{\mathcal{L}^2(\Sigma)}.
\end{aligned}$$

By comparison we thus have the *adjoint operator $Q^{\Sigma}(\tau,0)^*$ of the Laplace potential operator $Q^{\Sigma}(\tau,0)$* reads

$$\begin{aligned}
Q^{\Sigma}(\tau,0)^* F(x) &= Q^{\Sigma}(\tau,\sigma)^* F(x)\big|_{\Sigma=0} \\
&= \int_{\Sigma} F(y) \frac{1}{|x-y-\tau\mu(y)|} d\omega(y).
\end{aligned}$$

In an analogous way, we obtain the *adjoint operator of the directional derivative of a single layer*

$$Q^{\Sigma}_{|1}(\tau,0)^* F(x) = \int_{\Sigma} F(y) \frac{\mu(y)(x-y-\tau\mu(y))}{|x-y-\tau\mu(y)|^3} d\omega(y),$$

and the *adjoint operator of the Laplace potential operator of a double layer*

$$Q^{\Sigma}_{|2}(\tau,0)^* F(x) = -\int\limits_{\Sigma} F(y)\frac{\nu(x)(x-y-\tau\mu(y))}{|x-y-\tau\mu(y)|^3}d\omega(y),$$

where $\nu(x)$ may be replaced by $\mu(x)$ in all edges and corners x. This substitution has no influence on Lebesgue integrals, because the set of all edges and corners has the surface measure zero.

If we tighten the smoothed parallel surfaces $\Sigma(\tau)$ and $\Sigma(-\tau)$ to the regular surface Σ, we obtain the limit and jump relations for the Laplace potential operators. In doing so, we essentially follow [72].

As first result we mention two-sided limit relations for the single layer operator.

Lemma 2.4 *Let Σ be a regular surface as defined by Definition 1.12. Then*

$$\lim_{\substack{\tau\to 0\\ \tau>0}} \left\| \left(Q^{\Sigma}(\tau,0) - Q^{\Sigma}(-\tau,0)\right) \middle| \, \mathcal{C}(\Sigma)\right\|_{\mathcal{C}(\Sigma)} = 0.$$

Proof For $F \in \mathcal{C}(\Sigma)$ and the number δ, as defined by Definition 1.12, and a sufficiently small number $\epsilon > 0$ we get

$$\begin{aligned}
&\left|Q^{\Sigma}(\tau,0)F - Q^{\Sigma}(-\tau,0)F\right| \\
&\qquad = \left|\int\limits_{\Sigma} F(y)\left(\frac{1}{|x+\tau\mu(x)-y|} - \frac{1}{|x-\tau\mu(x)-y|}\right)d\omega(y)\right| \\
&\qquad \le \|F\|_{\mathcal{C}(\Sigma)}\left(\int\limits_{\Sigma\setminus\Omega^{int}_{\delta}(x)} \left|\frac{1}{|x+\tau\mu(x)-y|} - \frac{1}{|x-\tau\mu(x)-y|}\right| d\omega(y)\right. \\
&\qquad\qquad \left. + \int\limits_{\Sigma\cap\Omega^{int}_{\delta}(x)} \left|\frac{1}{|x+\tau\mu(x)-y|} - \frac{1}{|x-\tau\mu(x)-y|}\right| d\omega(y)\right).
\end{aligned}$$

For $y \in \Sigma \setminus \Omega^{int}_{\delta}(x)$ and $|\tau| < \frac{\delta}{2}$, we have the estimate

$$|x \pm \tau\mu(x) - y| \ge ||x-y| - |\tau|| \ge \frac{\delta}{2}.$$

Observing the last estimate we find

$$\begin{aligned}
&\left|\frac{1}{|x+\tau\mu(x)-y|} - \frac{1}{|x-\tau\mu(x)-y|}\right| \\
&\qquad = \frac{||x-\tau\mu(x)-y| - |x+\tau\mu(x)-y||}{|x+\tau\mu(x)-y||x-\tau\mu(x)-y|} \le \frac{2|\tau|}{\left(\frac{\delta}{2}\right)^2} = \frac{8|\tau|}{\delta^2}.
\end{aligned}$$

For sufficiently small $|\tau|$, it therefore follows that

$$\int\limits_{\Sigma\setminus\Omega_\delta^{int}(x)} \left| \frac{1}{|x+\tau\mu(x)-y|} - \frac{1}{|x-\tau\mu(x)-y|} \right| d\omega(y) \leq \frac{8|\tau|}{\delta^2}\|\Sigma\| < \frac{\epsilon}{2}, \quad (2.12)$$

where, as always, $\|\Sigma\|$ denotes the surface area of Σ.

Next, using the local surface construction of a regular surface and the estimate provided by Remark 1.16, we obtain

$$\int\limits_{\Sigma\cap\Omega_\delta^{int}(x)} \left| \frac{1}{|x+\tau\mu(x)-y|} - \frac{1}{|x-\tau\mu(x)-y|} \right| d\omega(y) \leq \int\limits_{\Sigma\cap\Omega_\delta^{int}(x)} \frac{2|\tau|}{(1-\alpha)\left(|x-y|^2+\tau^2\right)} d\omega(y). \quad (2.13)$$

$\Sigma\cap\Omega_\delta^{int}(x)$ consists of $\tilde{n}$ regular surface elements Ξ^l, $l=1,\ldots,\tilde{n}$. Converting the integral on the right side in Equation (2.13) to the parameter domain T and after that to the polar coordinates, we find

$$\begin{aligned}
\int\limits_{\Sigma\cap\Omega_\delta^{int}(x)} \frac{2|\tau|d\omega(y)}{(1-\alpha)\left(|x-y|^2+\tau^2\right)} &\leq \int\limits_{\Omega_\delta^{int}} \frac{2|\tau|\sqrt{1+H_{|1}^2+H_{|2}^2}}{(1-\alpha)\left(|y|^2+\tau^2\right)} dy_1 dy_2 \\
&\leq 2\left(1+M\right)|\tau|\frac{1}{(1-\alpha)} \int\limits_{\Omega_\delta^{int}} \frac{dy_1 dy_2}{|y|^2+\tau^2} \\
&\leq \frac{2\left(1+M\right)}{1-\alpha}|\tau| \int\limits_0^{2\pi}\int\limits_0^{\delta} \frac{r dr d\phi}{r^2+\tau^2} \\
&\leq \frac{2\left(1+M\right)\pi}{1-\alpha}|\tau| \ln\left\{\frac{\delta^2+\tau^2}{\tau^2}\right\}.
\end{aligned}$$

By virtue of l'Hôpital's rule, we get

$$\lim_{\substack{\tau\to 0\\ \tau>0}} \frac{2\left(1+M\right)\pi}{1-\alpha}|\tau| \ln\left\{\frac{\delta^2+\tau^2}{\tau^2}\right\} = 0.$$

Thus we have for all sufficiently small $|\tau|$ the estimate:

$$\int\limits_{\Sigma\cap\Omega_\delta^{int}(x)} \left| \frac{1}{|x+\tau\mu(x)-y|} - \frac{1}{|x-\tau\mu(x)-y|} \right| d\omega(y) \leq \frac{2\left(1+M\right)\pi}{1-\alpha}|\tau| \ln\left\{\frac{\delta^2+\tau^2}{\tau^2}\right\} \leq \frac{\epsilon}{2}. \quad (2.14)$$

Summarizing the estimates (2.12), (2.14) for all sufficiently small τ we obtain

$$\left| \int_\Sigma F(y) \left(\frac{1}{|x+\tau\mu(x)-y|} - \frac{1}{|x-\tau\mu(x)-y|} \right) d\omega(y) \right| \leq \|F\|_{\mathcal{C}(\Sigma)} \epsilon,$$

as required. ■

Next we come to the adjoint operators.

Lemma 2.5 *For a regular surface* Σ

$$\lim_{\substack{\tau\to 0 \\ \tau>0}} \left\| \left(Q^\Sigma(\tau,0) - Q^\Sigma(-\tau,0) \right)^* \Big| \mathcal{C}(\Sigma) \right\|_{\mathcal{C}(\Sigma)} = 0.$$

Proof Our goal is to prove

$$\begin{aligned} &\lim_{\substack{\tau\to 0 \\ \tau>0}} \left\| \left(Q^\Sigma(\tau,0) - Q^\Sigma(-\tau,0) \right)^* \Big| \mathcal{C}(\Sigma) \right\|_{\mathcal{C}(\Sigma)} \\ &\quad = \lim_{\substack{\tau\to 0 \\ \tau>0}} \sup_{F\in\mathcal{C}(\Sigma)} \sup_{x\in\Sigma} \left| F(y) \left(\frac{1}{y+\tau\mu(y)-x} - \frac{1}{y-\tau\mu(y)-x} \right) d\omega(y) \right| = 0. \end{aligned}$$

Let $x \in \Sigma$, $F \in \mathcal{C}(\Sigma)$. For the constant δ as specified by Definition 1.12, we choose $\delta_0 < \delta$. Then, for $y^1, y^2 \in \Sigma$ satisfying $|y^1 - y^2| < \delta_0$, because of the continuity of μ we have

$$|\mu(y^1) - \mu(y^2)| \leq \frac{1-\alpha}{2}, \tag{2.15}$$

where α is the constant known from Lemma 1.14. Moreover, we have

$$\begin{aligned} &\left| \int_\Sigma F(y) \left(\frac{1}{|x+\tau\mu(x)-y|} - \frac{1}{|y+\tau\mu(y)-x|} \right) d\omega(y) \right| \\ &\quad \leq \|F\|_{\mathcal{C}(\Sigma)} \left(\int_{\Sigma\setminus\Omega^{int}_{\delta_0}(x)} \left| \frac{1}{|x+\tau\mu(x)-y|} - \frac{1}{|y+\tau\mu(y)-x|} \right| d\omega(y) \right. \\ &\qquad \left. + \int_{\Sigma\cap\Omega^{int}_{\delta_0}(x)} \left| \frac{1}{|x+\tau\mu(x)-y|} - \frac{1}{|y+\tau\mu(y)-x|} \right| d\omega(y) \right). \end{aligned}$$

With the assumption that $|\tau| < \frac{\delta_0}{2}$, we obtain

$$|x \pm \tau\mu(x) - y| \geq ||x-y| - |\tau|| > \frac{\delta_0}{2}.$$

According to the last inequality, we immediately obtain (analogously to Lemma 2.4) the estimate

$$\int\limits_{\Sigma\setminus\Omega^{int}_{\delta_0}(x)} \left|\frac{1}{|x+\tau\mu(x)-y|}-\frac{1}{|y+\tau\mu(y)-x|}\right| d\omega(y) \leq \frac{8|\tau|}{\delta_0^2}\|\Sigma\|.$$

Next we study the case $y \in \Sigma \cap \Omega^{int}_{\delta_0}(x)$:

$$\begin{aligned}\left|\frac{1}{|x+\tau\mu(x)-y|}-\frac{1}{|y+\tau\mu(y)-x|}\right| &= \frac{||y+\tau\mu(y)-x|-|x+\tau\mu(x)-y||}{|x+\tau\mu(x)-y||y+\tau\mu(y)-x|} \\ &\leq \frac{2|\tau|}{|x+\tau\mu(x)-y||y+\tau\mu(y)-x|}. \quad (2.16)\end{aligned}$$

The denominator can be further estimated as follows

$$\begin{aligned}|x+\tau\mu(x)-y|\,|y+\tau\mu(y)-x| &= |(x+\tau\mu(x)-y)\,(y+\tau\mu(y)-x)| \\ &= \left||y-x|^2+\tau^2-\tau(\mu(x)-\mu(y))(y-x)\right| \\ &\geq |y-x|^2+\tau^2-|\tau||\mu(x)-\mu(y)||y-x|. \quad (2.17)\end{aligned}$$

With respect to Equation (2.15), we can further estimate the term $|\tau||\mu(x)-\mu(y)||y-x|$ in the last inequality

$$\begin{aligned}|\tau||\mu(x)-\mu(y)||y-x| &\leq \frac{1-\alpha}{2}|\tau||y-x| \\ &\leq \frac{1+\alpha}{2}|\tau||y-x| \\ &\leq \frac{1+\alpha}{2}\left(|y-x|^2+\tau^2\right) \quad (2.18)\end{aligned}$$

In response to (2.16) and by use of (2.17), (2.18) we obtain

$$\begin{aligned}&\int\limits_{\Sigma\cap\Omega^{int}_{\delta_0}(x)} \left|\frac{1}{|x+\tau\mu(x)-y|}-\frac{1}{|y+\tau\mu(y)-x|}\right| d\omega(y) \\ &\qquad \leq \int\limits_{\Sigma\cap\Omega^{int}_{\delta_0}(x)} \frac{2|\tau|d\omega(y)}{|x+\tau\mu(x)-y||y+\tau\mu(y)-x|} \\ &\qquad\qquad \leq \int\limits_{\Sigma\cap\Omega^{int}_{\delta_0}(x)} \frac{2|\tau|d\omega(y)}{(1-\alpha)\left(|y-x|^2+\tau^2\right)}. \quad (2.19)\end{aligned}$$

The same manipulations as in Lemma 2.4 imply

$$\lim_{\substack{\tau\to 0\\ \tau>0}} \frac{2}{1-\alpha}|\tau| \int\limits_{\Sigma\cap\Omega^{int}_{\delta_0}(x)} \frac{d\omega(y)}{|y-x|^2+\tau^2} = 0,$$

which is already proven in Lemma 2.4. ■

Now we deal with one-sided limit relation for the single layer operator.

Lemma 2.6 *For a regular surface* Σ

$$\lim_{\substack{\tau\to 0\\ \tau>0}} \left\| \left(Q^{\Sigma}(\pm\tau,0) - Q^{\Sigma}(0,0)\right) \middle| \mathcal{C}(\Sigma)\right\|_{\mathcal{C}(\Sigma)} = 0.$$

Proof For $F \in \mathcal{C}(\Sigma)$ and the number δ, as defined by Definition 1.12, and a sufficiently small number $\epsilon > 0$, we have:

$$\begin{aligned}\left| \int\limits_{\Sigma} F(y) \left(\frac{1}{|x\pm\tau\mu(x)-y|} - \frac{1}{|x-y|} \right) \right| \\ = \|F\|_{\mathcal{C}(\Sigma)} \left(\int\limits_{\Sigma\setminus\Omega^{int}_{\delta}(x)} \left| \frac{1}{|x\pm\tau\mu(x)-y|} - \frac{1}{|x-y|} \right| d\omega(y) \right. \\ \left. + \int\limits_{\Sigma\cap\Omega^{int}_{\delta}(x)} \left| \frac{1}{|x\pm\tau\mu(x)-y|} - \frac{1}{|x-y|} \right| d\omega(y) \right).\end{aligned}$$

If $y \in \Sigma \setminus \Omega^{int}_{\delta}(x)$ and $\tau < \frac{\delta}{2}$, we are able to write

$$\begin{aligned}|x-y| &\geq \delta; \\ |x\pm\tau\mu(x)-y| &\geq ||x-y|-|\tau|| \geq \frac{\delta}{2}.\end{aligned}$$

The last relation implies

$$\left| \frac{1}{|x\pm\tau\mu(x)-y|} - \frac{1}{|x-y|} \right| = \left| \frac{|x-y|-|x\pm\tau\mu(x)-y|}{|x\pm\tau\mu(x)-y||x-y|} \right| \leq \frac{2|\tau|}{\delta^2}.$$

For a sufficiently small τ, we have

$$\int\limits_{\Sigma\setminus\Omega^{int}_{\delta}(x)} \left| \frac{1}{|x\pm\tau\mu(x)-y|} - \frac{1}{|x-y|} \right| d\omega(y) \leq \frac{2|\tau|}{\delta^2}\|\Sigma\| < \frac{\epsilon}{2},$$

where $\|\Sigma\|$ denotes as before the surface area of Σ.

Next we consider the case $y \in \Sigma \cap \Omega_\delta^{int}(x)$. We study

$$|x \pm \tau\mu(x) - y|\,|x - y| = \left|(x-y)^2 \pm \tau\mu(x)(x-y)\right|.$$

According to Equation (1.86), the last expression can be estimated as follows

$$\begin{aligned}\left|(x-y)^2 \pm \tau\mu(x)(x-y)\right| &\geq |x-y|^2 - |\tau||\mu(x)(x-y)| \\ &\geq |x-y|^2 - \frac{\alpha}{2}\left(|x-y|^2 + \tau^2\right) \\ &= \frac{2-\alpha}{2}|x-y|^2 - \frac{\alpha}{2}\tau^2.\end{aligned}$$

Consequently, using the same manipulations as in Lemma 2.4, we obtain

$$\begin{aligned}&\int\limits_{\Sigma\cap\Omega_\delta^{int}(x)} \left|\frac{1}{|x \pm \tau\mu(x) - y|} - \frac{1}{|x-y|}\right| d\omega(y) \\ &\qquad \leq \frac{2}{2-\alpha} \int\limits_{\Sigma\cap\Omega_\delta^{int}(x)} \frac{|\tau|}{|x-y|^2 - \frac{\alpha}{2-\alpha}\tau^2} d\omega(y) \\ &\qquad \leq \frac{2}{2-\alpha} \int\limits_{\Omega_\delta^{int}} \frac{|\tau|\sqrt{1 + H_{|1}^2 + H_{|2}^2}}{|y|^2 - \frac{\alpha}{2-\alpha}\tau^2} dy_1 dy_2 \\ &\qquad \leq (1+M)\frac{2|\tau|}{2-\alpha} \int\limits_0^{2\pi}\int\limits_0^{\delta} \frac{r\,dr\,d\phi}{r^2 - \frac{\alpha}{2-\alpha}\tau^2} \\ &\qquad = (1+M)\frac{2|\tau|\pi}{2-\alpha} \ln\left(\frac{(2-\alpha)\delta^2}{\alpha\tau^2} - 1\right),\end{aligned}$$

where H is as defined by Definition 1.12.

According to l'Hôpital's rule,

$$\lim_{\substack{\tau\to 0 \\ \tau>0}} (1+M)\frac{2|\tau|\pi}{2-\alpha} \ln\left(\frac{(2-\alpha)\delta^2}{\alpha\tau^2} - 1\right) = 0.$$

So that for all sufficiently small $|\tau|$ we get the estimate:

$$\begin{aligned}&\int\limits_{\Sigma\cap\Omega_\delta^{int}(x)} \left|\frac{1}{|x \pm \tau\mu(x) - y|} - \frac{1}{|x-y|}\right| d\omega(y) \\ &\qquad \leq (1+M)\frac{2|\tau|\pi}{2-\alpha} \ln\left(\frac{(2-\alpha)\delta^2}{\alpha\tau^2} - 1\right) \leq \frac{\epsilon}{2}.\end{aligned}$$

Finally, we obtain for all sufficiently small $|\tau|$

$$\int_{\Sigma} \left| \frac{1}{|x \pm \tau\mu(x) - y|} - \frac{1}{|x-y|} \right| d\omega(y) \leq \|F\|_{\mathcal{C}(\Sigma)} \epsilon,$$

as required. ■

It should be remarked that, according to Definition 1.8, the integral

$$\int_{\Sigma} F(y) \frac{\partial}{\partial \nu(y)} \frac{1}{|x-y|} d\omega(y)$$

exists for all continuous functions F on Σ and all $x \in \mathbb{R}^3$, so that the definition $Q_{|2}^{\Sigma}(0,0) : \mathcal{C}(\Sigma) \to \hat{\mathcal{C}}(\Sigma)$ makes sense, where $Q_{|2}^{\Sigma}(0,0)F$ is given by

$$Q_{|2}^{\Sigma}(0,0)F(x) = \int_{\Sigma} F(y) \frac{\partial}{\partial \nu(y)} \frac{1}{|x-y|} d\omega(y)$$

(see (2.10)).

The following lemma presents a one-sided limit relation for the double layer operator.

Lemma 2.7 *For a regular surface Σ and all $F \in \mathcal{C}(\Sigma)$*

$$(i) \quad \lim_{\substack{\tau \to 0 \\ \tau > 0}} \left\| Q_{|2}^{\Sigma}(\tau,0)F - Q_{|2}^{\Sigma}(0,0)F - \omega F \right\|_{\mathcal{C}(\Sigma)} = 0.$$

$$(ii) \quad \lim_{\substack{\tau \to 0 \\ \tau > 0}} \left\| Q_{|2}^{\Sigma}(-\tau,0)F - Q_{|2}^{\Sigma}(0,0)F - (4\pi - \omega) F \right\|_{\mathcal{C}(\Sigma)} = 0.$$

Proof To (i): Let $F \in \mathcal{C}(\Sigma)$, $x \in \Sigma$, $\epsilon > 0$, $0 < \tau < \tau_0$ be adapted. For the number δ as defined by Definition 1.12 we choose a number δ_0 satisfying

$0 < \delta_0 < \delta$. Then, we have

$$
\begin{aligned}
\left| Q^{\Sigma}_{|2}(\tau,0)F - Q^{\Sigma}_{|2}(0,0)F - \omega F \right| &= \left| \int_{\Sigma} F(y) \frac{\partial}{\partial \nu(y)} \frac{1}{|x+\tau\mu(x)-y|} d\omega(y) \right. \\
&\qquad \left. - \int_{\Sigma} F(y) \frac{\partial}{\partial \nu(y)} \frac{1}{|x-y|} d\omega(y) - \omega(x)F(x) \right| \\
&= \left| \int_{\Sigma} F(y) \frac{\partial}{\partial \nu(y)} \frac{1}{|x+\tau\mu(x)-y|} d\omega(y) - \int_{\Sigma} F(y) \frac{\partial}{\partial \nu(y)} \frac{1}{|x-y|} d\omega(y) \right. \\
&\qquad \left. - F(x) \int_{\Sigma} \frac{\partial}{\partial \nu(y)} \frac{1}{|x-y|} d\omega(y) \right| \\
&\leq \int_{\Sigma \cap \Omega^{int}_{\delta_0}(x)} |F(y)-F(x)| \left| \frac{\partial}{\partial \nu(y)} \frac{1}{|x+\tau\mu(x)-y|} \right| d\omega(y) \\
&\qquad + |F(x)| \left| \int_{\Sigma} \frac{\partial}{\partial \nu(y)} \frac{1}{|x+\tau\mu(x)-y|} d\omega(y) \right| \\
&\quad + \left| \int_{\Sigma \setminus \Omega^{int}_{\delta_0}(x)} F(x) \left(\frac{\partial}{\partial \nu(y)} \frac{1}{|x-y|} - \frac{\partial}{\partial \nu(y)} \frac{1}{|x+\tau\mu(x)-y|} \right) d\omega(y) \right| \\
&\qquad + \int_{\Sigma \cap \Omega^{int}_{\delta_0}(x)} |F(x)-F(y)| \left| \frac{\partial}{\partial \nu(y)} \frac{1}{|x-y|} \right| d\omega(y) \\
&\quad + \left| \int_{\Sigma \setminus \Omega^{int}_{\delta_0}(x)} F(y) \left(\frac{\partial}{\partial \nu(y)} \frac{1}{|x+\tau\mu(x)-y|} - \frac{\partial}{\partial \nu(y)} \frac{1}{|x-y|} \right) d\omega(y) \right| \\
&\leq \ell_F(\delta_0) \int_{\Sigma \cap \Omega^{int}_{\delta_0}(x)} \left| \frac{\partial}{\partial \nu(y)} \frac{1}{|x+\tau\mu(x)-y|} \right| d\omega(y) + |F(x)|\, 0 \\
&\qquad + C\|F\|_{\mathcal{C}(\Sigma)} \|\Sigma\| \frac{\tau}{\delta_0^3} + \ell_F(\delta_0) \int_{\Sigma \cap \Omega^{int}_{\delta_0}(x)} \left| \frac{\partial}{\partial \nu(y)} \frac{1}{|x-y|} \right| d\omega(y).
\end{aligned}
$$

The second integral is bounded according to Lemma 1.19 for a sufficiently small δ_0. And because $(x + \tau\mu(x)) \in \Sigma^{ext}$, we have for the first integral with

respect to Definition 1.8

$$\int_{\Sigma} \frac{\partial}{\partial \nu(y)} \frac{1}{|x+\tau\mu(x)-y|} d\omega(y) = 0.$$

If we assume that $\delta_0 = \tau^{\frac{1}{4}}$, we immediately obtain the proof for the case (i).

To (ii): We use the same splitting as in case (i). The proof is obtained with respect to Definition 1.8 because of $(x-\tau\mu(x)) \in \Sigma^{int}$

$$\int_{\Sigma} \frac{\partial}{\partial \nu(y)} \frac{1}{|x+\tau\mu(x)-y|} d\omega(y) = -4\pi.$$

■

Using results of Lemma 2.7, we formulate the next theorem.

Theorem 2.8 *The following statements are satisfied:*

(i) For all $F \in \mathcal{C}(\Sigma)$

$$\lim_{\substack{\tau \to 0 \\ \tau > 0}} \left\| Q^{\Sigma}_{|2}(\tau,0)F - Q_{|2}(-\tau,0)F - 4\pi F \right\|_{\mathcal{C}(\Sigma)} = 0.$$

(ii) There exist numbers M *and* $\tau_0 > 0$*, such that for all* $0 < \tau < \tau_0$

$$\left\| \left(Q^{\Sigma}_{|2}(\tau,0) - Q^{\Sigma}_{|2}(-\tau,0) - 4\pi\mathcal{I} \right) \middle| \mathcal{C}(\Sigma) \right\|_{\mathcal{C}(\Sigma)} \leq M.$$

(iii) There exist numbers M *and* $\tau_0 > 0$*, such that for all* $0 < \tau < \tau_0$

$$\left\| \left(Q^{\Sigma}_{|2}(\tau,0) - Q^{\Sigma}_{|2}(-\tau,0) - 4\pi\mathcal{I} \right)^{*} \middle| \mathcal{C}(\Sigma) \right\|_{\mathcal{C}(\Sigma)} \leq M,$$

where $\nu(x) = \mu(x)$ *for all edges and corners* x*.*

Proof To (i) and (ii): From the proof of Lemma 2.7, we have with respect to the triangle inequality

$$\begin{aligned}
&\left| Q^{\Sigma}_{|2}(\tau,0)F(x) - Q^{\Sigma}_{|2}(-\tau,0)F(x) - 4\pi F(x) \right| \\
&\leq \ell_F(\delta_0) \int_{\Sigma \cap \Omega^{int}_{\delta_0}(x)} \left| \frac{\partial}{\partial \nu(y)} \left(\frac{1}{|x+\tau\mu(x)-y|} + \frac{1}{|x-\tau\mu(x)-y|} \right) \right| d\omega(y) \\
&\qquad + 2\ell_F(\delta_0) \int_{\Sigma \cap \Omega^{int}_{\delta_0}(x)} \left| \frac{\partial}{\partial \nu(y)} \frac{1}{|x-y|} \right| d\omega(y) + C\|F\|_{\mathcal{C}(\Sigma)} \|\Sigma\| \frac{\tau}{\delta_0^3}
\end{aligned}$$

From this estimate with respect to Lemma 1.19 and according to the inequality $\ell_F(\delta_0) \leq 2\|F\|_{\mathcal{C}(\Sigma)}$, we obtain the proof for (ii). Suppose in Lemma 2.7 that $\delta_0 = \tau^{\frac{1}{4}}$. Then we have the proof for (i) from the last estimate too:

$$\lim_{\substack{\tau \to 0 \\ \tau > 0}} \left\| Q_{|2}^{\Sigma}(\tau, 0)F - Q_{|2}(-\tau, 0)F - 4\pi F \right\|_{\mathcal{C}(\Sigma)} = 0,$$

for all functions $F \in \mathcal{C}(\Sigma)$.

To (iii): Let $F \in \mathcal{C}(\Sigma)$, $x \in \Sigma$, $0 < \delta_0 < \delta$ be defined as in Lemma 2.4. Then, we have

$$\begin{aligned}
&\left| Q_{|2}^{\Sigma}(\tau, 0)^* F(x) - Q_{|2}^{\Sigma}(-\tau, 0)^* F(x) - 4\pi F(x) \right| \\
&\qquad \leq 4\pi \|F\|_{\mathcal{C}(\Sigma)} \\
&\quad + \left| \int_{\Sigma} F(y) \left(\frac{\nu(x)\,(y + \tau\mu(y) - x)}{|y + \tau\mu(y) - x|^3} - \frac{\nu(x)\,(y - \tau\mu(y) - x)}{|y - \tau\mu(y) - x|^3} \right) d\omega(y) \right| \\
&\qquad \leq 4\pi \|F\|_{\mathcal{C}(\Sigma)} \\
&\quad + \|F\|_{\mathcal{C}(\Sigma)} \int_{\Sigma} \left| \frac{\nu(x)\,(y + \tau\mu(y) - x)}{|y + \tau\mu(y) - x|^3} - \frac{\nu(x)\,(y - \tau\mu(y) - x)}{|y - \tau\mu(y) - x|^3} \right| d\omega(y) \\
&\qquad \leq 4\pi \|F\|_{\mathcal{C}(\Sigma)} \\
&\qquad + \|F\|_{\mathcal{C}(\Sigma)} \int_{\Sigma} \left| \frac{(y + \tau\mu(y) - x)\,|y - \tau\mu(y) - x|^3}{|y + \tau\mu(y) - x|^3 |y - \tau\mu(y) - x|^3} \right. \\
&\qquad\qquad \left. - \frac{(y - \tau\mu(y) - x)\,|y + \tau\mu(y) - x|^3}{|y + \tau\mu(y) - x|^3 |y - \tau\mu(y) - x|^3} \right| d\omega(y)
\end{aligned}$$

We split the last integral in the inequality into two parts $\displaystyle\int_{\Sigma \setminus \Omega_{\delta_0}^{int}(x)} (\ldots)\, d\omega(y)$ and $\displaystyle\int_{\Sigma \cap \Omega_{\delta_0}^{int}(x)} (\ldots)\, d\omega(y)$. For the denominator of the first part of splitting we have the estimate:

$$|y + \tau\mu(y) - x|^3 |y - \tau\mu(y) - x|^3 \geq \frac{\delta_0^6}{64}.$$

For the denominator of the second splitting part

$$|y + \tau\mu(y) - x|^3 |y - \tau\mu(y) - x|^3 \geq \left(\frac{1 - \alpha}{2} \right)^3 \left(|y - x|^2 + \tau^2 \right)^3.$$

In the same manner as in Lemma 2.4 for an adapted $\tau < \tau_0$, we obtain the estimate for the first integral:

$$\int\limits_{\Sigma\setminus\Omega_{\delta_0}^{int}(x)} |\ldots|\, d\omega(y) \leq \frac{C}{\delta_0^6}.$$

Because of $a^3 \pm b^3 = (a \pm b)\left(a^2 \mp ab + b^2\right)$, where $a = |y - x - \tau\mu(y)|$ and $b = |y - x + \tau\mu(y)|$, we have for the nominator of the second integral with respect to the triangle inequality:

$$\begin{aligned}
&\left|(y-x)\left(a^3 - b^3\right) + \tau\mu(y)\left(a^3 + b^3\right)\right| \\
&\quad \leq 2|\tau||y-x|\left(a^2 + ab + b^2\right) + |\tau|\left(2|y-x| + 2\tau\right)\left(a^2 - ab + b^2\right) \\
&\quad = 2|\tau||y-x|\left(a^2 + 2b\right) + 2|\tau|^2\left(a^2 - ab + b^2\right) \\
&\quad \leq 8|\tau||y-x|\left(|y-x|^2 + |\tau|^2\right) \\
&\quad + 2|\tau|^2\left(2|y-x|^2 - 2|\tau|^2 - \left||y-x|^2 - |\tau|^2\right|\right) \\
&\quad \leq 8|\tau||y-x|\left(|y-x|^2 + |\tau|^2\right) + 4|\tau|\left(|y-x|^2 + |\tau|^2\right) \\
&\quad = \left(8|\tau||y-x| + 4|\tau|^2\right)\left(|y-x|^2 + |\tau|^2\right).
\end{aligned}$$

Thus we have the following estimate in terms of polar coordinates:

$$\begin{aligned}
&\int\limits_{\Sigma\cap\Omega_{\delta_0}^{int}(x)} \frac{8|\tau||y-x| + 4|\tau|^2}{\left(\frac{1-\alpha}{2}\right)^3\left(|y-x|^2 + |\tau|^2\right)^2} d\omega(y) \\
&\qquad \leq C \int\limits_{\Sigma\cap\Omega_{\delta_0}^{int}(x)} \frac{|\tau||y-x| + |\tau|^2}{\left(|y-x|^2 + |\tau|^2\right)^2} d\omega(y) \\
&\qquad \leq C_1|\tau| \int\limits_0^{2\pi}\int\limits_0^{\delta_0} \frac{r^2 dr d\phi}{\left(r^2+\tau^2\right)^2} + C_1|\tau|^2 \int\limits_0^{2\pi}\int\limits_0^{\delta_0} \frac{r dr d\phi}{\left(r^2+\tau^2\right)^2} \\
&\qquad \leq C_2|\tau|\left(\frac{-\delta_0}{2\left(\delta_0^2+\tau^2\right)} + \frac{1}{2|\tau|}\arctan\frac{\delta_0}{|\tau|}\right) \\
&\qquad\qquad + C_2|\tau|^2\left(\frac{1}{2\tau^2} - \frac{1}{2\left(\delta_0^2+\tau^2\right)}\right) \leq C_3.
\end{aligned}$$

Collecting all estimates, we obtain the proof for the constant

$$M = \|F\|_{\mathcal{C}(\Sigma)}\left(4\pi + \frac{C}{\delta_0^6} + C_3\right).$$

■

The jump relations, known for smooth surfaces, lose their validity for the directional derivative of the single layer potential on surfaces possessing edges and corners, because of the singularity in the neighborhood of such points. For this reason, we use the potentials of single and double layer and the contour integral on regular surface elements as described in [57], [72], to determine the singular behavior.

Lemma 2.9 *For all $x \notin \Sigma$ and all $F \in \mathcal{C}^{(1)}(\Sigma)$*

$$\nabla_x \int_\Sigma F(y) \frac{1}{|x-y|} d\omega(y) = -\int_\Sigma F(y)\nu(y) \frac{\partial}{\partial \nu(y)} \frac{1}{|x-y|} d\omega(y) + \int_\Sigma \left(\nabla^* F + 2\Upsilon F \nu\right)(y) \frac{1}{|x-y|} d\omega(y) - \int_{\mathcal{Q}(\Sigma)} \nu(y) F(y) \frac{1}{|x-y|} d\sigma(y),$$

where the last integral denotes the contour integral over all boundaries of regular surfaces. (If the boundary Σ is a $\mathcal{C}^{(2)}$-surface, the last integral in the sum equals zero.)

From Lemma 2.9 it follows that

Lemma 2.10 *For all $x \notin \Sigma$ and all $F \in \tilde{\mathcal{C}}^{(1)}(\Sigma)$*

$$\nabla_x \int_\Sigma F(y) \frac{1}{|x-y|} d\omega(y) = -\int_\Sigma F(y)\nu(y) \frac{\partial}{\partial \nu(y)} \frac{1}{|x-y|} d\omega(y) + \int_\Sigma \left(\nabla^* F + 2\Upsilon F \nu\right)(y) \frac{1}{|x-y|} d\omega(y).$$

Because of $F \in \tilde{\mathcal{C}}^{(1)}(\Sigma)$, the terms $F\nu$ and $\nabla^* F + 2\Upsilon F\nu$ represent continuous vector fields in Lemma 2.10. Following the results of the previous subsections, the limit relations for the directional derivative of the single layer potential can be established.

Theorem 2.11 *For the operator $\tilde{\mathcal{I}}$ as defined by* (2.5)*, the following limit relations are satisfied:*

(i) For all $F \in \tilde{\mathcal{C}}^{(1)}(\Sigma)$

$$\lim_{\substack{\tau \to 0 \\ \tau > 0}} \left\| Q^\Sigma_{|1}(\tau, 0)F - Q^\Sigma_{|1}(-\tau, 0)F + 4\pi \tilde{\mathcal{I}} F \right\|_{\mathcal{C}(\Sigma)} = 0.$$

(ii) For all $F \in \tilde{\mathcal{C}}^{(1)}(\Sigma)$ *and constants* M, $\tau_0 > 0$ *and* $0 < \tau < \tau_0$

$$\left\| \left(Q^{\Sigma}_{|1}(\tau,0) - Q^{\Sigma}_{|1}(-\tau,0) + 4\pi\tilde{\mathcal{I}} \right) \middle| \mathcal{C}(\Sigma) \right\|_{\mathcal{C}(\Sigma)} \leq M.$$

(iii) For all $F \in \tilde{\mathcal{C}}^{(1)}(\Sigma)$ *and constants* M, $\tau_0 > 0$ *and all* $0 < \tau < \tau_0$

$$\left\| \left(Q^{\Sigma}_{|1}(\tau,0)^{-} Q^{\Sigma}_{|1}(-\tau,0) + 4\pi\tilde{\mathcal{I}} \right)^{*} \middle| \mathcal{C}(\Sigma) \right\|_{\mathcal{C}(\Sigma)} \leq M.$$

Proof To (i): For $x \in \Sigma$ we have with respect to Lemma 2.10:

$$\begin{aligned}
&\left| Q^{\Sigma}_{|1}(\tau,0)F - Q^{\Sigma}_{|1}(-\tau,0)F + 4\pi(\mu(x)\nu(x))F \right| \\
&\qquad \left| = \int_{\Sigma} F(y) \frac{\mu(x)(x-\tau\mu(x)-y)}{|x-\tau\mu(x)-y|^3} d\omega(y) \right. \\
&\qquad \left. - \int_{\Sigma} F(y) \frac{\mu(x)(x+\tau\mu(x)-y)}{|x+\tau\mu(x)-y|^3} d\omega(y) + 4(\mu(x)\nu(y))F(x) \right| \\
&\qquad\qquad \leq \left| \int_{\Sigma} F(y)(\mu(x)\nu(y)) \frac{\partial}{\partial\nu(y)} \frac{1}{|x+\tau\mu(x)-y|} d\omega(y) \right. \\
&\left. - \int_{\Sigma} F(y)(\mu(x)\nu(y)) \frac{\partial}{\partial\nu(y)} \frac{1}{|x-\tau\mu(x)-y|} d\omega(y) + 4\pi(\mu(x)\nu(x))F(x) \right| \\
&\qquad\qquad + \left| \int_{\Sigma} (\nu(x)\nabla^{*}F(y) + 2\Upsilon(y)F(y)\mu(x)\nu(y)) \times \right. \\
&\qquad\qquad\qquad \left. \times \left(\frac{1}{|x+\tau\mu(x)-y|} - \frac{1}{|x-\tau\mu(x)-y|} \right) d\omega(y) \right|.
\end{aligned}$$

According to Lemma 2.4 and Theorem 2.8(i), the limit on the right side in the last inequality is zero. As the limit relation is uniformly relative to $x \in \Sigma$, this result is valid for all functions $F \in \tilde{\mathcal{C}}^{(1)}(\Sigma)$.

To (ii): The proof can be directly obtained from the estimates from

Lemma 1.14 and Theorem 2.8. We have for all functions $F \in \mathcal{C}(\Sigma)$:

$$\begin{aligned}
&\left|Q^{\Sigma}_{|1}(\tau,0)F - Q^{\Sigma}_{|1}(-\tau,0)F + 4\pi(\mu(x)\nu(x))F\right| \\
&\qquad = \left| \int\limits_{\Sigma} F(y) \frac{\mu(x)(x-\tau\mu(x)-y)}{|x-\tau\mu(x)-y|^3} d\omega(y) \right. \\
&\qquad \left. - \int\limits_{\Sigma} F(y) \frac{\mu(x)(x+\tau\mu(x)-y)}{|x+\tau\mu(x)-y|^3} d\omega(y) + 4(\mu(x)\nu(y))F(x) \right| \\
&\qquad \leq 4\pi \|F\|_{\mathcal{C}(\Sigma)} \\
&\quad + \left| \int\limits_{\Sigma} F(y) \left(\frac{\mu(x)(x-\tau\mu(x)-y)}{|x-\tau\mu(x)-y|^3} - \frac{\mu(x)(x+\tau\mu(x)-y)}{|x+\tau\mu(x)-y|^3} \right) d\omega(y) \right|
\end{aligned}$$

$$\begin{aligned}
&\leq 4\pi \|F\|_{\mathcal{C}(\Sigma)} + \|F\|_{\mathcal{C}(\Sigma)} \int\limits_{\Sigma} \left| \frac{(x-\tau\mu(x)-y)|x+\tau\mu(x)-y|^3}{|x-\tau\mu(x)-y|^3|x+\tau\mu(x)-y|^3} \right. \\
&\qquad \left. - \frac{(x+\tau\mu(x)-y)|x-\tau\mu(x)-y|^3}{|x-\tau\mu(x)-y|^3|x+\tau\mu(x)-y|^3} \right| d\omega(y)
\end{aligned}$$

$$\leq \|F\|_{\mathcal{C}(\Sigma)} \left(4\pi + \frac{C}{\delta_0^6}\right) + \|F\|_{\mathcal{C}(\Sigma)} \int\limits_{\Sigma \cap \Omega^{int}_{\delta_0}(x)} \frac{8|\tau||y-x| + 4|\tau|^2}{(1-\alpha)^3 \left(|y-x|^2+\tau^2\right)^2} d\omega(y).$$

The final estimate is obtained for the constant $M = \left(4\pi + \dfrac{C}{\delta_0^6}\right) \|F\|_{\mathcal{C}(\Sigma)}$.

To (iii): Because $|\mu(x)| = |\nu(y)| = 1$ for all $x \in \Sigma$, the proof completely matches the proof of Theorem 2.8(iii). ■

Remark 2.12 *With conventional agreements for the vector field, we deduce from the proof of Theorem 2.11(ii) also uniform boundedness of the difference*

$$\int\limits_{\Sigma} F(y) \frac{y-x-\tau\mu(x)}{|y-x-\tau\mu(x)|^3} d\omega(y) - \int\limits_{\Sigma} F(y) \frac{y-x+\tau\mu(x)}{|y-x+\tau\mu(x)|^3} d\omega(y),$$

for all $0 < \tau < \tau_0$ and all $F \in \mathcal{C}(\Sigma)$ relative to the supremum norm.

The jump and limit relations can be generalized to the Hilbert space $\mathcal{L}^2(\Sigma)$. The main tool for this assertion is a lemma known form functional analysis (cf. [50], [55]).

Lemma 2.13 *Let H be a Hilbert space with the scalar product $(.,.)$. Let $B \subset H$ be a normed subspace with norms $\|.\|_1$ and $\|.\|_2 = (.,.)^{\frac{1}{2}}$. Assume that there exists a constant C, such that*

$$\|x\|_2 \leq C\|x\|_1$$

for all $x \in B$. Moreover, let the operator $\mathcal{T} : B \to B$ be linear and bounded relative to $\|.\|_1$. Let $\mathcal{T}^*|_B : B \to B$ be the adjoint operator of $\mathcal{T}$ with respect to the scalar product $(.,.)$ and be further bounded relative to $\|.\|_1$. Then, the operator $\mathcal{T}$ is also bounded relative to $\|.\|_2$.

Proof The operator $\mathcal{T}^*$ is the adjoint operator of $\mathcal{T}$ with respect to the scalar product $(.,.)$. Then, after the application of the Cauchy-Schwarz's inequality we obtain for all $x \in B$:

$$\|\mathcal{T}x\|_2^2 = (\mathcal{T}x, \mathcal{T}x) = (x, \mathcal{T}^*\mathcal{T}x) \leq \|x\|_2\|\mathcal{T}^*\mathcal{T}x\|_2.$$

Hence, the next estimate is valid

$$\|\mathcal{T}x\|_2^4 \leq \|x\|_2^2\|\mathcal{T}^*\mathcal{T}x\|_2^2 \leq \|x\|_2\|x\|_2\|(\mathcal{T}^*\mathcal{T})^2x\|_2.$$

Then, by the application of the induction and with use of the properties of $\mathcal{T}$ and $\mathcal{T}^*$ we have

$$\begin{aligned}\|\mathcal{T}x\|_2^{2^n} &\leq \|x\|_2^{2^n-1}\left\|(\mathcal{T}^*\mathcal{T})^{2^{n-1}}x\right\|_2 \\ &\leq \|x\|_2^{2^n-1}C\left\|(\mathcal{T}^*\mathcal{T})^{2^{n-1}}x\right\|_1 \\ &\leq \|x\|_2^{2^n-1}CC_1^{2^n}\|x\|_1.\end{aligned}$$

Consequently, we obtain for all $n \in \mathbb{N}$ and $x \neq 0$

$$\frac{\|\mathcal{T}x\|_2^{2^n}}{\|x\|_2^{2^n}} \leq CC_1^{2^n}\frac{\|x\|_1}{\|x\|_2},$$

so that after some manipulations

$$\frac{\|\mathcal{T}x\|_2}{\|x\|_2} \leq C_1\left(\frac{C\|x\|_1}{\|x\|_2}\right)^{2^{-n}}.$$

This shows that

$$\|\mathcal{T}\|_2 \leq C_1$$

holds true for $n \to \infty$, as required. ■

Because the function spaces $\mathcal{C}(\Sigma)$ and $\tilde{\mathcal{C}}^{(1)}(\Sigma)$ with the scalar product $(.,.)_{\mathcal{L}^2(\Sigma)}$ can be used as linear subspaces of $\mathcal{L}^2(\Sigma)$, the next lemmas are valid (cf. [72]):

Lemma 2.14 *The space $\mathcal{C}(\Sigma)$ is dense in $\mathcal{L}^2(\Sigma)$.*

Lemma 2.15 *The space $\tilde{\mathcal{C}}^{(1)}(\Sigma)$ is dense as subspace of $\mathcal{L}^2(\Sigma)$.*

Proof Let $\Xi \subset \Sigma$ be closed. χ_Ξ is a characteristic function on Ξ. Then, according to [67], it is sufficient to prove, that for each $\epsilon > 0$ there exists a function $F \in \tilde{\mathcal{C}}^{(1)}(\Sigma)$ satisfying the estimate

$$\|\chi_\Xi - F\|_{\mathcal{L}^2(\Sigma)} \leq \epsilon. \tag{2.20}$$

Really, because each function of $\mathcal{L}^2(\Sigma)$ is a limit function of a sequence of piecewise constant functions W, so that with respect to

$$W = \sum_{l=1}^{n} c_l \chi_{\Xi^l},\ \Xi^l \subset \Sigma,\ l = 1, \ldots, n,$$

for all $F_l \in \tilde{\mathcal{C}}^{(1)}(\Sigma), l = 1, \ldots, n$ from the equality

$$\sum_{l=1}^{n} c_l F_l = \tilde{F},$$

follows the estimate

$$\left\| W - \tilde{F} \right\|_{\mathcal{L}^2(\Sigma)} \leq \sum_{l=1}^{n} |c_l| \, \|\chi_{\Xi^l} - F_l\|_{\mathcal{L}^2(\Sigma)}.$$

Each $\Xi \subset \Sigma$ can be divided into a finite number of regular surface elements. According to Definition 1.11, there exists a Cartesian coordinate system (tangential-normal-system) for each of these regular surface elements. Without loss of generality, we assume that Ξ is a regular surface element with the tangential-normal-system defined in an inner point $x \in \Xi$, so that the boundary of Ξ consists of edges and corners. In this case Ξ corresponds to a closed parameter domain $T \subset \mathbb{R}^2$ possessing the origin.

Now we define a continuous function on T that equals the constant 1 outside the boundary stripes of the width $2a$ and declines to 0 at the boundaries (as shown in the figure below).

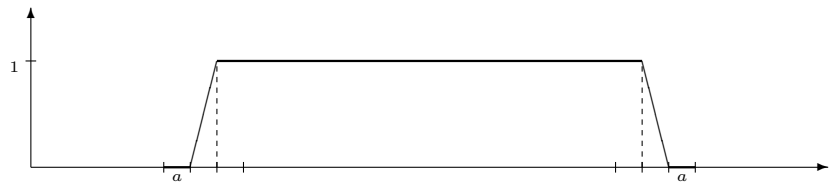

By use of the integral smoothing process (described, e.g., in [81]), we obtain infinitely differentiable function F_1 on T that equals 1 beyond the boundary stripes and declines to zero at the boundaries with all its derivatives. If we set all values of F_1 at the remains of Σ to zero, we again obtain the function $F \in \tilde{\mathcal{C}}^{(1)}(\Sigma)$ because of the bijection between Ξ and T.

With a sufficiently small number a relative to $\epsilon > 0$, the ratio of the surface, corresponding to the boundary stripes relative to Ξ is less then $\frac{\epsilon}{2}$. This implies the estimate

$$\|\chi_\Xi - F\|_{\mathcal{L}^2(\Sigma)} \leq \epsilon.$$

■

We obtain the continuation of operators from a subspace to $\mathcal{L}^2$ from the next lemma.

Lemma 2.16 *(cf. [51]) Let H be a Banach space. $B \subset H$ is a linear subspace, dense in H. $\mathcal{T} : B \to H$ is linear and bounded. Then the operator $\mathcal{T}$ can be continued to the whole space according to the linearity and the norm.*

For simplicity we introduce the following notation (cf. [31]).

Definition 2.17 *For sufficiently small $\tau > 0$, the operators*

$$\begin{aligned} J_1^\Sigma(\tau) &= Q^\Sigma(\tau, 0) - Q^\Sigma(-\tau, 0), \\ J_2^\Sigma(\tau) &= Q_{|1}^\Sigma(\tau, 0) - Q_{|1}^\Sigma(-\tau, 0) + 4\pi\tilde{\mathcal{I}}, \\ J_3^\Sigma(\tau) &= Q_{|2}^\Sigma(\tau, 0) - Q_{|2}^\Sigma(-\tau, 0) - 4\pi\mathcal{I}, \end{aligned} \tag{2.21}$$

*are called **jump operators**.*

Now we can prove the jump relations in $\mathcal{L}^2(\Sigma)$ (see, e.g., [28], [72]).

Theorem 2.18 *For a regular surface Σ and all $F \in \mathcal{L}^2(\Sigma)$*

(i) $\lim\limits_{\substack{\tau \to 0 \\ \tau > 0}} \left\| Q^\Sigma(\tau, 0)F - Q^\Sigma(-\tau, 0)F \right\|_{\mathcal{L}^2(\Sigma)} = 0.$

(ii) $\lim\limits_{\substack{\tau\to 0\\ \tau>0}} \left\| Q^{\Sigma}_{|2}(\tau,0)F - Q^{\Sigma}_{|2}(-\tau,0)F - 4\pi F \right\|_{\mathcal{L}^2(\Sigma)} = 0.$

(iii) $\lim\limits_{\substack{\tau\to 0\\ \tau>0}} \left\| Q^{\Sigma}_{|1}(\tau,0)F - Q^{\Sigma}_{|1}(-\tau,0)F + 4\pi\tilde{\mathcal{I}}F \right\|_{\mathcal{L}^2(\Sigma)} = 0.$

Proof Because Σ^{int} is a bounded region with a finite surface, the next inequality holds for the supremum norm and $\mathcal{L}^2$-norm:

$$\|F\|_{\mathcal{L}^2(\Sigma)} \leq D\|F\|_{\mathcal{C}(\Sigma)},$$

where D is a constant that depending only on Σ.

To (i): With respect to $J_1^{\Sigma}(\tau) : \mathcal{C}(\Sigma) \to \mathcal{C}(\Sigma)$ and Lemmas 2.4, 2.5, we have that $J_1^{\Sigma}(\tau)\big|\,\mathcal{C}(\Sigma)$ (and resp. $J_1^{\Sigma}(\tau)^*\big|\,\mathcal{C}(\Sigma)$) is uniformly bounded for $0 < \tau < \tau_0$ relative to the $\|.\|_{\mathcal{C}(\Sigma)}$ norm. Under consideration of Lemma 2.13 (by letting $\mathcal{T} = J_1^{\Sigma}(\tau)$, $H = \mathcal{L}^2(\Sigma)$, $B = \mathcal{C}(\Sigma)$, $\|.\|_1 = \|.\|_{\mathcal{C}(\Sigma)}$, $\|.\|_2 = \|.\|_{\mathcal{L}^2(\Sigma)}$) we obtain that $J_1^{\Sigma}(\tau)$ is also bounded relative to $\|.\|_{\mathcal{L}^2(\Sigma)}$, i.e., there exists a constant K that

$$\|J_1^{\Sigma}(\tau)F\|_{\mathcal{L}^2(\Sigma)} \leq K\|F\|_{\mathcal{L}^2(\Sigma)} \tag{2.22}$$

holds true for all $F \in \mathcal{C}(\Sigma)$ and $0 < \tau < \tau_0$. According to Lemma 2.14, the space $\mathcal{C}(\Sigma)$ is a dense subspace in $\mathcal{L}^2(\Sigma)$. Hence, with respect to Lemma 2.16, the operator $J_1^{\Sigma}(\tau)$ can be continued on $\mathcal{L}^2(\Sigma)$ by using of the norm $\|.\|_{\mathcal{L}^2(\Sigma)}$, and Equation (2.22) is satisfied for all $F \in \mathcal{L}^2(\Sigma)$ and $0 < \tau < \tau_0$.

Let $F \in \mathcal{L}^2(\Sigma)$ be given. Then there exists a series of functions $\{F_n\}_{n\in\mathbb{N}}$, $F_n \in \mathcal{C}(\Sigma)$, such that for every $\epsilon > 0$ a number $N(\epsilon) \in \mathbb{N}$ exists, so that for all numbers $n \geq N(\epsilon)$ the estimate

$$\|F - F_n\|_{\mathcal{L}^2(\Sigma)} < \epsilon,$$

holds true. So that we have

$$\begin{aligned}
\left\|J_1^{\Sigma}(\tau)F\right\|_{\mathcal{L}^2(\Sigma)} &= \left\|J_1^{\Sigma}(\tau)F - J_1^{\Sigma}(\tau)F_n + J_1^{\Sigma}(\tau)F_n\right\|_{\mathcal{L}^2(\Sigma)} \\
&\leq \left\|J_1^{\Sigma}(\tau)F_n\right\|_{\mathcal{L}^2(\Sigma)} + \left\|J_1^{\Sigma}(\tau)F - J_1^{\Sigma}(\tau)F_n\right\|_{\mathcal{L}^2(\Sigma)} \\
&\leq D\left\|J_1^{\Sigma}(\tau)F_n\right\|_{\mathcal{C}(\Sigma)} + \left\|J_1^{\Sigma}(\tau)\left(F - F_n\right)\right\|_{\mathcal{L}^2(\Sigma)} \\
&\leq D\left\|J_1^{\Sigma}(\tau)F_n\right\|_{\mathcal{C}(\Sigma)} + K\left\|F - F_n\right\|_{\mathcal{L}^2(\Sigma)}.
\end{aligned}$$

With respect to Lemma 1.14,

$$\lim_{\substack{\tau\to 0\\ \tau>0}} \left\|J_1^{\Sigma}(\tau)F_n\right\|_{\mathcal{C}(\Sigma)} = 0.$$

holds for each $n \in \mathbb{N}$. And the limit $n \to \infty$ yields

$$\lim_{\substack{\tau \to 0 \\ \tau > 0}} \left\| J_1^{\Sigma}(\tau) F \right\|_{\mathcal{L}^2(\Sigma)} = 0.$$

To (ii): Let B be the space $\hat{\mathcal{C}}(\Sigma)$ as defined in Lemma 2.13. For a continuous function F, the operator $J_3^{\Sigma}(\tau)^* F$ is not continuous in general in edges and corners. For the space H, we substitute $\mathcal{L}^2(\Sigma)$ and set the operator $\mathcal{T}$ to $J_3^{\Sigma}(\tau)$. Thus, according to Theorem 2.8(ii) and (iii), we get the estimate for $J_3^{\Sigma}(\tau)$ in the $\mathcal{L}^2$-norm:

$$\left\| J_3^{\Sigma}(\tau) F \right\|_{\mathcal{L}^2(\Sigma)} \leq K \left\| F \right\|_{\mathcal{L}^2(\Sigma)}.$$

The last estimate is satisfied for all functions $F \in \hat{\mathcal{C}}(\Sigma)$, and $0 < \tau < \tau_0$, ($J_3^{\Sigma}(\tau)$, according to Theorem 2.8, is also bounded on $\hat{\mathcal{C}}(\Sigma)$ relative to the supremum norm) as well as for all functions $F \in \mathcal{L}^2(\Sigma)$, and $0 < \tau < \tau_0$ with respect to Lemma 2.14. The approximation of $F \in \mathcal{L}^2(\Sigma)$ by a series of functions $\{F_n\}_{n \in \mathbb{N}}$, $F_n \in \mathcal{C}(\Sigma)$ satisfying $\lim_{n \to 0} \left\| F - F_n \right\|_{\mathcal{L}^2(\Sigma)} = 0$ implies, analogously, as in case (i), the jump relation for all functions $F \in \mathcal{L}^2(\Sigma)$:

$$\lim_{\substack{\tau \to 0 \\ \tau > 0}} \left\| J_3^{\Sigma}(\tau) F \right\|_{\mathcal{L}^2(\Sigma)} = 0.$$

To (iii): According to Theorem 2.11(i), the jump relations for the directional derivative of the single layer potential are proved only for the space $\tilde{\mathcal{C}}^{(1)}(\Sigma)$. But, with respect to Theorem 2.11(ii), the operator $J_2^{\Sigma}(\tau) \big| \hat{\mathcal{C}}(\Sigma)$ is uniformly bounded in the supremum norm for $0 < \tau < \tau_0$ and $J_2^{\Sigma}(\tau)(\hat{\mathcal{C}}(\Sigma))$ is a subset of $\hat{\mathcal{C}}(\Sigma)$. So that we can apply Lemma 2.13 and Theorem 2.8(iii) by letting $H = \mathcal{L}^2(\Sigma)$, $B = \hat{\mathcal{C}}(\Sigma)$, $\|.\|_1 = \|.\|_{\mathcal{C}(\Sigma)}$, $\mathcal{T} = J_2^{\Sigma}(\tau)$ because of uniform boundedness of the operator $J_2^{\Sigma}(\tau)$ in the supremum norm for $0 < \tau < \tau_0$.

Again, with respect to Lemma 2.14, we obtain the boundedness of $J_2^{\Sigma}(\tau)$ in $\mathcal{L}^2(\Sigma)$ with $\mathcal{L}^2$-norm, i.e., there exists a constant K, such that for all $F \in \mathcal{L}^2(\Sigma)$

$$\left\| J_2^{\Sigma}(\tau) F \right\|_{\mathcal{L}^2(\Sigma)} \leq K \left\| F \right\|_{\mathcal{L}^2(\Sigma)}$$

holds for $0 < \tau < \tau_0$. In addition, for $F \in \mathcal{L}^2(\Sigma)$ there exists a series of functions $\{F_n\}_{n \in \mathbb{N}}$, $F_n \in \mathcal{C}(\Sigma)$ that for every $\epsilon > 0$ there exists $N(\epsilon) \in \mathbb{N}$, such that

$$\left\| F - F_n \right\|_{\mathcal{L}^2(\Sigma)} < \epsilon,$$

holds for all $n \geq N(\epsilon)$. Then we have

$$\begin{aligned}\left\|J_2^{\Sigma}(\tau)F\right\|_{\mathcal{L}^2(\Sigma)} &\leq \left\|J_2^{\Sigma}(\tau)F_n\right\|_{\mathcal{L}^2(\Sigma)} + \left\|J_2^{\Sigma}(\tau)\left(F-F_n\right)\right\|_{\mathcal{L}^2(\Sigma)} \\ &\leq D\left\|J_2^{\Sigma}(\tau)F_n\right\|_{\mathcal{C}(\Sigma)} + K\left\|F-F_n\right\|_{\mathcal{L}^2(\Sigma)}\end{aligned}$$

Analogously, as in case (i), according to Theorem 2.11(i), we obtain for all functions $F \in \mathcal{L}^2(\Sigma)$

$$\lim_{\substack{\tau\to 0\\ \tau>0}} \left\|J_2^{\Sigma}(\tau)F\right\|_{\mathcal{L}^2(\Sigma)} = 0.$$

■

Remark 2.19 *With assumptions of Theorem 2.18 and with respect to Remark 2.12, the uniform boundedness of the difference*

$$\int_{\Sigma} F(y)\frac{y-x-\tau\mu(x)}{|y-x-\tau\mu(x)|^3}d\omega(y) - \int_{\Sigma} F(y)\frac{y-x+\tau\mu(x)}{|y-x+\tau\mu(x)|^3}d\omega(y),$$

can be shown for all $0<\tau<\tau_0$ *and all* $F \in \mathcal{L}^2(\Sigma)$ *relative to the* $\mathcal{L}^2$*-norm.*

2.3 Helmholtz Potential Operators

After the consideration of limit and jump relations for the Laplace operator we now go over to the Helmholtz operator $\Delta + \kappa^2$, $\kappa \in \mathbb{C}$.

We introduce the Helmholtz potential operators which allow a unified concept for the formulation of the boundary integrals involving the Helmholtz equation to be needed for our wavelet concept.

Definition 2.20 *Let numbers* $\tau, \sigma \in \mathbb{R}$, $\tau \neq 0$ *satisfy the requirements known from Lemma 1.15 and Definition 1.17, for a regular surface* Σ*, i.e.,*

$$|\sigma| \leq \frac{1-\alpha}{4}|\tau| \leq \frac{1-\alpha}{5-\alpha}\frac{\delta}{2},\ |\tau| \leq \tau_0.$$

Then, the operator $P^{\Sigma}(\tau,\sigma;\kappa) : \mathcal{L}^2(\Sigma) \to \mathcal{C}(\Sigma)$ *defined for* $F \in \mathcal{L}^2(\Sigma)$ *by*

$$P^{\Sigma}(\tau,\sigma;\kappa)F(x) = \int_{\Sigma} F(y)\frac{\exp\left(\mathrm{i}\kappa\left|x+\tau\mu(x)-(y+\sigma\nu(y))\right|\right)}{\left|x+\tau\mu(x)-(y+\sigma\nu(y))\right|}d\omega(y),\ \kappa \in \mathbb{C},$$

is called a ***Helmholtz potential operator*** *on* Σ*.*

In the sense of this definition we are able to introduce the potential operators for a single and double layer on the regular surface Σ.

The *Helmholtz potential operator of a single layer* on Σ for values on the smoothed parallel surface $\Sigma(\tau)$: $P^{\Sigma}(\tau,0;\kappa):\mathcal{L}^2(\Sigma)\to\mathcal{C}(\Sigma)$ is given by

$$P^{\Sigma}(\tau,0;\kappa)F(x)=\int\limits_{\Sigma}F(y)\frac{\exp\left(\mathrm{i}\kappa\left|x+\tau\mu(x)-y\right|\right)}{\left|x+\tau\mu(x)-y\right|}d\omega(y). \tag{2.23}$$

Analogously, we can introduce the *Helmholtz potential operator of a double layer* on Σ for values on $\Sigma(\tau)$, $P^{\Sigma}_{|2}(\tau,0;\kappa):\mathcal{L}^2(\Sigma)\to\mathcal{C}(\Sigma)$ by

$$\begin{aligned}P^{\Sigma}_{|2}(\tau,0;\kappa)F(x)&=\frac{\partial}{\partial\sigma}P^{\Sigma}(\tau,\sigma;\kappa)F(x)\Big|_{\sigma=0}\\&=\int\limits_{\Sigma}F(y)\left(\frac{\partial}{\partial\nu(y)}\frac{\exp\left(\mathrm{i}\kappa\left|x+\tau\mu(x)-(y+\sigma\nu(y))\right|\right)}{\left|x+\tau\mu(x)-(y+\sigma\nu(y))\right|}\right)\Big|_{\sigma=0}d\omega(y)\\&=\int\limits_{\Sigma}F(y)\frac{\nu(y)\left(x+\tau\mu(x)-y\right)\exp\left(\mathrm{i}\kappa\left|x+\tau\mu(x)-y\right|\right)}{\left|x+\tau\mu(x)-y\right|^2}\times\\&\quad\times\left(-\mathrm{i}\kappa+\frac{1}{\left|x-\tau\mu(x)-y\right|}\right)d\omega(y).\end{aligned} \tag{2.24}$$

In the same manner, we are able to introduce the *Helmholtz operator of the directional derivative of a single layer potential* for values on $\Sigma(\tau)$:

$$\begin{aligned}P^{\Sigma}_{|1}(\tau,0;\kappa)F(x)&=\frac{\partial}{\partial\tau}P(\tau,\sigma;\kappa)F(x)\Big|_{\sigma=0}\\&=-\int\limits_{\Sigma}F(y)\frac{\mu(x)\left(x+\tau\mu(x)-y\right)\exp\left(\mathrm{i}\kappa\left|x+\tau\mu(x)-y\right|\right)}{\left|x+\tau\mu(x)-y\right|^2}\times\\&\quad\times\left(-\mathrm{i}\kappa+\frac{1}{\left|x+\tau\mu(x)-y\right|}\right)d\omega(y).\end{aligned} \tag{2.25}$$

If $\tau=\sigma=0$, the kernels of the formally defined potentials have weak singularities. The associated potential operators are given by the weakly singular integral expressions

$$P^{\Sigma}(0,0;\kappa)F(x)=\int\limits_{\Sigma}F(y)\frac{\exp\left(\mathrm{i}\kappa|x-y|\right)}{|x-y|}d\omega(y), \tag{2.26}$$

$$P^{\Sigma}_{|2}(0,0;\kappa)F(x)=\int\limits_{\Sigma}F(y)\frac{\partial}{\partial\nu(y)}\frac{\exp\left(\mathrm{i}\kappa|x-y|\right)}{|x-y|}d\omega(y), \tag{2.27}$$

$$P^{\Sigma}_{|1}(0,0;\kappa)F(x)=\frac{\partial}{\partial\mu(x)}\int\limits_{\Sigma}F(y)\frac{\exp\left(\mathrm{i}\kappa|x-y|\right)}{|x-y|}d\omega(y), \tag{2.28}$$

where $P^{\Sigma}, P^{\Sigma}_{|1}, P^{\Sigma}_{|2}$ define linear bounded operators on $\mathcal{L}^2(\Sigma)$ (cf. [31]).

Remark 2.21 *Let F be a continuous function on Σ. Then, the functions* (2.26), (2.27), *and* (2.28) *are infinitely often differentiable and satisfy the Helmholtz equation in Σ_{int} and Σ_{ext}. Moreover, these functions fulfill the Sommerfeld radiation condition in Σ_{ext}. According to classical potential theory (see, e.g., [58]), these function can be continued continuously for all $F \in \mathcal{C}(\Sigma)$ to the surface Σ, but the limits depend from which (smoothed) parallel surface (inner or outer) the point x tends to Σ. On the other hand, these functions are also defined on the surface Σ, i.e., all integrals* (2.26), (2.27), *and* (2.28) *exist for $x \in \Sigma$.*

In order to give concise formulations of the classical limit formulas and jump relations, the adjoint operators come into play.

Definition 2.22 *The operator $P^{\Sigma}(\tau,\sigma;\kappa)^* : \mathcal{L}^2(\Sigma) \to \mathcal{C}(\Sigma)$ satisfying*

$$\left(F, P^{\Sigma}(\tau,\sigma;\kappa)G\right)_{\mathcal{L}^2(\Sigma)} = \left(P^{\Sigma}(\tau,\sigma;\kappa)^*F, G\right)_{\mathcal{L}^2(\Sigma)},$$

for all functions $F, G \in \mathcal{L}^2(\Sigma)$ is called the ***adjoint Helmholtz operator*** *of $P^{\Sigma}(\tau,\sigma;\kappa)$ with respect to the scalar product $(.,.)_{\mathcal{L}^2(\Sigma)}$.*

According to Fubini's theorem we are able to interchange the order of integration

$$\begin{aligned}
&\left(F, P^{\Sigma}(\tau,\sigma;\kappa)G\right)_{\mathcal{L}^2(\Sigma)} \\
&= \int_{\Sigma} F(x) \overline{\int_{\Sigma} G(y) \frac{\exp\left(\mathrm{i}\kappa\left|x+\tau\mu(x)-(y+\sigma\nu(y))\right|\right)}{\left|x+\tau\mu(x)-(y+\sigma\nu(y))\right|} d\omega(y)} d\omega(x) \\
&= \int_{\Sigma} \overline{G(y)} \int_{\Sigma} F(x) \frac{\exp\left(\mathrm{i}\overline{\kappa}\left|x+\tau\mu(x)-(y+\sigma\nu(y))\right|\right)}{\left|x+\tau\mu(x)-(y+\sigma\nu(y))\right|} d\omega(x) d\omega(y) \\
&= \left(P^{\Sigma}(\tau,\sigma;\kappa)^*F, G\right)_{\mathcal{L}^2(\Sigma)}.
\end{aligned}$$

By comparison we thus have the *adjoint operator $P^{\Sigma}(\tau,0;\kappa)^*$ of the Helmholtz potential operator $P^{\Sigma}(\tau,0;\kappa)$*

$$\begin{aligned}
P^{\Sigma}(\tau,0;\kappa)^*F(x) &= P^{\Sigma}(\tau,\sigma;\kappa)^*F(x)\big|_{\sigma=0} \\
&= \int_{\Sigma} F(y) \frac{\exp\left(-\mathrm{i}\overline{\kappa}\left|x-y-\tau\mu(y)\right|\right)}{\left|x-y-\tau\mu(y)\right|} d\omega(y).
\end{aligned}$$

In an analogous way, we obtain the *adjoint operator of the potential operator of a double layer*

$$P^{\Sigma}_{|2}(\tau,0;\kappa)^*F(x) = \int_{\Sigma} F(y)\frac{\nu(x)(x-y-\tau\mu(y))\exp\left(-\mathrm{i}\overline{\kappa}\,|x-y-\tau\mu(y)|\right)}{|x-y-\tau\mu(y)|^2}\times \times\left(-\mathrm{i}\overline{\kappa}-\frac{1}{|x-y-\tau\mu(y)|}\right)d\omega(y).$$

and the *adjoint operator of the directional derivative of a single layer*

$$P^{\Sigma}_{|1}(\tau,0;\kappa)^*F(x) = \int_{\Sigma} F(y)\frac{\mu(y)(x-y-\tau\mu(y))\exp\left(-\mathrm{i}\overline{\kappa}\,|x-y-\tau\mu(y)|\right)}{|x-y-\tau\mu(y)|^2}\times \times\left(\mathrm{i}\overline{\kappa}+\frac{1}{|x-y-\tau\mu(y)|}\right)d\omega(y),$$

For the defined Helmholtz potential operators we present the limit and jump relations in a Hilbert space $\mathcal{L}^2(\Sigma)$ (see, e.g., [31], [72]).

Theorem 2.23 *For a regular surface Σ as defined by Definition 1.12, the next propositions are satisfied:*

(i) For all $F \in \mathcal{L}^2(\Sigma)$ and $\kappa \in \mathbb{C}$

$$\lim_{\substack{\tau\to 0\\ \tau>0}} \left\|P^{\Sigma}(\tau,0;\kappa)F - P^{\Sigma}(-\tau,0;\kappa)F\right\|_{\mathcal{L}^2(\Sigma)} = 0,$$
$$\lim_{\substack{\tau\to 0\\ \tau>0}} \left\|P^{\Sigma}(\tau,0;\kappa)^*F - P^{\Sigma}(-\tau,0;\kappa)^*F\right\|_{\mathcal{L}^2(\Sigma)} = 0.$$

(ii) For all $F \in \mathcal{L}^2(\Sigma)$ and $\kappa \in \mathbb{C}$

$$\lim_{\substack{\tau\to 0\\ \tau>0}} \left\|P^{\Sigma}_{|2}(\tau,0;\kappa)F - P^{\Sigma}_{|2}(-\tau,0;\kappa)F - 4\pi F\right\|_{\mathcal{L}^2(\Sigma)} = 0,$$
$$\lim_{\substack{\tau\to 0\\ \tau>0}} \left\|P^{\Sigma}_{|2}(\tau,0;\kappa)^*F - P^{\Sigma}_{|2}(-\tau,0;\kappa)^*F - 4\pi F\right\|_{\mathcal{L}^2(\Sigma)} = 0.$$

(iii) For all $F \in \mathcal{L}^2(\Sigma)$ and $\kappa \in \mathbb{C}$

$$\lim_{\substack{\tau\to 0\\ \tau>0}} \left\|P^{\Sigma}_{|1}(\tau,0;\kappa)F - P^{\Sigma}_{|1}(-\tau,0;\kappa)F + 4\pi\tilde{\mathcal{I}}F\right\|_{\mathcal{L}^2(\Sigma)} = 0,$$
$$\lim_{\substack{\tau\to 0\\ \tau>0}} \left\|P^{\Sigma}_{|1}(\tau,0;\kappa)^*F - P^{\Sigma}_{|1}(-\tau,0;\kappa)^*F + 4\pi\tilde{\mathcal{I}}^*F\right\|_{\mathcal{L}^2(\Sigma)} = 0,$$

where the operator $\tilde{\mathcal{I}} : \mathcal{L}^2(\Sigma) \to \mathcal{L}^2(\Sigma)$ *is represented by* $\tilde{\mathcal{I}}F(x) = (\mu(x)\nu(x))F(x)$.

Proof To (i): By use of series expansions of the exponential function to the kernel of the Helmholtz potential operators, we obtain

$$\frac{\exp(\mathrm{i}\kappa|x+\tau\mu(x)-y|)}{|x+\tau\mu(x)-y|} - \frac{\exp(\mathrm{i}\kappa|x-\tau\mu(x)-y|)}{|x-\tau\mu(x)-y|} = \frac{1}{|x+\tau\mu(x)-y|} - \frac{1}{|x-\tau\mu(x)-y|} + \mathcal{O}(|\tau|),$$

and, analogously, we have for the kernel of the adjoint operator

$$\frac{\exp(-\mathrm{i}\overline{\kappa}|y+\tau\mu(y)-x|)}{|y+\tau\mu(y)-x|} - \frac{\exp(-\mathrm{i}\overline{\kappa}|y-\tau\mu(y)-x|)}{|y-\tau\mu(y)-x|} = \frac{1}{|y+\tau\mu(y)-x|} - \frac{1}{|y-\tau\mu(y)-x|} + \mathcal{O}(|\tau|).$$

As a consequence, we obtain for $M > 0$, $0 < \tau < \tau_0$ and all functions $F \in \mathcal{C}(\Sigma)$ the following estimates:

$$\begin{aligned}&\left\|P^{\Sigma}(\tau,0;\kappa)F - P^{\Sigma}(-\tau,0;\kappa)F\right\|_{\mathcal{C}(\Sigma)} \\ &\qquad\qquad \leq \left\|Q^{\Sigma}(\tau,0)F - Q^{\Sigma}(-\tau,0)F\right\|_{\mathcal{C}(\Sigma)} < M,\end{aligned}$$

$$\begin{aligned}&\left\|P^{\Sigma}(\tau,0;\kappa)^*F - P^{\Sigma}(-\tau,0;\kappa)^*F\right\|_{\mathcal{C}(\Sigma)} \\ &\qquad\qquad \leq \left\|Q^{\Sigma}(\tau,0)^*F - Q^{\Sigma}(-\tau,0)^*F\right\|_{\mathcal{C}(\Sigma)} < M.\end{aligned}$$

From the last inequalities we obtain immediately for all $F \in \mathcal{C}(\Sigma)$

$$\begin{aligned}&\lim_{\substack{\tau\to 0\\ \tau>0}} \left\|P^{\Sigma}(\tau,0;\kappa)F - P^{\Sigma}(-\tau,0;\kappa)F\right\|_{\mathcal{C}(\Sigma)} = 0, \\ &\left\|\left(P^{\Sigma}(\tau,0;\kappa) - P^{\Sigma}(-\tau,0;\kappa)\right)\middle|\,\mathcal{C}(\Sigma)\right\|_{\mathcal{C}(\Sigma)} < M,\ 0 < \tau < \tau_0,\end{aligned} \tag{2.29}$$

and

$$\begin{aligned}&\lim_{\substack{\tau\to 0\\ \tau>0}} \left\|P^{\Sigma}(\tau,0;\kappa)^*F - P^{\Sigma}(-\tau,0;\kappa)^*F\right\|_{\mathcal{C}(\Sigma)} = 0, \\ &\left\|\left(P^{\Sigma}(\tau,0;\kappa) - P^{\Sigma}(-\tau,0;\kappa)\right)^*\middle|\,\mathcal{C}(\Sigma)\right\|_{\mathcal{C}(\Sigma)} < M,\ 0 < \tau < \tau_0.\end{aligned} \tag{2.30}$$

With respect to the uniform boundedness and analogously to the proof of Theorem 2.18(i), the expressions (2.29), (2.30) can be continued on $\mathcal{L}^2(\Sigma)$ with the norm $\|.\|_{\mathcal{L}^2(\Sigma)}$.

To (ii): After the application of the same series expansion of the exponential function, we obtain

$$\frac{\partial}{\partial\nu(y)}\left(\frac{\exp\left(\mathrm{i}\kappa|x+\tau\mu(x)-y|\right)}{|x+\tau\mu(x)-y|}-\frac{\exp\left(\mathrm{i}\kappa|x-\tau\mu(x)-y|\right)}{|x-\tau\mu(x)-y|}\right)=$$
$$\frac{\partial}{\partial\nu(y)}\left(\frac{1}{|x+\tau\mu(x)-y|}-\frac{1}{|x-\tau\mu(x)-y|}\right)$$
$$+\frac{\partial}{\partial\nu(y)}\frac{\kappa^2}{2}\left(|x-\tau\nu(x)-y|-|x+\tau\nu(x)-y|\right)+\mathcal{O}(|\tau|),$$

and

$$\frac{\partial}{\partial\nu(y)}\left(\frac{\exp\left(-\mathrm{i}\overline{\kappa}|y+\tau\mu(y)-x|\right)}{|y+\tau\mu(y)-x|}-\frac{\exp\left(-\mathrm{i}\overline{\kappa}|y-\tau\mu(y)-x|\right)}{|y-\tau\mu(y)-x|}\right)=$$
$$\frac{\partial}{\partial\nu(y)}\left(\frac{1}{|y+\tau\mu(y)-x|}-\frac{1}{|y-\tau\mu(y)-x|}\right)$$
$$+\frac{\partial}{\partial\nu(y)}\frac{\kappa^2}{2}\left(|y-\tau\nu(y)-x|-|y+\tau\nu(y)-x|\right)+\mathcal{O}(|\tau|).$$

Additionally, we have

$$\left|\int_\Sigma\frac{\partial}{\partial\nu(y)}\left(|x-\tau\mu(x)-y|-|x+\tau\mu(x)-y|\right)d\omega(y)\right|$$

$$\leq\int_\Sigma\left|\frac{(x+\tau\mu(x)-y)|x-\tau\mu(x)-y|}{|x-\tau\mu(x)-y||x+\tau\mu(x)-y|}\right.$$
$$\left.-\frac{(x-\tau\mu(x)-y)|x+\tau\mu(x)-y|}{|x-\tau\mu(x)-y||x+\tau\mu(x)-y|}\right|d\omega(y)$$
$$\leq\int_\Sigma\frac{4|\tau||x-y|+2|\tau|^2}{(1-\alpha)\left(\tau^2+|x-y|^2\right)}d\omega(y)\leq C|\tau|,$$

and

$$\left|\int_\Sigma\frac{\partial}{\partial\nu(y)}\left(|y-\tau\mu(y)-x|-|y+\tau\mu(y)-x|\right)d\omega(y)\right|$$
$$\leq\int_\Sigma\frac{8|\tau||x-y|+2|\tau|^2}{(1-\alpha)\left(\tau^2+|x-y|^2\right)}d\omega(y)\leq C|\tau|.$$

Accumulating all these estimates, we obtain

$$\left|P^\Sigma_{|2}(\tau,0;\kappa)F(x)-P^\Sigma_{|2}(-\tau,0;\kappa)F(x)-4\pi F(x)\right|$$
$$\leq\left|Q^\Sigma_{|2}(\tau,0)F(x)-Q^\Sigma_{|2}(-\tau,0)F(x)-4\pi F(x)\right|+C|\tau|.$$

As in Theorem 2.8, we have for a continuous function F and $0 < \tau < \tau_0$:

$$\begin{aligned}
&\lim_{\substack{\tau\to 0\\ \tau>0}} \left\| P_{|2}^{\Sigma}(\tau,0;\kappa)F - P_{|2}^{\Sigma}(-\tau,0;\kappa)F - 4\pi F \right\|_{\mathcal{C}(\Sigma)} = 0,\\
&\left\| \left(P_{|2}^{\Sigma}(\tau,0;\kappa) - P_{|2}^{\Sigma}(-\tau,0;\kappa) - 4\pi\mathcal{I} \right) \middle| \, \mathcal{C}(\Sigma) \right\|_{\mathcal{C}(\Sigma)} \leq M, \qquad (2.31)\\
&\left\| \left(P_{|2}^{\Sigma}(\tau;\kappa) - P_{|2}^{\Sigma}(-\tau,0;\kappa) - 4\pi\mathcal{I} \right)^{*} \middle| \, \mathcal{C}(\Sigma) \right\|_{\mathcal{C}(\Sigma)} \leq M,
\end{aligned}$$

where the operator $\mathcal{I}$ denotes the identity operator in $\mathcal{L}^2(\Sigma)$.

Analogously, as in case (i), the expressions (2.31) can be continuated on $\mathcal{L}^2(\Sigma)$ with the norm $\|.\|_{\mathcal{L}^2(\Sigma)}$.

To (iii): After the application of the same series expansion of the exponential function, we have the estimate

$$\begin{aligned}
&\left| P_{|1}^{\Sigma}(\tau,0;\kappa)F(x) - P_{|1}^{\Sigma}(-\tau,0;\kappa)F(x) + 4\pi(\mu(x)\nu(x))F(x) \right|\\
&\qquad \leq \left| Q_{|1}^{\Sigma}(\tau,0)F(x) - Q_{|1}^{\Sigma}(-\tau,0)F(x) + 4\pi(\mu(x)\nu(x))F(x) \right| + C|\tau|,
\end{aligned}$$

for all $F \in \tilde{\mathcal{C}}^{(1)}(\Sigma)$, $x \in \Sigma$. Hence, the equality

$$\lim_{\substack{\tau\to 0\\ \tau>0}} \left\| P_{|1}^{\Sigma}(\tau,0;\kappa)F - P_{|1}^{\Sigma}(-\tau,0;\kappa)F + 4\pi\tilde{\mathcal{I}}F \right\|_{\mathcal{C}(\Sigma)} = 0$$

holds true for all $F \in \tilde{\mathcal{C}}^{(1)}(\Sigma)$. With the analogous proof to Theorem 2.11, we obtain for $0 < \tau < \tau_0$:

$$\begin{aligned}
&\left\| \left(P_{|1}^{\Sigma}(\tau,0;\kappa) - P_{|1}^{\Sigma}(-\tau,0;\kappa) + 4\pi\tilde{\mathcal{I}} \right) \middle| \, \mathcal{C}(\Sigma) \right\|_{\mathcal{C}(\Sigma)} \leq M,\\
&\left\| \left(P_{|1}^{\Sigma}(\tau,0;\kappa) - P_{|1}^{\Sigma}(-\tau,0;\kappa) + 4\pi\tilde{\mathcal{I}} \right)^{*} \middle| \, \mathcal{C}(\Sigma) \right\|_{\mathcal{C}(\Sigma)} \leq M.
\end{aligned}$$

Because $\tilde{\mathcal{C}}^{(1)}(\Sigma)$ is dense in $\mathcal{L}^2(\Sigma)$, analogously to the last cases, we obtain the proof. ■

In the sequel, we define the limit and jump relations with respect to the Helmholtz case in potential theory. Let $\mathcal{I}$ be the identity operator in $\mathcal{L}^2(\Sigma)$, the operator $\tilde{\mathcal{I}} : \mathcal{L}^2(\Sigma) \to \mathcal{L}^2(\Sigma)$ is defined by $\tilde{\mathcal{I}}F(x) = (\mu(x)\nu(x))F(x)$. Then, for all sufficiently small $\tau > 0$, the operators

$$\begin{aligned}
J_1^{\Sigma}(\tau;\kappa) &= P^{\Sigma}(\tau,0;\kappa) - P^{\Sigma}(-\tau,0;\kappa),\\
J_2^{\Sigma}(\tau;\kappa) &= P_{|1}^{\Sigma}(\tau,0;\kappa) - P_{|1}^{\Sigma}(-\tau,0;\kappa) + 4\pi\tilde{\mathcal{I}},\\
J_3^{\Sigma}(\tau;\kappa) &= P_{|2}^{\Sigma}(\tau,0;\kappa) - P_{|2}^{\Sigma}(-\tau,0;\kappa) - 4\pi\tilde{\mathcal{I}}
\end{aligned}$$

are called *jump operators*, and

$$\begin{aligned} L_1^\Sigma(\pm\tau;\kappa) &= P^\Sigma(\pm\tau,0;\kappa) - P^\Sigma(0,0;\kappa), \\ L_2^\Sigma(\pm\tau;\kappa) &= P_{|1}^\Sigma(\pm\tau,0;\kappa) - P_{|1}^\Sigma(0,0;\kappa) \pm 2\pi\tilde{\mathcal{I}}, \\ L_3^\Sigma(\pm\tau;\kappa) &= P_{|2}^\Sigma(\pm\tau,0;\kappa) - P_{|2}^\Sigma(0,0;\kappa) \mp 2\pi\tilde{\mathcal{I}}, \end{aligned}$$

are called *limit operators*.

In analogy to the Laplace case we can now prove the following theorem (see, e.g., [31], [32]).

Theorem 2.24 *For all $F \in \mathcal{L}^2(\Sigma)$ and $i = 1, 2, 3$*

$$\begin{aligned} &\lim_{\substack{\tau\to 0\\ \tau>0}} \left\| L_i^\Sigma(\pm\tau;\kappa)F \right\|_{\mathcal{L}^2(\Sigma)} = 0, && \lim_{\substack{\tau\to 0\\ \tau>0}} \left\| J_i^\Sigma(\tau;\kappa)F \right\|_{\mathcal{L}^2(\Sigma)} = 0, \\ &\lim_{\substack{\tau\to 0\\ \tau>0}} \left\| L_i^\Sigma(\pm\tau;\kappa)^* F \right\|_{\mathcal{L}^2(\Sigma)} = 0, && \lim_{\substack{\tau\to 0\\ \tau>0}} \left\| J_i^\Sigma(\tau;\kappa)^* F \right\|_{\mathcal{L}^2(\Sigma)} = 0. \end{aligned}$$

2.4 Multiscale Modeling

Based on the limit and jump relations provided in Section 2.3, we formulate in this section scaling and wavelet functions, and their important properties.

2.4.1 Scaling and Wavelet Functions

We reformulate the limit and jump relations in integral form.

Corollary 2.25 *For all $F \in \mathcal{L}^2(\Sigma)$*

$$\lim_{\substack{\tau\to 0\\ \tau>0}} \int_\Sigma \Phi_\tau^{i,\Sigma}(\cdot,y;\kappa)F(y)d\omega(y) = \begin{cases} F, & i = 3,4; \\ 0, & i = 2; \\ P^\Sigma(0,0;\kappa)F, & i = 1; \\ P_{|1}^\Sigma(0,0;\kappa)F, & i = 5; \\ P_{|2}^\Sigma(0,0;\kappa)F, & i = 6; \end{cases}$$

where $\Phi_\tau^{i,\Sigma}(\cdot,y;\kappa)$, $i = 1,\ldots,6$ are explicitly given by

$$\Phi_{\pm\tau}^{1,\Sigma}(x,y;\kappa) = \frac{\exp(\mathrm{i}\kappa|x \pm \tau\mu(x) - y|)}{|x \pm \tau\mu(x) - y|}, \tag{2.32}$$

$$\Phi_\tau^{2,\Sigma}(x,y;\kappa) = \frac{\exp(\mathrm{i}\kappa|x + \tau\mu(x) - y|)}{|x + \tau\mu(x) - y|} - \frac{\exp(\mathrm{i}\kappa|x - \tau\mu(x) - y|)}{|x - \tau\mu(x) - y|}, \tag{2.33}$$

$$\begin{aligned}
&\Phi_\tau^{3,\Sigma}(x,y;\kappa)\\
&= \frac{\exp\left(\mathrm{i}\kappa\left|x-\tau\mu(x)-y\right|\right)\left(x-\tau\mu(x)-y\right)\mu(x)}{4\pi\mu(x)\nu(y)\left|x-\tau\mu(x)-y\right|^2}\left(\frac{1}{|x-\tau\mu(x)-y|}-\mathrm{i}\kappa\right)\\
&- \frac{\exp\left(\mathrm{i}\kappa\left|x+\tau\mu(x)-y\right|\right)\left(x+\tau\mu(x)-y\right)\mu(x)}{4\pi\mu(x)\nu(y)\left|x+\tau\mu(x)-y\right|^2}\left(\frac{1}{|x+\tau\mu(x)-y|}-\mathrm{i}\kappa\right),
\end{aligned} \tag{2.34}$$

$$\begin{aligned}
&\Phi_\tau^{4,\Sigma}(x,y;\kappa)\\
&= \frac{\exp\left(\mathrm{i}\kappa\left|x+\tau\mu(x)-y\right|\right)\left(x+\tau\mu(x)-y\right)\nu(y)}{4\pi\left|x+\tau\mu(x)-y\right|^2}\left(\frac{1}{|x+\tau\mu(x)-y|}-\mathrm{i}\kappa\right)\\
&- \frac{\exp\left(\mathrm{i}\kappa\left|x-\tau\mu(x)-y\right|\right)\left(x-\tau\mu(x)-y\right)\nu(y)}{4\pi\left|x-\tau\mu(x)-y\right|^2}\left(\frac{1}{|x-\tau\mu(x)-y|}-\mathrm{i}\kappa\right),
\end{aligned} \tag{2.35}$$

$$\begin{aligned}
&\Phi_\tau^{5,\Sigma}(x,y;\kappa)\\
&= \frac{\exp\left(\mathrm{i}\kappa\left|x+\tau\mu(x)-y\right|\right)\left(x+\tau\mu(x)-y\right)\mu(x)}{2\left|x+\tau\mu(x)-y\right|^2}\left(\frac{1}{|x+\tau\mu(x)-y|}-\mathrm{i}\kappa\right)\\
&- \frac{\exp\left(\mathrm{i}\kappa\left|x-\tau\mu(x)-y\right|\right)\left(x-\tau\mu(x)-y\right)\mu(x)}{2\left|x-\tau\mu(x)-y\right|^2}\left(\frac{1}{|x-\tau\mu(x)-y|}-\mathrm{i}\kappa\right),
\end{aligned} \tag{2.36}$$

$$\begin{aligned}
&\Phi_\tau^{6,\Sigma}(x,y;\kappa)\\
&= \frac{\exp\left(\mathrm{i}\kappa\left|x+\tau\mu(x)-y\right|\right)\left(x+\tau\mu(x)-y\right)\nu(y)}{2\left|x+\tau\mu(x)-y\right|^2}\left(\frac{1}{|x+\tau\mu(x)-y|}-\mathrm{i}\kappa\right)\\
&- \frac{\exp\left(\mathrm{i}\kappa\left|x-\tau\mu(x)-y\right|\right)\left(x-\tau\mu(x)-y\right)\nu(y)}{2\left|x-\tau\mu(x)-y\right|^2}\left(\frac{1}{|x-\tau\mu(x)-y|}-\mathrm{i}\kappa\right).
\end{aligned} \tag{2.37}$$

From the limit and jump relations for the dual operators, we are able to deduce the following result.

Corollary 2.26 *For all* $F \in \mathcal{L}^2(\Sigma)$

$$\lim_{\substack{\tau\to 0\\ \tau>0}} \int_\Sigma \Phi_\tau^{i,\Sigma}(\cdot,y;\kappa)^* F(y)\,d\omega(y) = \begin{cases} F, & i=3,4;\\ 0, & i=2;\\ P^\Sigma(0,0;\kappa)^* F, & i=1;\\ P_{|1}^\Sigma(0,0;\kappa)^* F, & i=5;\\ P_{|2}^\Sigma(0,0;\kappa)^* F, & i=6; \end{cases}$$

where $\Phi_\tau^{i,\Sigma}(\cdot,y;\kappa)^*$, $i=1,\dots,6$ *are explicitly representable by*

$$\Phi_{\pm\tau}^{1,\Sigma}(x,y;\kappa)^* = \frac{\exp(-\mathrm{i}\overline{\kappa}|x\mp\tau\mu(y)-y|)}{|x\mp\tau\mu(y)-y|}, \tag{2.38}$$

$$\Phi_\tau^{2,\Sigma}(x,y;\kappa)^* = \frac{\exp(-\mathrm{i}\overline{\kappa}|x-\tau\mu(y)-y|)}{|x-\tau\mu(y)-y|} - \frac{\exp(-\mathrm{i}\overline{\kappa}|x+\tau\mu(y)-y|)}{|x+\tau\mu(y)-y|}, \tag{2.39}$$

$$\begin{aligned}
&\Phi_\tau^{3,\Sigma}(x,y;\kappa)^* \\
&= \frac{\exp\left(-\mathrm{i}\overline{\kappa}\,|x+\tau\mu(y)-y|\right)(x+\tau\mu(y)-y)\,\mu(y)}{4\pi\mu(x)\nu(y)\,|x+\tau\mu(y)-y|^2}\left(\frac{1}{|x+\tau\mu(y)-y|}+\mathrm{i}\overline{\kappa}\right) \\
&- \frac{\exp\left(-\mathrm{i}\overline{\kappa}\,|x-\tau\mu(y)-y|\right)(x-\tau\mu(y)-y)\,\mu(y)}{4\pi\mu(x)\nu(y)\,|x-\tau\mu(y)-y|^2}\left(\frac{1}{|x-\tau\mu(y)-y|}+\mathrm{i}\overline{\kappa}\right),
\end{aligned} \tag{2.40}$$

$$\begin{aligned}
&\Phi_\tau^{4,\Sigma}(x,y;\kappa)^* \\
&= \frac{\exp\left(\mathrm{i}\overline{\kappa}\,|x-\tau\mu(y)-y|\right)(x-\tau\mu(y)-y)\,\nu(x)}{4\pi\,|x-\tau\mu(y)-y|^2}\left(-\frac{1}{|x-\tau\mu(y)-y|}-\mathrm{i}\overline{\kappa}\right) \\
&- \frac{\exp\left(\mathrm{i}\overline{\kappa}\,|x+\tau\mu(y)-y|\right)(x+\tau\mu(y)-y)\,\nu(x)}{4\pi\,|x+\tau\mu(y)-y|^2}\left(-\frac{1}{|x+\tau\mu(y)-y|}-\mathrm{i}\overline{\kappa}\right),
\end{aligned} \tag{2.41}$$

$$\begin{aligned}
&\Phi_\tau^{5,\Sigma}(x,y;\kappa)^* \\
&= \frac{\exp\left(-\mathrm{i}\overline{\kappa}\,|x-\tau\mu(y)-y|\right)(x-\tau\mu(y)-y)\,\mu(y)}{2\,|x-\tau\mu(y)-y|^2}\left(\frac{1}{|x-\tau\mu(y)-y|}+\mathrm{i}\overline{\kappa}\right) \\
&- \frac{\exp\left(-\mathrm{i}\overline{\kappa}\,|x+\tau\mu(y)-y|\right)(x+\tau\mu(y)-y)\,\mu(y)}{2\,|x+\tau\mu(y)-y|^2}\left(\frac{1}{|x+\tau\mu(y)-y|}+\mathrm{i}\overline{\kappa}\right),
\end{aligned} \tag{2.42}$$

$$\begin{aligned}
&\Phi_\tau^{6,\Sigma}(x,y;\kappa)^* \\
&= \frac{\exp\left(\mathrm{i}\overline{\kappa}\,|x-\tau\mu(y)-y|\right)(x-\tau\mu(y)-y)\,\nu(x)}{2\,|x-\tau\mu(y)-y|^2}\left(-\frac{1}{|x-\tau\mu(y)-y|}-\mathrm{i}\overline{\kappa}\right) \\
&- \frac{\exp\left(\mathrm{i}\overline{\kappa}\,|x+\tau\mu(y)-y|\right)(x+\tau\mu(y)-y)\,\nu(x)}{2\,|x+\tau\mu(y)-y|^2}\left(-\frac{1}{|x+\tau\mu(y)-y|}-\mathrm{i}\overline{\kappa}\right).
\end{aligned} \tag{2.43}$$

Definition 2.27 *For $\tau > 0$ and $i \in \{1, \ldots, 6\}$, the family $\left\{\Phi_\tau^{i,\Sigma}\right\}_{\tau>0}$ of kernels $\Phi_\tau^{i,\Sigma} : \Sigma \times \Sigma \to \mathbb{C}$ is called a* ***Σ-scaling function*** *of type i. Moreover, $\Phi_1^{i,\Sigma} : \Sigma \times \Sigma \to \mathbb{C}$ (i.e.: $\tau = 1$) is called the* ***mother kernel*** *of the Σ-scaling function of type i.*

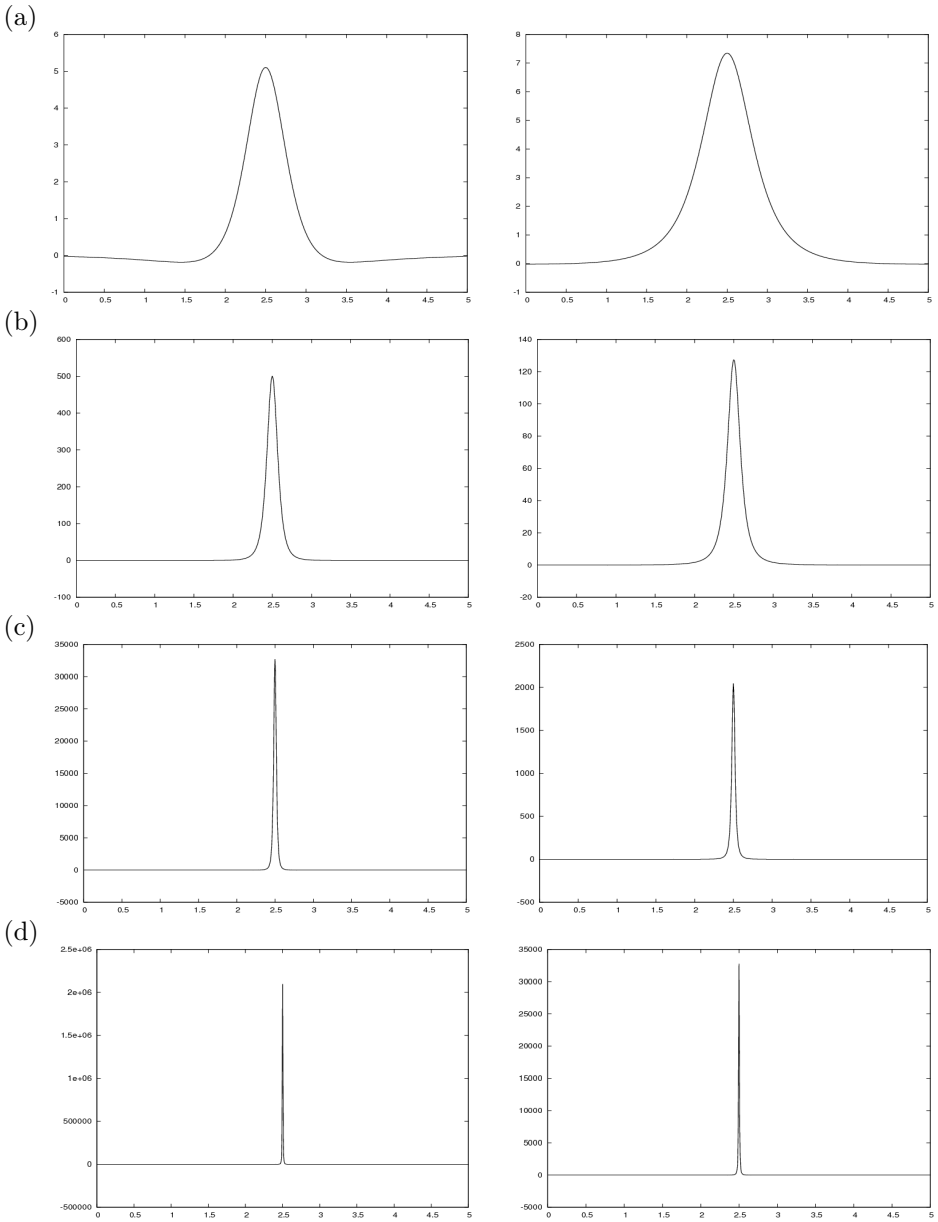

Figure 2.1: Scaling functions $\Phi_\tau^{6,\Sigma}(2.5, y; 1.0)$, $y \in [0, 5]$: (a) $\tau = 2^{-1}$, (b) $\tau = 2^{-3}$, (c) $\tau = 2^{-5}$, (d) $\tau = 2^{-7}$. (left: real part, right: imaginary part).

The scaling functions for different scales τ are illustrated in Figure 2.1. In addition, Figure 2.2 (right column) shows the real parts of scaling functions for different parameter κ.

Definition 2.28 *Correspondingly, for $\tau > 0$, a weight function α and the integer $i \in \{1, \ldots, 6\}$, the family $\left\{\Psi_\tau^{i,\Sigma}\right\}_{\tau>0}$ of kernels $\Psi_\tau^{i,\Sigma} : \Sigma \times \Sigma \to \mathbb{C}$ given by*

$$\Psi_\tau^{i,\Sigma}(x, y; \kappa) = -\tau \frac{d}{d\tau} \Phi_\tau^{i,\Sigma}(x, y; \kappa), \ x, y \in \Sigma, \kappa \in \mathbb{C}, \tag{2.44}$$

*is called a Σ-**wavelet function** of type i. The differential equation (2.44) is called the **(scale continuous) Σ-scaling equation** of type i.*

For simplicity we omit explicit representations of the wavelet functions $\Psi_\tau^{i,\Sigma}(x, y; \kappa)$, $x, y \in \Sigma$, $i \in \{1, \ldots, 6\}$. But it should be pointed out, that all of them allow explicit representations. For example, the wavelet function $\Psi_\tau^{1,\Sigma}(x, y; \kappa)$ is given by

$$\Psi_\tau^{1,\Sigma}(x, y; \kappa) = \tau \frac{\exp(\mathrm{i}\kappa|x + \tau\mu(x) - y|)(x + \tau\mu(x) - y)\mu(x)}{|x + \tau\mu(x) - y|} \times \\ \times \left(\frac{1}{|x + \tau\mu(x) - y|} - \mathrm{i}\kappa \right).$$

The real part of the wavelet function $\Psi_\tau^{1,\Sigma}$ for different parameters κ is shown in Figure 2.2 (right column). The wavelet function $\Psi_\tau^{6,\Sigma}$ for different τ is illustrated in Figure 2.3.

Definition 2.29 *Let $\left\{\Phi_\tau^{i,\Sigma}\right\}_{\tau>0}$ be a Σ-scaling function of type i. Then, the associated Σ-**wavelet transform** of type i $\mathfrak{W}_\kappa^{i,\Sigma} : \mathcal{L}^2(\Sigma) \to \mathcal{L}^2((0, \infty) \times \Sigma)$ is defined by*

$$\mathfrak{W}_\kappa^{i,\Sigma}(F)(\tau, x) = \int_\Sigma \Psi_\tau^{i,\Sigma}(x, y; \kappa) F(y) d\omega(y), \ \kappa \in \mathbb{C}.$$

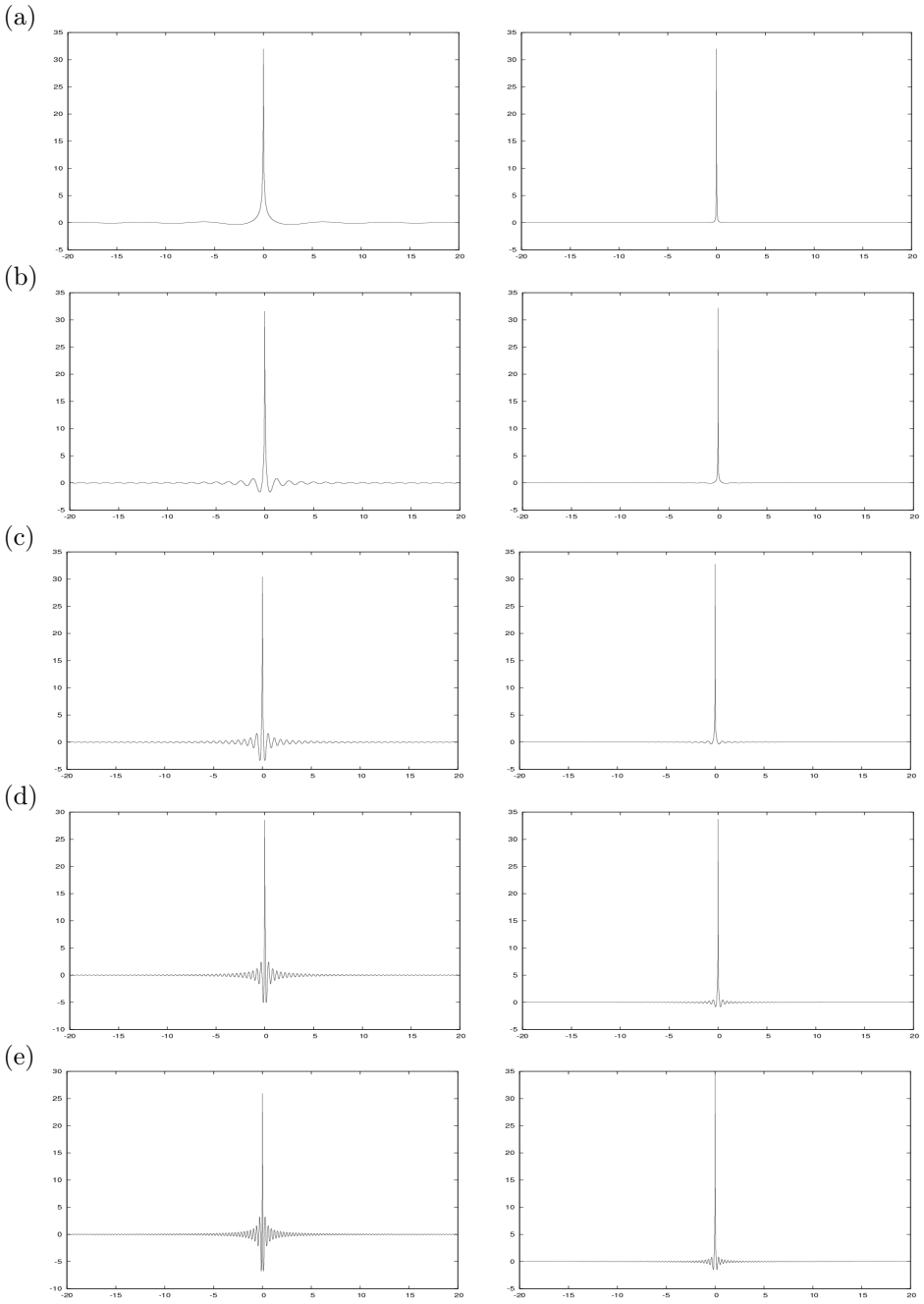

Figure 2.2: The real part of the scaling function $\Phi_\tau^{1,\Sigma}(x,0;\kappa)$ (left), the real part of the wavelet function $\Psi_\tau^{1,\Sigma}(x,0;\kappa)$ (right), where $\tau = 2^{-5}$, $x = -20,\ldots,20$: (a) $\kappa = 1.0$, (b) $\kappa = 5.0$, (c) $\kappa = 10.0$, (d) $\kappa = 15.0$, (e) $\kappa = 20.0$.

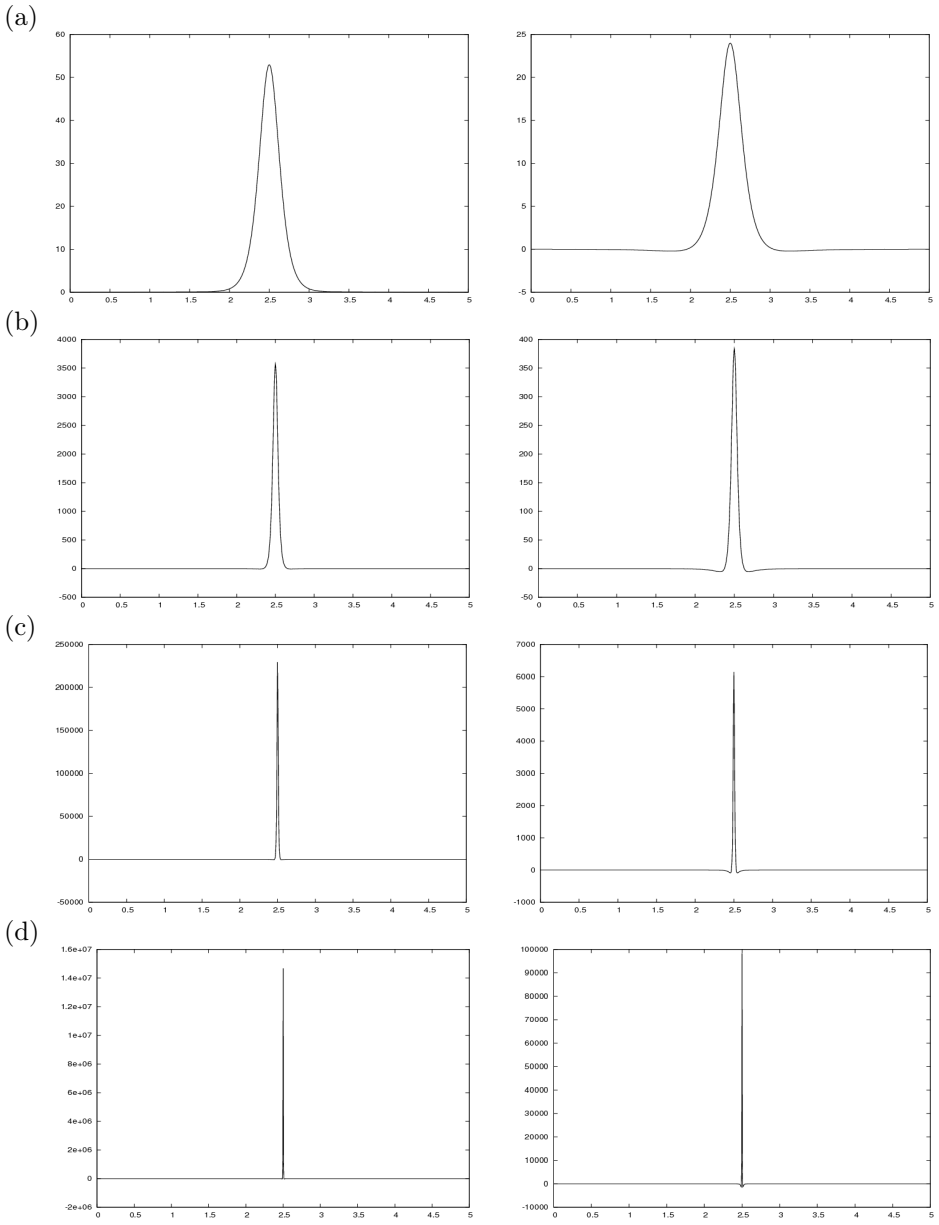

Figure 2.3: Wavelet functions $\Psi_\tau^{6,\Sigma}(2.5, y; 1.0)$, $y \in [0, 5]$: (a) $\tau = 1$, (b) $\tau = 2^{-2}$, (c) $\tau = 2^{-4}$, (d) $\tau = 2^{-6}$. (left: real part, right: imaginary part).

2.4.2 Scale Continuous Reconstruction Formula

Of course, the convergence of the following integrals in the reconstruction theorem is guaranteed.

Theorem 2.30 *Let* $\left\{\Phi_\tau^{i,\Sigma}\right\}_{\tau>0}$ *be a* Σ*-scaling function of type* i*. Suppose, that* F *is of class* $\mathcal{C}(\Sigma)$*. Then, the reconstruction formula (the* Σ*-wavelet transform of type* i*)*

$$\int_0^\infty \mathfrak{W}_\kappa^{i,\Sigma}(F)(\tau,\cdot)\frac{d\tau}{\tau} = \begin{cases} F, & i=3,4; \\ 0, & i=2; \\ P^\Sigma(0,0;\kappa)F, & i=1; \\ P_{|1}^\Sigma(0,0;\kappa)F, & i=5; \\ P_{|2}^\Sigma(0,0;\kappa)F, & i=6; \end{cases}$$

holds in the pointwise sense and in the sense of the $\mathcal{C}$*-norm for all* $\kappa \in \mathbb{C}$*. If* F *is of class* $\mathcal{L}^2(\Sigma)$*, then*

$$\int_0^\infty \mathfrak{W}_\kappa^{i,\Sigma}(F)(\tau,\cdot)\frac{d\tau}{\tau} = \begin{cases} F, & i=3,4; \\ 0, & i=2; \\ P^\Sigma(0,0;\kappa)F, & i=1; \\ P_{|1}^\Sigma(0,0;\kappa)F, & i=5; \\ P_{|2}^\Sigma(0,0;\kappa)F, & i=6; \end{cases}$$

holds in the sense of the $\mathcal{L}^2$*-norm for all* $\kappa \in \mathbb{C}$*.*

Proof Let $R > 0$ be arbitrary. By observing the Fubini's theorem and the identity

$$\Phi_R^{i,\Sigma}(x,y;\kappa) = \int_R^\infty \Psi_\tau^{i,\Sigma}(x,y;\kappa)\frac{d\tau}{\tau},\ (x,y) \in \Sigma\times\Sigma, \kappa \in \mathbb{C},$$

we obtain

$$\begin{aligned} \int_R^\infty \mathfrak{W}_\kappa^{i,\Sigma}(F)(\tau,\cdot)\frac{d\tau}{\tau} &= \int_R^\infty \int_\Sigma \Psi_\tau^{i,\Sigma}(\cdot,y;\kappa)F(y)d\omega(y)\frac{d\tau}{\tau} \\ &= \int_\Sigma \int_R^\infty \Psi_\tau^{i,\Sigma}(\cdot,y;\kappa)\frac{d\tau}{\tau}F(y)d\omega(y) \\ &= \int_\Sigma \Phi_R^{i,\Sigma}(\cdot,y;\kappa)F(y)d\omega(y). \end{aligned}$$

The limit $R \to 0$ in connection with Corollary 2.25 yields the desired result.
■

Our next interest is to reformulate the wavelet transform and the reconstruction theorem by means of the dilated and shifted versions of the mother kernel. For that purpose we introduce the x-translation and τ-dilation operator of the mother kernel as follows:

$$T_x : \Psi_1^{i,\Sigma} \mapsto T_x \Psi_1^{i,\Sigma} = \Psi_{1;x}^{i,\Sigma} = \Psi_1^{i,\Sigma}(x, \cdot; \cdot), \ x \in \Sigma; \tag{2.45}$$

$$D_\tau : \Psi_1^{i,\Sigma} \mapsto D_\tau \Psi_1^{i,\Sigma} = \Psi_\tau^{i,\Sigma}, \ \tau > 0. \tag{2.46}$$

Consequently, it follows that

$$T_x D_\tau \Psi_1^{i,\Sigma} = T_x \Psi_\tau^{i,\Sigma} = \Psi_{\tau;x}^{i,\Sigma} = \Psi_\tau^{i,\Sigma}(x, \cdot; \cdot),$$

for $i = 1, \ldots, 6$. In other words,

$$\mathfrak{W}_\kappa^{i,\Sigma}(F)(\tau, x) = \int\limits_\Sigma \Psi_{\tau;x}^{i,\Sigma}(y; \kappa) F(y) d\omega(y), \ x \in \Sigma, \ \kappa \in \mathbb{C}, \ \tau > 0.$$

Moreover, we have the following limit results.

Theorem 2.31 *For $x \in \Sigma$, $F \in \mathcal{C}(\Sigma)$ and all $\kappa \in \mathbb{C}$*

$$\lim_{\substack{R \to 0 \\ R>0}} \int\limits_\Sigma \Phi_{R;x}^{i,\Sigma}(y; \kappa) F(y) d\omega(y) = \begin{cases} F(x), & i = 3, 4; \\ 0, & i = 2; \\ P^\Sigma(0, 0; \kappa) F(x), & i = 1; \\ P_{|1}^\Sigma(0, 0; \kappa) F(x), & i = 5; \\ P_{|2}^\Sigma(0, 0; \kappa) F(x), & i = 6; \end{cases} \tag{2.47}$$

and

$$\int\limits_0^\infty \int\limits_\Sigma \Psi_{\tau;x}^{i,\Sigma}(y; \kappa) F(y) d\omega(y) \frac{d\tau}{\tau} = \begin{cases} F(x), & i = 3, 4; \\ 0, & i = 2; \\ P^\Sigma(0, 0; \kappa) F(x), & i = 1; \\ P_{|1}^\Sigma(0, 0; \kappa) F(x), & i = 5; \\ P_{|2}^\Sigma(0, 0; \kappa) F(x), & i = 6, \end{cases} \tag{2.48}$$

holds in the pointwise sense and in the sense of $\mathcal{C}$-norm.
For $x \in \Sigma$, $F \in \mathcal{L}^2(\Sigma)$ and all $\kappa \in \mathbb{C}$

$$\lim_{\substack{R \to 0 \\ R>0}} \int\limits_\Sigma \Phi_{R;x}^{i,\Sigma}(y; \kappa) F(y) d\omega(y) = \begin{cases} F(x), & i = 3, 4; \\ 0, & i = 2; \\ P^\Sigma(0, 0; \kappa) F(x), & i = 1; \\ P_{|1}^\Sigma(0, 0; \kappa) F(x), & i = 5; \\ P_{|2}^\Sigma(0, 0; \kappa) F(x), & i = 6; \end{cases} \tag{2.49}$$

and

$$\int_0^\infty \int_\Sigma \Psi^{i,\Sigma}_{\tau;x}(y;\kappa)F(y)d\omega(y)\frac{d\tau}{\tau} = \begin{cases} F(x), & i=3,4; \\ 0, & i=2; \\ P^\Sigma(0,0;\kappa)F(x), & i=1; \\ P^\Sigma_{|1}(0,0;\kappa)F(x), & i=5; \\ P^\Sigma_{|2}(0,0;\kappa)F(x), & i=6, \end{cases} \tag{2.50}$$

holds in the sense of the $\mathcal{L}^2$-norm.

Remark 2.32 *Note that the properties of the Σ-wavelets of type i (analogously to variants of spherical wavelets developed in [30], [29]) do not presume the zero-mean property of $\Phi^{i,\Sigma}_\tau$. The wavelets constructed in such a way, therefore, do not satisfy a substantial condition of the Euclidean concept. However, it should be pointed out, that a construction of wavelets possessing the zero-mean property (see [30]), is obvious and will not be discussed here.*

Remark 2.33 *The dual wavelets can be constructed in the same manner as presented in this section. Their representation, discussion, and application are omitted here.*

2.4.3 Scale Discretized Reconstruction Formula

Until now we were concerned with a scale continuous approach to wavelets. In what follows, scale discrete Σ-scaling functions and wavelets of type i will be introduced. We start with the choice of a sequence, which divides the continuous scale interval $(0,\infty)$ into discrete pieces. More explicitly, $(\tau_j)_{j\in\mathbb{Z}}$ denotes a sequence of real numbers satisfying

$$\lim_{j\to\infty} \tau_j = 0. \tag{2.51}$$

As examples for sequences (τ_j), we choose in the following the dyadic sequence $\tau_j = 2^{-j}, j\in\mathbb{Z}$, where $2\tau_{j+1} = \tau_j, j\in\mathbb{Z}$, or the sequence (τ_j) with $\tau_j = 1-\cos(2^{-j}\pi)$, $j\in\mathbb{Z}$.

For a given Σ-scaling function $\left\{\Phi^{i,\Sigma}_{\tau_j}\right\}_{\tau_j>0}$ of type i, we define the *(scale) discretized Σ-scaling function of type i* and denote $\left\{\Phi^{i,\Sigma}_{\tau_j}\right\}_{j\in\mathbb{Z}}$ by $\Phi^{i,\Sigma}_j$.

Using the (scale) discretized Σ-scaling function and according to Theorem 2.31, we can formulate the next theorem.

Theorem 2.34 *For all* $F \in \mathcal{C}(\Sigma)$

$$\lim_{j\to\infty} \int_{\Sigma} \Phi_j^{i,\Sigma}(\cdot, y; \kappa) F(y) d\omega(y) = \begin{cases} F, & i = 3, 4; \\ 0, & i = 2; \\ P^{\Sigma}(0, 0; \kappa) F, & i = 1; \\ P_{|1}^{\Sigma}(0, 0; \kappa) F, & i = 5; \\ P_{|2}^{\Sigma}(0, 0; \kappa) F, & i = 6; \end{cases}$$

holds in the pointwise sense and in the sense of $\mathcal{C}$*-norm.*
For all $F \in \mathcal{L}^2(\Sigma)$

$$\lim_{j\to\infty} \int_{\Sigma} \Phi_j^{i,\Sigma}(\cdot, y; \kappa) F(y) d\omega(y) = \begin{cases} F, & i = 3, 4; \\ 0, & i = 2; \\ P^{\Sigma}(0, 0; \kappa) F, & i = 1; \\ P_{|1}^{\Sigma}(0, 0; \kappa) F, & i = 5; \\ P_{|2}^{\Sigma}(0, 0; \kappa) F, & i = 6; \end{cases}$$

holds in the sense of $\mathcal{L}^2$*-norm.*

This allows us to define scale discretized wavelets.

Definition 2.35 *Let* $\left\{\Phi_j^{i,\Sigma}\right\}_{j\in\mathbb{Z}}$ *be a discretized* Σ*-scaling function of type* i*. Then, the* ***scale discretized*** Σ***-wavelet function of type*** i *is defined by*

$$\Psi_j^{i,\Sigma}(\cdot, \cdot; \kappa) = -\int_{\tau_{j+1}}^{\tau_j} \Psi_\tau^{i,\Sigma}(\cdot, \cdot; \kappa) \frac{d\tau}{\tau}, \ j \in \mathbb{Z}, \kappa \in \mathbb{C}.$$

By virtue of the equation (2.44)*, we get the formula*

$$\Psi_j^{i,\Sigma}(\cdot, \cdot; \kappa) = -\int_{\tau_{j+1}}^{\tau_j} \tau \frac{d}{d\tau} \Phi_\tau^{i,\Sigma}(\cdot, \cdot; \kappa) \frac{d\tau}{\tau} = \Phi_{j+1}^{i,\Sigma}(\cdot, \cdot; \kappa) - \Phi_j^{i,\Sigma}(\cdot, \cdot; \kappa), \quad (2.52)$$

which is called the ***(scale) discretized*** Σ***-scaling equation of type*** i*.*

Observing the discretized Σ-scaling equation of type i, we obtain for the

function $F \in \mathcal{L}^2(\Sigma)$ and numbers $J \in \mathbb{Z}$ and $N \in \mathbb{N}$:

$$\int_{\Sigma} \Phi_{J+N}^{i,\Sigma}(\cdot, y; \kappa) F(y) d\omega(y)$$
$$= \int_{\Sigma} \Phi_{J}^{i,\Sigma}(\cdot, y; \kappa) F(y) d\omega(y) + \sum_{j=J}^{J+N-1} \int_{\Sigma} \Psi_{j}^{i,\Sigma}(\cdot, y; \kappa) F(y) d\omega(y). \quad (2.53)$$

Corollary 2.36 *Let* $\left\{\Phi_j^{i,\Sigma}\right\}_{j\in\mathbb{Z}}$ *be a (scale) discretized* Σ*-scaling function of type* i*. Then, the multiscale representation of a function* $F \in \mathcal{C}(\Sigma)$

$$\sum_{j=-\infty}^{\infty} \int_{\Sigma} \Psi_j^{i,\Sigma}(\cdot, y; \kappa) F(y) d\omega(y) = \begin{cases} F, & i = 3, 4; \\ 0, & i = 2; \\ P^{\Sigma}(0, 0; \kappa) F, & i = 1; \\ P_{|1}^{\Sigma}(0, 0; \kappa) F, & i = 5; \\ P_{|2}^{\Sigma}(0, 0; \kappa) F, & i = 6; \end{cases}$$

holds in the pointwise sense and in the sense of $\|.\|_{\mathcal{C}}$*-norm.*
If F *is of class* $\mathcal{L}^2(\Sigma)$*, then*

$$\sum_{j=-\infty}^{\infty} \int_{\Sigma} \Psi_j^{i,\Sigma}(\cdot, y; \kappa) F(y) d\omega(y) = \begin{cases} F, & i = 3, 4; \\ 0, & i = 2; \\ P^{\Sigma}(0, 0; \kappa) F, & i = 1; \\ P_{|1}^{\Sigma}(0, 0; \kappa) F, & i = 5; \\ P_{|2}^{\Sigma}(0, 0; \kappa) F, & i = 6; \end{cases}$$

holds in the sense of $\mathcal{L}^2$*-norm.*

Corollary 2.37 *Under assumption of Corollary 2.36*

$$P_J^{i,\Sigma}(F; \kappa) + \sum_{j=J}^{+\infty} \int_{\Sigma} \Psi_j^{i,\Sigma}(\cdot, y; \kappa) F(y) d\omega(y) = \begin{cases} F, & i = 3, 4; \\ 0, & i = 2; \\ P^{\Sigma}(0, 0; \kappa) F, & i = 1; \\ P_{|1}^{\Sigma}(0, 0; \kappa) F, & i = 5; \\ P_{|2}^{\Sigma}(0, 0; \kappa) F, & i = 6; \end{cases}$$

for every $F \in \mathcal{C}(\Sigma)$ *(in the pointwise sense and in the sense of* $\mathcal{C}$*-norm), and for every* $F \in \mathcal{L}^2(\Sigma)$ *(in the sense of* $\mathcal{L}^2$*-norm), where* $P_J^{i,\Sigma}(F; \kappa)$*,* $J \in \mathbb{Z}$ *is*

defined by

$$P_J^{i,\Sigma}(F;\kappa) = \int_\Sigma \Phi_J^{i,\Sigma}(\cdot, y;\kappa)F(y)d\omega(y).$$

According to the scale discretized Σ-wavelets, we introduce, analogously to [31], the following formulation:

$$T_x D_j \Psi_1^{i,\Sigma} = T_x \Psi_j^{i,\Sigma} = \Psi_{j;x}^{i,\Sigma} = \Psi_j^{i,\Sigma}(x,\cdot;\cdot)$$

for $i = 1,\ldots,6$ and $x \in \Sigma$.

Definition 2.38 *The **(scale) discretized Σ-wavelet transform** of type i is defined by*

$$\mathfrak{W}_\kappa^{i,\Sigma} : \mathcal{L}^2(\Sigma) \mapsto \left\{ H : \mathbb{Z}\times\Sigma \,\middle|\, \sum_{j=-\infty}^{\infty} \int_\Sigma \left(H(j;y)\right)^2 d\omega(y) < \infty \right\}$$

with

$$\mathfrak{W}_\kappa^{i,\Sigma}(F)(j;x) = \int_\Sigma \Psi_{j;x}^{i,\Sigma}(y;\kappa)F(y)d\omega(y).$$

Theorem 2.39 *For all functions $F \in \mathcal{C}(\Sigma)$, the reconstruction formula*

$$\sum_{j=-\infty}^{\infty} \mathfrak{W}_\kappa^{i,\Sigma}(F)(j;\cdot) = \begin{cases} F, & i = 3,4; \\ 0, & i = 2; \\ P^\Sigma(0,0;\kappa)F, & i = 1; \\ P_{|1}^\Sigma(0,0;\kappa)F, & i = 5; \\ P_{|2}^\Sigma(0,0;\kappa)F, & i = 6, \end{cases}$$

holds in the pointwise sense and in the sense of $\mathcal{C}$-norm.
For all functions $F \in \mathcal{L}^2(\Sigma)$, the reconstruction formula

$$\sum_{j=-\infty}^{\infty} \mathfrak{W}_\kappa^{i,\Sigma}(F)(j;\cdot) = \begin{cases} F, & i = 3,4; \\ 0, & i = 2; \\ P^\Sigma(0,0;\kappa)F, & i = 1; \\ P_{|1}^\Sigma(0,0;\kappa)F, & i = 5; \\ P_{|2}^\Sigma(0,0;\kappa)F, & i = 6, \end{cases}$$

holds in the sense of $\mathcal{L}^2$-norm.

2.4.4 Scale and Detail Spaces

In this subsection we show that the subdivision of the continuous scale interval $(0, \infty)$ into discrete pieces and the corresponding substitution of the integral over τ by an associated discrete sum provide a multiscale analysis of $\mathcal{L}^2(\Sigma)$.

In fact, analogously to the conventional theory of wavelets (see [34] for the spherical case), the operators $P_j^{i,\Sigma}$, $R_j^{i,\Sigma}$ defined by

$$P_j^{i,\Sigma}(F;\kappa) = \int_\Sigma \Phi_j^{i,\Sigma}(\cdot, y; \kappa) F(y) d\omega(y), \ \kappa \in \mathbb{C}, \ F \in \mathcal{L}^2(\Sigma); \tag{2.54}$$

$$R_j^{i,\Sigma}(F;\kappa) = \int_\Sigma \Psi_j^{i,\Sigma}(\cdot, y; \kappa) F(y) d\omega(y), \ \kappa \in \mathbb{C}, \ F \in \mathcal{L}^2(\Sigma); \tag{2.55}$$

may be understood as *low pass* and *band pass filter*, respectively. Then, the scale spaces $\mathcal{V}_j^i(\Sigma)$ and the detail spaces $\mathcal{W}_j^i(\Sigma)$ of type i are defined by

$$\mathcal{V}_j^i(\Sigma) = P_j^{i,\Sigma}(\mathcal{L}^2(\Sigma);\kappa) = \left\{ P_j^{i,\Sigma}(F;\kappa) \middle| \, F \in \mathcal{L}^2(\Sigma) \right\}; \tag{2.56}$$

$$\mathcal{W}_j^i(\Sigma) = R_j^{i,\Sigma}(\mathcal{L}^2(\Sigma);\kappa) = \left\{ R_j^{i,\Sigma}(F;\kappa) \middle| \, F \in \mathcal{L}^2(\Sigma) \right\}; \tag{2.57}$$

for a fixed value $\kappa \in \mathbb{C}$, respectively. And according to the identity

$$\int_\Sigma \Phi_{j+1}^{i,\Sigma}(\cdot, y; \kappa) F(y) d\omega(y) = \int_\Sigma \Phi_j^{i,\Sigma}(\cdot, y; \kappa) F(y) d\omega(y) + \int_\Sigma \Psi_j^{i,\Sigma}(\cdot, y; \kappa) F(y) d\omega(y),$$

we obtain for all $j \in \mathbb{Z}$

$$P_{j+1}^{i,\Sigma}(F;\kappa) = P_j^{i,\Sigma}(F;\kappa) + R_j^{i,\Sigma}(F;\kappa).$$

From the last identity, we obtain

$$\mathcal{V}_{j+1}^i(\Sigma) = \mathcal{V}_j^i(\Sigma) + \mathcal{W}_j^i(\Sigma).$$

The last equation may be interpreted in the following way: The set $\mathcal{V}_j^i(\Sigma)$ contains a $P_j^{i,\Sigma}$-filtered version of a function F belonging to the class $\mathcal{L}^2(\Sigma)$. The lower the scale, the stronger the intensity of the filtering. By adding $R_j^{i,\Sigma}$-details contained in the space $\mathcal{W}_j^i(\Sigma)$, the space $\mathcal{V}_{j+1}^i(\Sigma)$, which consists

of a filtered versions at resolution $j+1$ is created. Obviously, for $i = 3, 4$, we have the multiscale analysis

$$\overline{\bigcup_{j=-\infty}^{\infty} \mathcal{V}_j^i(\Sigma)}^{\|.\|_{\mathcal{L}^2(\Sigma)}} = \mathcal{L}^2(\Sigma).$$

Furthermore, the next expressions are satisfied for a fixed value $\kappa \in \mathbb{C}$

$$\begin{aligned}
\overline{\bigcup_{j=-\infty}^{\infty} \mathcal{V}_j^1(\Sigma)}^{\|.\|_{\mathcal{L}^2(\Sigma)}} &= P^{\Sigma}(0,0;\kappa)\left(\mathcal{L}^2(\Sigma)\right), \\
\overline{\bigcup_{j=-\infty}^{\infty} \mathcal{V}_j^5(\Sigma)}^{\|.\|_{\mathcal{L}^2(\Sigma)}} &= P_{|1}^{\Sigma}(0,0;\kappa)\left(\mathcal{L}^2(\Sigma)\right), \\
\overline{\bigcup_{j=-\infty}^{\infty} \mathcal{V}_j^6(\Sigma)}^{\|.\|_{\mathcal{L}^2(\Sigma)}} &= P_{|2}^{\Sigma}(0,0;\kappa)\left(\mathcal{L}^2(\Sigma)\right).
\end{aligned}$$

2.5 A Tree Algorithm

By use of the multiscale representation properties of scaling functions (Section 2.4.4), we introduce in this section some aspects for the scientific numerical computation. Our goal is to deduce a pyramid (decomposition) scheme for the recursive computation of the integrals $P_j^{i,\Sigma}(F;\kappa)$ and $R_j^{i,\Sigma}(F;\kappa)$ for $i \in \{1,\ldots,6\}$ and $j = J_0,\ldots,J$ starting from the scale $J \in \mathbb{N}$ of a given function F of class $\mathcal{C}(\Sigma)$ (or $\mathcal{L}^2(\Sigma)$). This scheme can further be applied to the decomposition of seismic data. The tree algorithm is based on the existence of the 'reproducing kernel function' on each regular surface element $\Xi^l,\ l = 1,\ldots,n$ defined in Definition 1.12. We assume that the sequence $\tau_j,\ j = J_0,\ldots,J$ satisfies Equations (2.51).

In order to construct the recursive decomposition scheme, we consider a pyramid scheme and decompose a given function $G \in \mathcal{C}(\Sigma)$ (or $G \in \mathcal{L}^2(\Sigma)$) in a series of the scaling functions. For this reason, we assume, that for suitable, sufficiently large $J \in \mathbb{N}$, the integral $P_J^{i,\Sigma}(F;\kappa)$ is close to the function G, so that for all $x \in \Sigma$, a fixed $\kappa \in \mathbb{C}$ satisfies[1]:

$$P_J^{i,\Sigma}(F;\kappa)(x) \simeq \sum_{k=1}^{N_J} \alpha_k^{N_J} \Phi_J^{i,\Sigma}(x, y_k^{N_J};\kappa) \simeq G(x), \tag{2.58}$$

[1]The symbol $\simeq$ always means, that the error is assumed to be negligible.

where the function G is defined by

$$G = \begin{cases} F, & i = 3, 4; \\ 0, & i = 2; \\ P^{\Sigma}(0,0;\kappa)F, & i = 1; \\ P^{\Sigma}_{|1}(0,0;\kappa)F, & i = 5; \\ P^{\Sigma}_{|2}(0,0;\kappa)F, & i = 6. \end{cases}$$

We want to calculate coefficients

$$\alpha^{N_j} \in \mathbb{R}^{N_j},\ \alpha^{N_j} = \left(\alpha_1^{N_j}, \ldots, \alpha_{N_j}^{N_j}\right)^T,\ j = J_0, \ldots, J,$$

which satisfy the statements:

- The vectors $\alpha^{N_j},\ j = J_0, \ldots, J-1$, are obtainable by recursion starting from the vector α^{N_J}.
- For $j = J_0, \ldots, J$

$$P_j^{i,\Sigma}(F;\kappa)(x) = \int_{\Sigma} \Phi_j^{i,\Sigma}(x,y;\kappa)F(y)d\omega(y) \simeq \sum_{k=1}^{N_j} \alpha_k^{N_j} \Phi_j^{i,\Sigma}(x, y_k^{N_j};\kappa).$$

  For $j = J_0, \ldots, J-1$

$$R_j^{i,\Sigma}(F;\kappa)(x) = \int_{\Sigma} \Psi_j^{i,\Sigma}(x,y;\kappa)F(y)d\omega(y) \simeq \sum_{k=1}^{N_j} \alpha_k^{N_j} \Psi_j^{i,\Sigma}(x, y_k^{N_j};\kappa).$$

In this tree algorithm (pyramid scheme), we base the numerical integration on certain approximate formulas associated to known weights $w_k^{N_j} \in \mathbb{C}$ and prescribed knots $y_k^{N_j} \in \Sigma,\ j = J_0, \ldots, J$. Note that j denotes the scale of the discretized scaling function, N_j is the number of integration points to the accompanying scale j, and k denotes the index of the integration knots within the integration formulas under consideration, i.e.,

$$P_j^{i,\Sigma}(F;\kappa)(x) \simeq \sum_{k=1}^{N_j} w_k^{N_j} F(y_k^{N_j}) \Phi_j^{i,\Sigma}(x, y_k^{N_j};\kappa), \qquad j = J_0, \ldots, J, \quad (2.59)$$

$$R_j^{i,\Sigma}(F;\kappa)(x) \simeq \sum_{k=1}^{N_j} w_k^{N_j} F(y_k^{N_j}) \Psi_j^{i,\Sigma}(x, y_k^{N_j};\kappa), \quad j = J_0, \ldots, J-1. \quad (2.60)$$

The pyramid scheme, as every recursive implementation, is divided into two parts, the initial step and the recursion step, as in [31], called pyramid step.

Initial step As mentioned before $P_J^{i,\Sigma}(F;\kappa)$ approximates, for a suitable, sufficiently large integer $J \in \mathbb{N}$, the right side of Equation (2.58) for all $x \in \Sigma$ with negligible error. Thus, according to Equation (2.59) we simply get

$$\alpha_k^{N_J} = w_k^{N_J} F(y_k^{N_J}),\ k = 1, \ldots, N_J.$$

Pyramid step (decomposition) The essential idea for the development of the recursive scheme is the existence of a (symmetric) kernel function $\Theta_j : \Sigma \times \Sigma \to \mathbb{C}$, such that

$$\Phi_j^{i,\Sigma}(x, y; \kappa) \simeq \int_\Sigma \Phi_j^{i,\Sigma}(z, x; \kappa)\Theta_j(y, z; \kappa)d\omega(z)$$

and

$$\Theta_j(x, y; \kappa) \simeq \int_\Sigma \Theta_j(z, x; \kappa)\Theta_{j+1}(y, z; \kappa)d\omega(z)$$

for $j = J_0, \ldots, J$.

Since the scaling functions are non-band-limited, the scale spaces $\mathcal{V}_j$ are infinite dimensional. This leads us to choose the functions Θ_j, for example, to be equal to

$$\Theta_j = \Phi_{j+L}^{i,\Sigma},\ j = J_0, \ldots, J,$$

for suitable $L \in \mathbb{N}_0$. By virtue of the approximate integration rules we thus obtain

$$\begin{aligned}
\int_\Sigma \Phi_j^{i,\Sigma}(\cdot, y; \kappa)F(y)d\omega(y) &\simeq \int_\Sigma \Theta_j(y, z; \kappa) \int_\Sigma \Phi_j^{i,\Sigma}(\cdot, z; \kappa)F(y)d\omega(z)d\omega(y) \\
&\simeq \int_\Sigma \Phi_j^{i,\Sigma}(\cdot, z; \kappa) \int_\Sigma \Theta_j(y, z; \kappa)F(y)d\omega(y)d\omega(z) \\
&\simeq \sum_{k=1}^{N_j} \alpha_k^{N_j} \Phi_j^{i,\Sigma}(\cdot, y_k^{N_j}; \kappa)
\end{aligned} \tag{2.61}$$

for $j = J_0, \ldots, J-1$, where

$$\alpha_k^{N_j} = w_k^{N_j} \int_\Sigma \Theta_j(y_k^{N_j}, y; \kappa)F(y)d\omega(y)$$

for $j = J_0, \ldots . J-1$ and $k = 1, \ldots, N_j$. Hence, according to Equation (2.61), we obtain

$$\begin{aligned}
\alpha_k^{N_j} &= w_k^{N_j} \int_\Sigma \Theta_j(y_k^{N_j}, y; \kappa) F(y) d\omega(y) \\
&\simeq w_k^{N_j} \int_\Sigma \int_\Sigma \Theta_{j+1}(z, y; \kappa) \Theta_j(y_k^{N_j}, z; \kappa) d\omega(z) F(y) d\omega(y) \\
&\simeq w_k^{N_j} \sum_{s=1}^{N_{j+1}} w_s^{N_{j+1}} \Theta_j(y_k^{N_j}, y_s^{N_{j+1}}; \kappa) \int_\Sigma \Theta_{j+1}(y_s^{N_{j+1}}, y; \kappa) F(y) d\omega(y) \\
&= w_k^{N_j} \sum_{s=1}^{N_{j+1}} w_s^{N_{j+1}} \Theta_j(y_k^{N_j}, y_s^{N_{j+1}}; \kappa) \alpha_s^{N_{j+1}}.
\end{aligned}$$

for all $j = J_0, \ldots, J-1$ and $k = 1, \ldots, N_j$.

In other words, the coefficients $\alpha_s^{N_{J-1}}$ can be calculated recursively from $\alpha_s^{N_J}$ given on the initial level J; $\alpha_k^{N_{J-2}}$ can be deduced from $\alpha_s^{N_{J-1}}$; etc. Finally, we obtain the decomposition scheme

$$P_j^{i,\Sigma}(F; \kappa) \simeq \sum_{k=1}^{N_j} \alpha_k^{N_j} \Phi_j^{i,\Sigma}(\cdot, y_k^{N_j}; \kappa), \qquad j = J_0, \ldots, J, \tag{2.62}$$

$$R_j^{i,\Sigma}(F; \kappa) \simeq \sum_{k=1}^{N_j} \alpha_k^{N_j} \Psi_j^{i,\Sigma}(\cdot, y_k^{N_j}; \kappa), \qquad j = J_0, \ldots, J-1. \tag{2.63}$$

Note that the coefficients α^{N_J} in the initial step do not depend on the choice of $\Theta_J = \Phi_{J+L}^{i,\Sigma}$. Furthermore, the functions Θ_j, $j = J_0, \ldots, J-1$, can be chosen independently of scaling function $\{\Phi_j^{i,\Sigma}\}_{j \in \mathbb{Z}}$ used in Equations (2.62) and (2.63).

In conclusion, the above considerations lead us to formulate (schematically) the *decomposition scheme* for a fixed value $\kappa \in \mathbb{C}$:

$F \to \alpha^{N_J} \to$	$\alpha^{N_{J-1}} \to \ldots \to$	$\alpha^{N_{J_0+1}} \to$	$\alpha^{N_{J_0}}$
$\downarrow$	$\downarrow$	$\downarrow$	$\downarrow$
$P_J^{i,\Sigma}(F; \kappa)$	$P_{J-1}^{i,\Sigma}(F; \kappa)$	$P_{J_0+1}^{i,\Sigma}(F; \kappa)$	$P_{J_0}^{i,\Sigma}(F; \kappa)$

Because the described scheme has a tree representation form, we can easily construct also the *reconstruction scheme* by inversion of the decom-

position scheme:

$$
\begin{array}{lll}
\alpha^{N_{J_0}} & \alpha^{N_{J_0+1}} & \alpha^{N_{J-1}} \\
\downarrow & \downarrow & \downarrow \\
P_{J_0}^{i,\Sigma}(F;\kappa) & P_{J_0+1}^{i,\Sigma}(F;\kappa) & P_{J-1}^{i,\Sigma}(F;\kappa) \\
\quad \searrow & \quad \searrow & \quad \searrow \\
R_{J_0}^{i,\Sigma}(F;\kappa) + \rightarrow & R_{J_0+1}^{i,\Sigma}(F;\kappa) + \rightarrow \ldots \rightarrow & R_{J-1}^{i,\Sigma}(F;\kappa) + \rightarrow P_{J}^{i,\Sigma}(F;\kappa)
\end{array}
$$

where $P_j^{i,\Sigma}(F;\kappa)$, $R_j^{i,\Sigma}(F;\kappa)$ are given by Equations (2.62), (2.62), respectively.

The idea of the reconstruction scheme can be described as follows: We start from a trend solution, a rough approximation on the low level $J_0 \in \mathbb{N}_0$. Regarding the more and more space-localizing properties of the wavelet functions, the solution on the next level $P_{J_0+1}^{i,\Sigma}(F;\kappa)$ can be obtained by addition of the detail information $R_{J_0}^{i,\Sigma}(F;\kappa)$ on the current level. This procedure can be recursively continued. Schematically, by way of an example, the reconstruction algorithm with the (2D) scaling and wavelet functions of type 6 is shown in Figure 2.4.

The idea of the decomposition scheme is completely different (see Figure 2.5): We start from a scaling function with high level J. The data will be „read in“ at this level and recursively decomposed by the tree algorithm (pyramid scheme). The decomposition provides a decorrelation of the data at different levels and at different positions.

The numerical effort of a pyramid step can be drastically reduced by use of a panel-clustering method (e.g., fast multipole procedures as developed by [36], [37], [38], [39]). In doing so, the evaluations take advantage of the localizing structure of the kernels.Roughly spoken, the kernel is split into a near field and a far field component. The far field component is approximated by a certain expression obtaining the ‘low frequency contributions’. For the points close to the evaluation position, the evaluation uses the exact near field of the kernel. For the remaining points, the approximate far field contributions are put together.

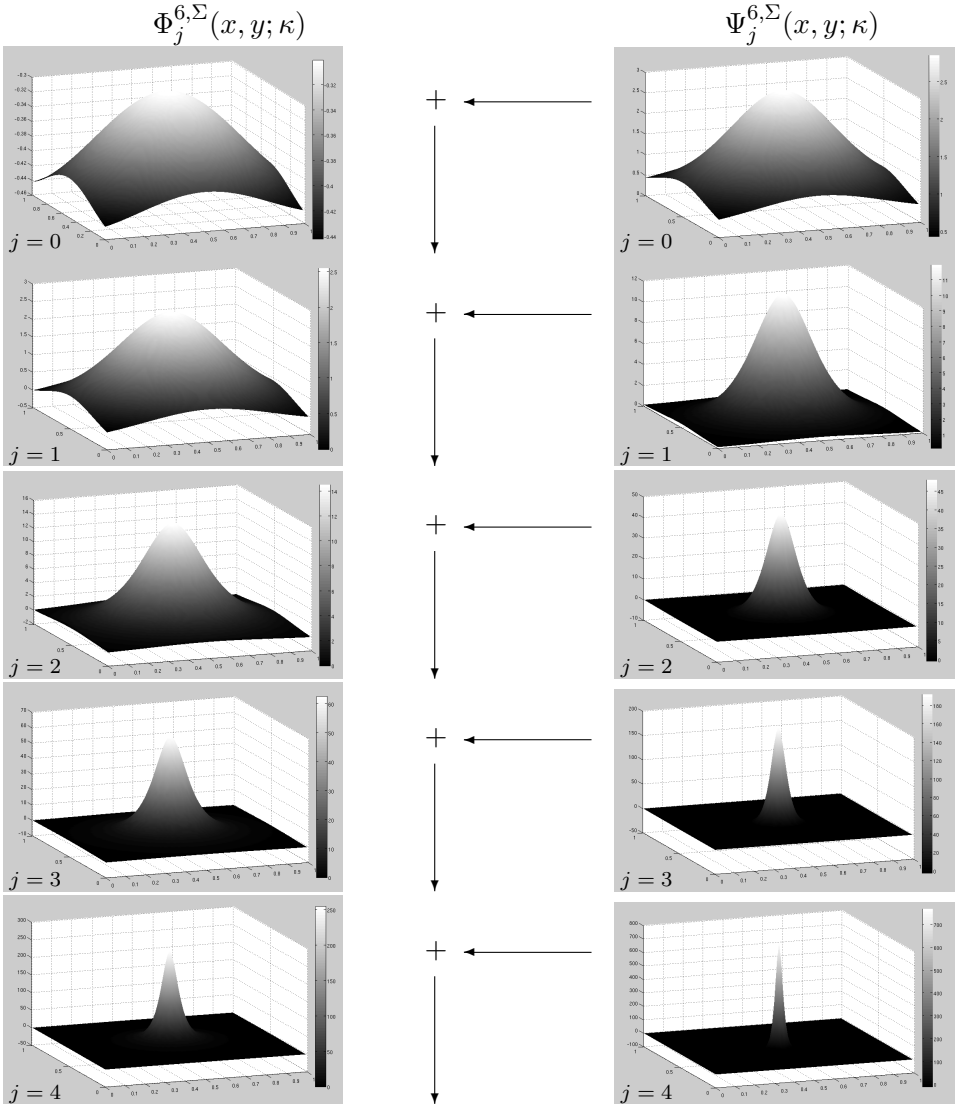

Figure 2.4: Reconstruction scheme (a tree algorithm) with (2D) wavelet functions of type 6. ($\tau = 2^{-j}, 0 \leq y_1, y_2 \leq 1$, $x_1 = 0.5, x_2 = 0.5$, $\kappa = 1.0$)

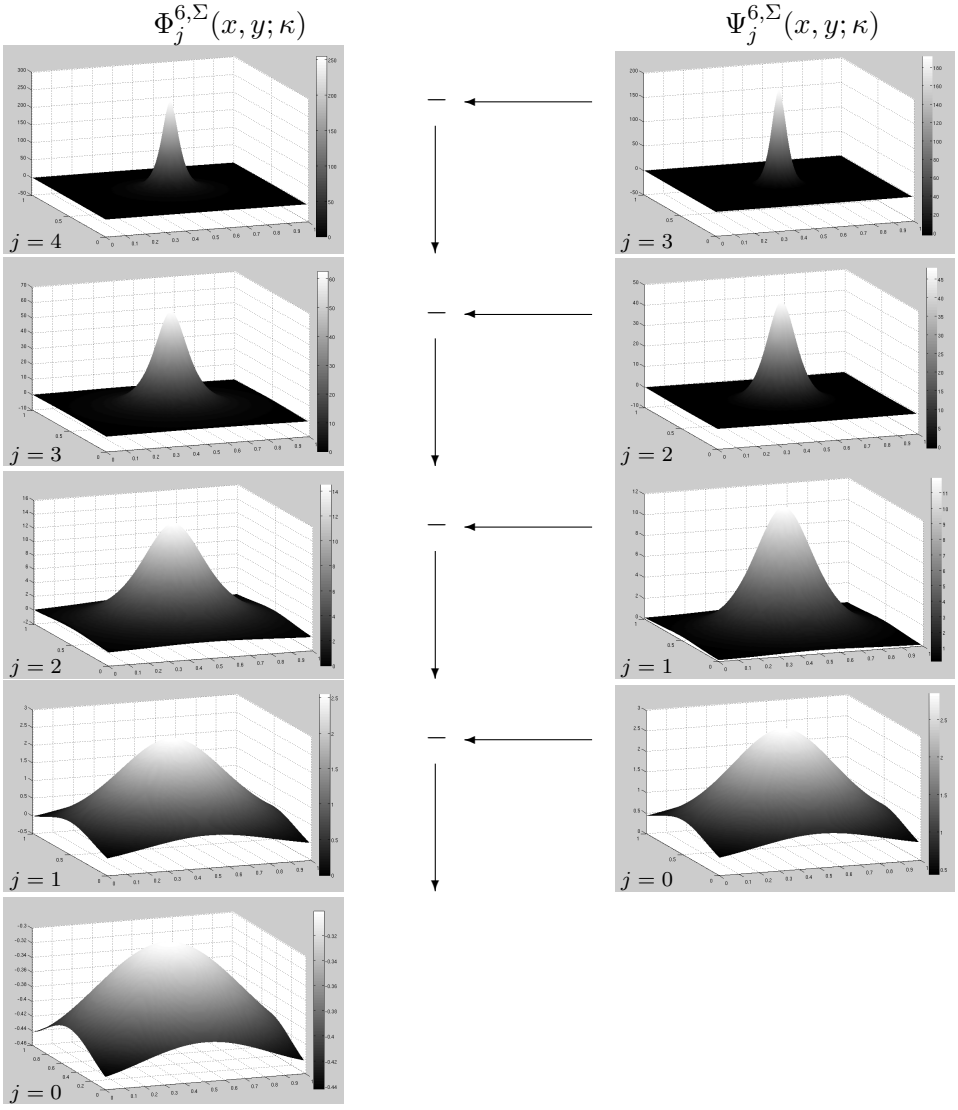

Figure 2.5: Decomposition scheme (a tree algorithm) with (2D) wavelet functions of type 6. ($\tau = 2^{-j}, 0 \leq y_1, y_2 \leq 1$, $x_1 = 0.5, x_2 = 0.5$, $\kappa = 1.0$)

Chapter 3

An Additive Scheme for Seismic Modeling

This chapter is devoted to a finite-difference approach applied to the modeling of the acoustic wave transmission in inhomogeneous media. We base our high performance computation on an additive scheme developed by Samarskij, Vabishevich (see [74]) that approximates a second order differential equation. In fact, such a scheme can be successfully used for the construction of the alternating direction implicit (ADI) method (e.g., [26]) as well as for the domain decomposition. At the end of this chapter, we present an algorithm for seismic migration by use of the additive scheme.

3.1 Additive Scheme for a Second Order Differential Equation

We begin our consideration with the brief recapitulation of the theory developed by Samarskij, Vabishevich (cf. [74]).

We search for a function U in a suitable reference space (allowing the specification of a Hilbert space structure, i.e., norms and angles), which satisfies

$$\frac{d^2}{dt^2}U(t) + \mathcal{A}U(t) = F(t),\ t > 0, \tag{3.1}$$

$$U(0) = u^0, \tag{3.2}$$

$$\frac{d}{dt}U(0) = v^0. \tag{3.3}$$

If the operator $\mathcal{A}$ is positive definite, self-adjoint, and stationary, the following operator decomposition can be used

$$\mathcal{A} = \sum_{\alpha=1}^{p} \mathcal{A}^{(\alpha)}. \tag{3.4}$$

We focus on the explicit scheme according to the operator decomposition (3.4):

$$\frac{u^{n+1} - 2u^n + u^{n-1}}{\tau^2} + \mathcal{A}u^n = \phi^n.$$

By using of the simplest multiplicative regularization, we have

$$\frac{u^{n+1} - 2u^n + u^{n-1}}{\tau^2} + (\mathcal{I} + \mu\mathcal{A})^{-1} \mathcal{A}u^n = \phi^n. \tag{3.5}$$

Now, regarding the operator decomposition (3.4), we rewrite the explicit scheme as follows

$$\frac{u^{n+1} - 2u^n + u^{n-1}}{\tau^2} + \sum_{\alpha=1}^{p} \mathcal{A}^{(\alpha)} u^n = \phi^n.$$

The multiplicative perturbation of each operator components yields the additive difference scheme

$$\frac{u^{n+1} - 2u^n + u^{n-1}}{\tau^2} + \sum_{\alpha=1}^{p} (\mathcal{I} + \mu\mathcal{A}^{\alpha})^{-1} \mathcal{A}^{\alpha} u^n = \phi^n. \tag{3.6}$$

Theorem 3.1 *(cf. [74]) For* $\sigma \geq \frac{p}{4}$ $(\mu = \sigma\tau^2)$ *and all* $\tau > 0$, *the additive difference scheme* (3.6) *for the problem* (3.1)-(3.3) *is unconditionally stable, i.e., the scheme* (3.6) *converges for all time-steps* τ.

3.2 Approximate Solution of the Wave Equation

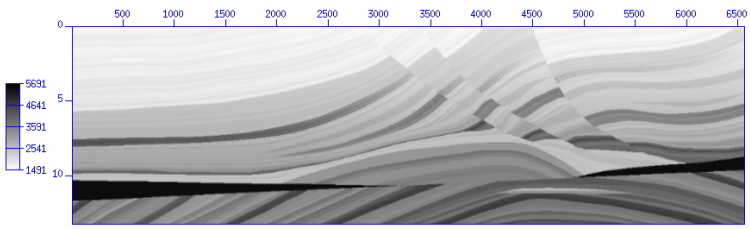

Figure 3.1: The strong velocity field of the 'Marmousi' model

In this section we apply the additive difference scheme to the problem of the wave propagation in an inhomogeneous medium. For this reason, we rewrite the acoustic wave equation according to the form (3.1)

$$\frac{\partial^2}{\partial t^2}\tilde{U}(x,t) - C(x)^2\Delta\tilde{U}(x,t) = \tilde{F}(x,t), \text{ in } \Sigma^{int}\times[0,T], \tag{3.7}$$

$$\tilde{U}(x,0) = 0, \tag{3.8}$$

$$\frac{\partial}{\partial t}U(x,0) = 0, \tag{3.9}$$

where $\tilde{U}$ is the solution of the wave equation (the pressure wave field) and $\tilde{F}$ is defined by

$$\tilde{F}(x,t) = \begin{cases} F(t), & x = x_s; \\ 0, & x \neq x_s, \end{cases} \tag{3.10}$$

where F denoted the seismogram recorded at position x_s.

In accordance with the theory described in Section 3.1, we have for the problem (3.8)-(3.9) the following representation

$$\frac{\tilde{u}^{n+1} - 2\tilde{u}^n + \tilde{u}^{n-1}}{\tau^2} + \sum_{\alpha=1}^{p}\left(\mathcal{I} + \mu\mathcal{A}^{\alpha}\right)^{-1}\mathcal{A}^{\alpha}\tilde{u}^n = \tilde{\phi}^n, \tag{3.11}$$

where $\tilde{u}^n$ denotes the discretized value of the function $\tilde{U}$ at the time-step $t_n, n = 1,\ldots,N$, while $\tilde{\phi}^n$ is the discretization of $\tilde{F}$. The operator $\mathcal{A}$ denotes the finite difference approximation of $-C(x)^2\Delta\tilde{U}(x,t)$ and can be represented as $\mathcal{A} = \sum_{\alpha=1}^{p}\mathcal{A}^{(\alpha)}$, where $A^{(\alpha)}$ can be used for the domain decomposition into p domains (usually applied for three-dimensional models) as well as for direction splitting into p directions (usually applied for two-dimensional models).

Actually, the difference representation (3.11) contains two parts, i.e., implicit and explicit one. In this sequence, Equation (3.11) has to be solved

(i) For each $\alpha = 1,\ldots,p$ the linear system of equation is to solve

$$\left(\mathcal{I} + \mu\mathcal{A}^{(\alpha)}\right)w^{(\alpha)} = \mathcal{A}^{(\alpha)}\tilde{u}^n. \tag{3.12}$$

(ii) The explicit step is to calculate

$$\frac{\tilde{u}^{n+1} - 2\tilde{u}^n + \tilde{u}^{n-1}}{\tau^2} + \sum_{\alpha=1}^{p} w^{(\alpha)} = \tilde{\phi}^n. \tag{3.13}$$

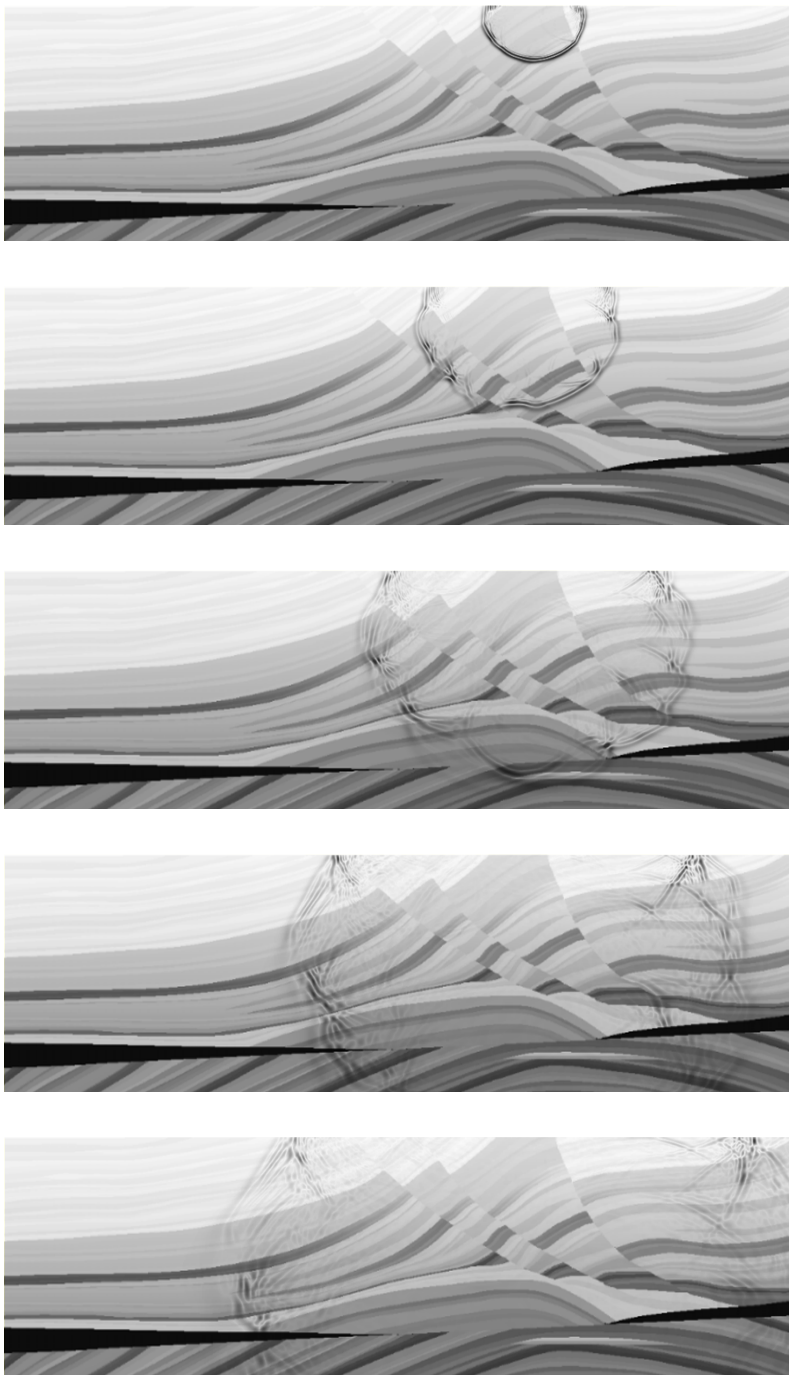

Figure 3.2: Wave transmission illustrated to $0.6, 1.1, 1.6, 2.1, 2.6 sec$ in the strong velocity field of the 'Marmousi' model (Fig. 3.1)

Example We consider the commonly used (2D) 'Marmousi' model described by Versteeg in [75]. This model is the most useful model in the history of geophysics, and is applied to calibrate imaging algorithms. We focus on the strong velocity field of the 'Marmousi' model, which is illustrated in Figure 3.1. In order to demonstrate examples of the transmission of seismic waves, we consider the function F (that has to be substitute into Equation (3.10))

$$F(t) = \exp(-\gamma^2 t^2)\cos(2\pi\omega_{peak}t), \tag{3.14}$$

which according to the practical experience is used to simulate an impulse of an energy source in seismic experiment. In Equation (3.14) γ denotes a damping parameter, ω_{peak} is a peak angular frequency. We demonstrate an example of the wave propagation by setting the function F on the surface at point $x = 6000m$ as an initial value. Then, we apply the numerical scheme (3.12), (3.13) in combination with non-reflecting boundary conditions (e.g. [63]). The resulting snapshots of the wave transmission to $0.6, 1.1, 1.6, 2.1, 2.6sec$ are illustrated in Figure 3.2.

3.3 Imaging Condition and Seismic Migration

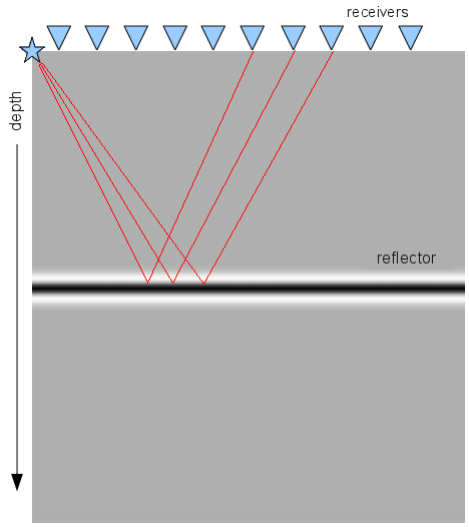

Figure 3.3: Seismic experiment.

In this section we construct a seismic migration method. For this purpose, we again use the example of seismic data collecting illustrated in Figure

3.3. This seismic experiment can be considered as two separate problems, i.e., the simulation of the source wave field, and the extrapolation of the receivers wave field by recorded seismogram. Such configuration is usually called a (shot-gather) *pre-stack migration*. If, in the seismic experiment, we have only one source and only one receiver, which occupy the same position, we obtain the *post-stack migration* (or migration of *zero-offset data set*).

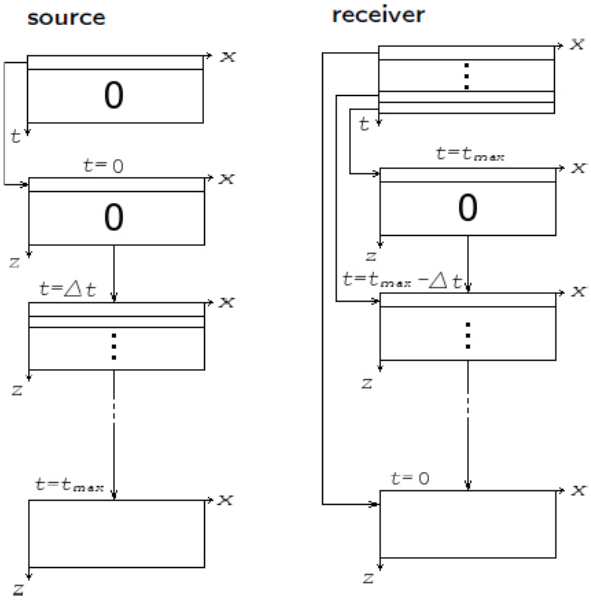

Figure 3.4: Schematic representation of the source wave field modeling (left) and of the receiver wave field extrapolation (right). t_{max} denotes here the last recorded time T, Δt is the time sampling.

In order to compute the desired seismic image M of the subsurface interior, the *imaging condition* (e.g., [6] and the references therein; [40]), which is mathematically represented as the convolution of both wave fields to the time zero, applies

$$M(x) = \int_0^T S(x,t)R(x,t)dt,$$

where S and R denote source and receiver wave fields, respectively. Moreover, if we have more than one source position, we obtain for the image M

the following representation

$$M(x) = \sum_{s} \int_{0}^{T} S_s(x,t) R_s(x,t) dt, \tag{3.15}$$

where the sum over s denotes the sum over all source positions, S_s is the source wave field in the initial position s, and R_s is the receiver wave field corresponding to the current source position s.

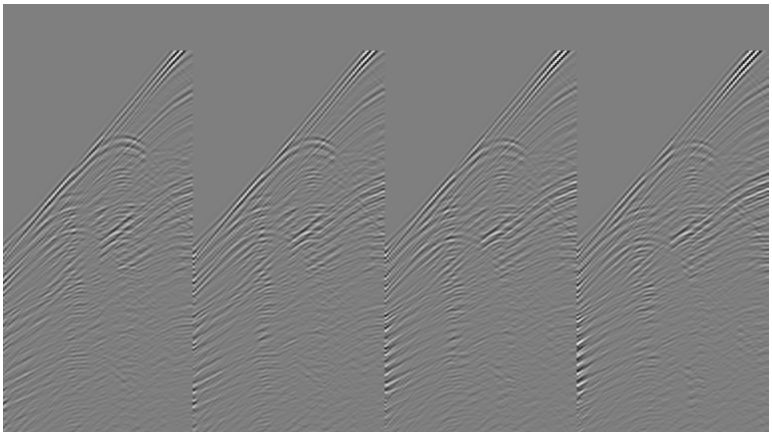

Figure 3.5: The 121-124th shot gathers of the 'Marmousi' model.

Remark 3.2 *In order to reduce some modeling artifacts, modified imaging conditions can be used (for more details the reader is referred, e.g., to [44], [45] and the references therein).*

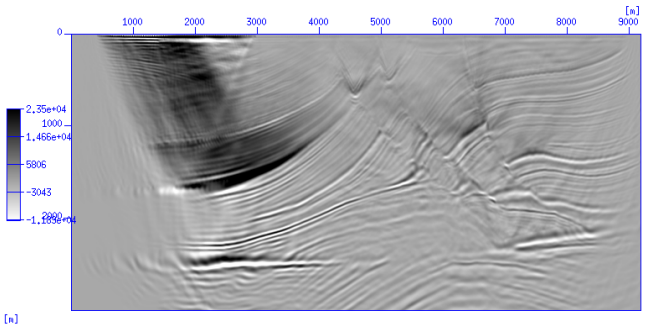

Figure 3.6: The migration result of the 'Marmousi' model.

By using of the imaging condition (3.15), we present a seismic migration method. The most intuitive understandable migration algorithm is the

reverse-time migration developed by Baysal (see [2], [3]). This method is schematically illustrated in Figure 3.4: the source wave field is simulated in direct time by using the Ricker wavelet as initial value; the receiver wave field is extrapolated in reverse time by using recorded seismogram as initial value.

Example We turn back to the 'Marmousi' model (see [75]). This data set consists of 240 shot gathers recorded during $2.7s$ with the time sampling $4ms$. Each shot gather contains 96 receiver positions. The 121^{st}-124^{th} shot gather is illustrated in Figure 3.5. We apply the aforementioned additive scheme with absorbing boundary conditions [63] to the data set and calculate the seismic image by applying the reverse time approach using imaging condition (3.15). The (migrated) seismic image is illustrated in Figure 3.6.

Chapter 4

Postprocessing by Helmholtz FWT

This chapter is devoted to the application of the developed Helmholtz wavelet theory for seismic data postprocessing. In Section 4.1 we recapitulate the Helmholtz FWT in accordance with goals of noise and artifact attenuation. Afterwards, in Section 4.2, we demonstrate some numerical results.

4.1 Construction of a Postprocessing Algorithm

In the previous chapter we briefly described the well-known procedure of reverse time migration and demonstrated its numerical implementation by use of an additive scheme. This migration algorithm is a powerful tool for imaging complex geological structures because of its ability to calculate all types of waves (e.g., head waves, multi-pathing, turning waves, etc), and also to handle steep dips. However, the reverse time migration is very sensitive to the accuracy of the velocity model, and, therefore, produces low-frequency artifacts at the places of sharp velocity contrasts (see, e.g., [40], [45]). These artifacts are created by the unwanted cross-correlation of head-waves, diving waves and back-scattered waves by the application of the imaging condition.

The low-frequency events exert negative influence on the recognition of seismic attributes from seismic data needed for geological interpretation and analysis. These attributes can help to predict physical properties of the Earth subsurface, and to map of faults and fractures. Their classification may be based on time, amplitude, frequency, and attenuation (cf. [12], [13]).

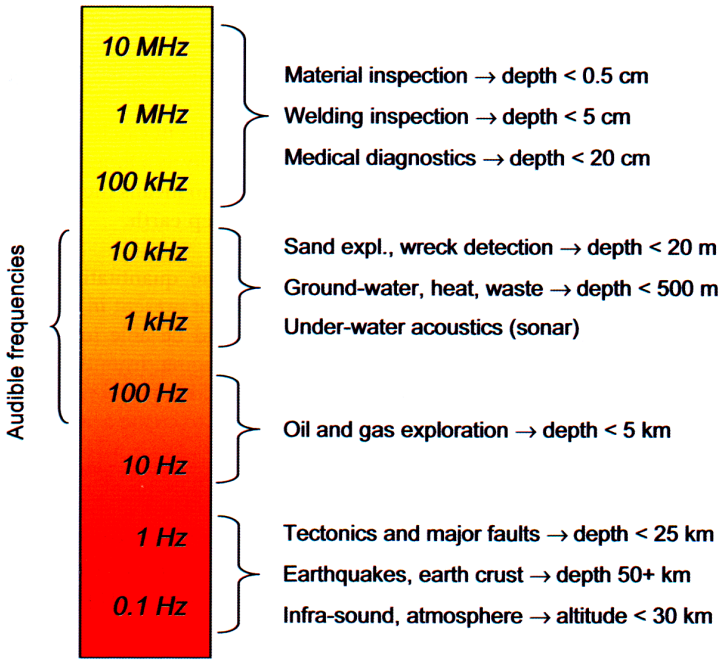

Figure 4.1: Experienced frequency range of currently used acoustical imaging applications, with depth of penetration (source [35]).

Because each currently used acoustical imaging application corresponds to the frequency range specific only for this application as illustrated in Figure 4.1, we can apply a postprocessing algorithm that filters out significant frequencies and, in addition, attenuates noise and artifacts. For this purpose, we apply our wavelet theory as proposed in Chapters 1, 2.

The main reason for our work is the Helmholtz wavelet decomposition, which is provided by Corollary 2.37, i.e., for a regular surface $\Sigma \subset \mathbb{R}^3$, a continuous or square-integrable function F on Σ, an integer $J_0 \in \mathbb{Z}$, and a sufficiently large number $J \in \mathbb{N}$

$$F \simeq \int_\Sigma \Phi_{J_0}^{3,\Sigma}(\cdot, y; \kappa) F(y) d\omega(y) + \sum_{j=J_0}^{J-1} \int_\Sigma \Psi_j^{3,\Sigma}(\cdot, y; \kappa) F(y) d\omega(y) \tag{4.1}$$

$$\simeq P_{J_0}^{3,\Sigma}(F; \kappa) + \sum_{j=J_0}^{J-1} R_j^{3,\Sigma}(F; \kappa). \tag{4.2}$$

The scaling functions $\Phi_j^{3,\Sigma}(x, 0; \kappa)$ and the wavelet functions $\Psi_j^{3,\Sigma}(x, 0; \kappa)$ are illustrated in Figure 4.2. The efficient and economical implementation

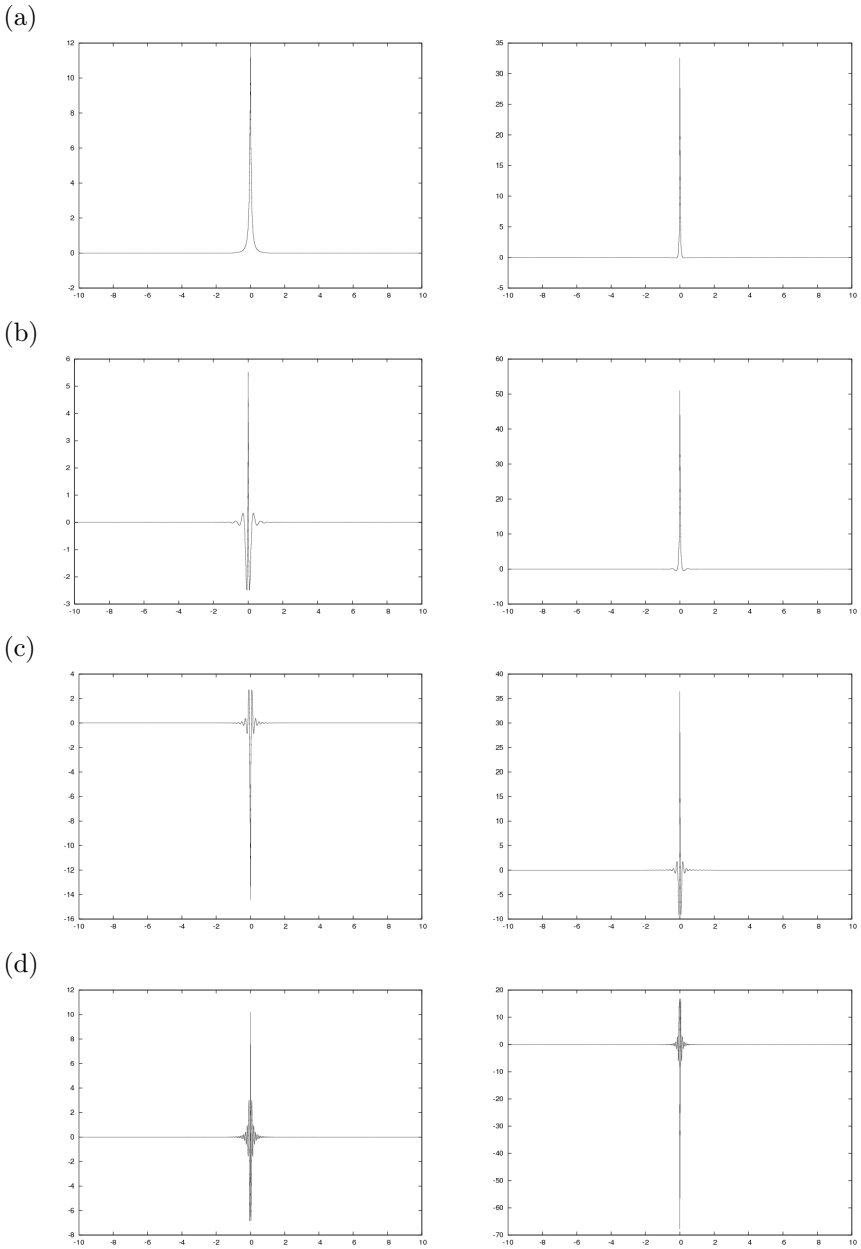

Figure 4.2: The scaling functions $\Phi_j^{3,\Sigma}(x,0;\kappa)$ (left) and the wavelet functions $\Psi_j^{3,\Sigma}(x,0;\kappa)$ (right), where $j=-3$, $x=-10,\ldots,10$, $C=2.0km/s$: (a) $f=0.5Hz$, (b) $f=5Hz$, (c) $f=10Hz$, (d) $f=20Hz$.

of the last equation can be accomplished by the Helmholtz FWT in form of the tree algorithm described in Section 2.5.

The multiscale representation (4.2) may be applied to perform the analysis of seismic attributes from a given seismic section (the given function F), as well as to obtain the multiscale analysis and to calculate the attributes for each resolution scale (e.g., [64]).

Remark 4.1 *Note that - because of the space localization properties of scaling as well as wavelet functions - for the computation of the filtered versions of the function F on the coarser scale, we need fewer control points. That allows for the use of the same allocated memory for saving the decomposition coefficients used, for example, for the further entropy coding in order to compress a seismic section (cf. [5]).*

4.2 Numerical Tests

We consider the migration result of the 'Marmousi' model presented in Chapter 3, and shown in Figure 3.6. Our goal is to reduce the low-frequency artifacts, and to reveal additional informations relevant for seismic data interpreters.

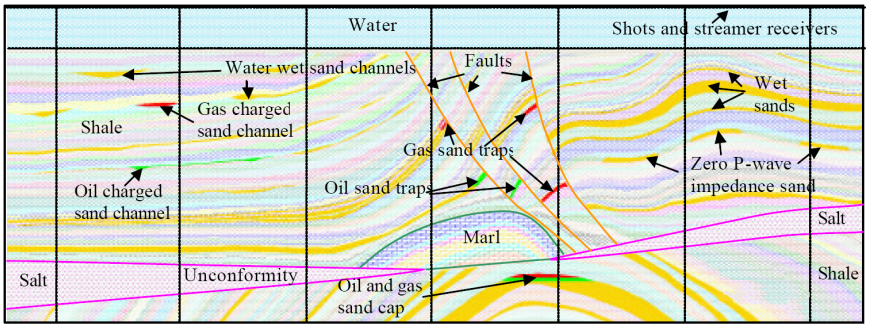

Figure 4.3: Lithology and model features including the location of hydrocarbons surfaces (source [53]).

In order to be able to verify further results, we briefly review the geological interpretation illustrated in Figure 4.3 of the 'Marmousi' model (cf. [53], [75]): The geologic history underlying this model consists of two quite different phases. The first corresponds to a continuous sedimentation of marls and carbonates. At the end of the sedimentation, these deposits were slightly folded and then eroded with erosion surface being flat. The second began with the deposition of an isopachous seliferous evaporitic series. On

this series a clayeymarly series rich in organic matter was deposited. These sediments were followed by a thick deposit of shaly-sandy detrital sediments with a western source whose facies thickness was governed by continuous lateral creep of the salt resulting from the overburden pressure. Linked to this salt creep, which locally causes complete disappearance of the salt, slanting growth faults appeared which were continuously active during the deposition of the detrital series.

Thereby, the main targets of this data set are salt structure related traps and the deeper anticlinal structure, under which a single gas and oil accumulation is located (see Figure 4.3).

In what follows we are interested in the multiscale decomposition of seismic data. For this reason we treat Σ as a boundary of a cube with the length $9.125km$, the width $3.000km$, and an arbitrary height. Each side of this cube is represented by a regular surface element Ξ^i, $i = 1, \ldots, 6$, so that $\Sigma = \cup_{i=1}^{6} \overline{\Xi^i}$. The seismic data set, i.e., the collection of discrete values of F is assumed to be given on the upper rectangular surface element Ξ^1. For the purposes of numerical tests, we associate the function F with the migration result of the 'Marmousi' model calculated by the additive scheme in Section 3.3 with the sampling interval $12.5m$ (corresponds to 730 pixels) in the lateral direction and $4.0m$ (750 pixels) in the depth and illustrated in Figure 3.6. The discrete data set of F is then handled by the tree algorithm (decomposition scheme) as described in Section 2.5, i.e., according to the formulas (4.1), (4.2) on a rectangular surface element Ξ^i in pointwise sense.

With respect to the tableau, which is illustrated in Figure 4.1, the frequency range applied in the hydrocarbon industry lies approximatively between 10 and $100Hz$. We use the aforementioned decomposition scheme in order to reveal additional information about the geological structure, and in order to attenuate noise and artifacts. We focus on the parameter κ (wave number) given by

$$\kappa = \frac{2\pi}{\lambda} = \frac{\omega}{C}, \tag{4.3}$$

where λ is the wave length, ω is an angular frequency ($\omega = 2\pi f$), C is a medium velocity. For fixed f and after the application of the Helmholtz FWT, we obtain the multiscale representation, which is associated to the wave number κ, of a given seismic section.

In order to explain our postprocessing procedure we have to comment on the role of κ from numerical point of view. On the one hand, our wavelet

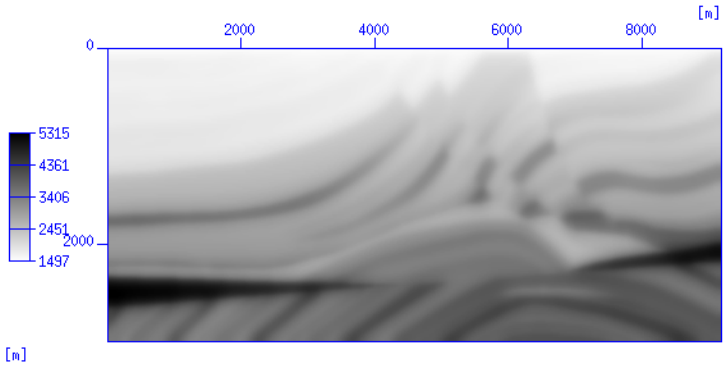

Figure 4.4: The smooth velocity field of the 'Marmousi' model.

theory as presented in Chapter 2 provides multiscale decomposition globally on Σ for a constant κ. On the other hand, the Helmholtz wavelets – at least for large J – show extreme space localization for which a constant value κ has to be taken into account. In consequence, when we are interested in numerics, the tree algorithm (decomposition scheme) for a data point x of the seismic section involves only extremely localized areas with constant κ. This is the reason why we finally decided – for numerical purposes – to consider „the constant κ to be different from point to point", such that seismic sections become attackable in a realistic way. In other words, our wavelet theory enables us to use the values κ to be dependent on the position x to be discussed.

Contrary to the theoretical approach as presented in this thesis, but consistently with the space localization properties of the Helmholtz wavelets we therefore understand κ as given by Equation (4.3) to be a function of the point x of the regular surface element of Σ containing the given information for postprocessing. More concretely, the decomposition scheme can be further represented as follows.

Initial (read-in) step For a suitable sufficiently large $J \in \mathbb{N}$, and a given frequency f, we read in the (discrete) seismic data F and the corresponding (discrete) velocity model C. F is associated by P_J^{3,Ξ^i}.

Pyramid (decomposition) step For a given $J_0 \in \mathbb{N}, J_0 < J$ the sections P_j^{3,Ξ^i} are to be calculated for $j = J-1, \ldots, J_0$.

1. We choose the integration knots $y_k^{N_j} \in \Xi^i$ and the corresponding weights $w_k^{N_j} \in \mathbb{C}$.
2. For each $x \in \Xi^i$ we set $\kappa_x = \dfrac{2\pi f}{C(x)}$ and compute
   (a) $R_j^{3,\Xi^i}(F;\kappa_x) \simeq \sum_{k=1}^{N_j} \alpha_k^{N_j} \Psi_j^{3,\Xi^i}(x, y_k^{N_j}; \kappa_x)$.
   (b) $P_{j-1}^{3,\Xi^i}(F;\kappa_x) = P_j^{3,\Xi^i}(F;\kappa_x) - R_j^{3,\Xi^i}(F;\kappa_x)$.
3. While $j > J_0$ we set the current scale $j = j-1$, repeat step 1.

By use of our algorithm we obtain multiscale representations of the input seismic data, i.e., discrete values of F (Figure 3.6) over the selected frequency into the low-pass filtered (scale) information and band-pass filtered (detail) information. For the discrete choices of the scaling parameter we use $\tau_j = 1 - \cos(2^{-j}\pi)$, and for C in Equation (4.3) we use the smooth velocity field illustrated in Figure 4.4. In order to understand how the decomposition works, we study, for example, the result of the Helmholtz FWT illustrated in Figure 4.5. The original values of F (730×750 pixels) is recovered from the sum of the low-pass filtered information $P_{10}^{3,\Xi^1}(F;\kappa)$ (365×375 pixels) and the band-pass filtered information $R_{10}^{3,\Xi^1}(F;\kappa)$ (365×375 pixels). The section $P_{10}^{3,\Xi^1}(F;\kappa)$ is obtained as a sum of $P_9^{3,\Xi^1}(F;\kappa)$ (182×187 pixels) and $R_9^{3,\Xi^1}(F;\kappa)$ (182×187 pixels). The section $P_9^{3,\Xi^1}(F;\kappa)$ is calculated from $P_8^{3,\Xi^1}(F;\kappa)$ (90×93 pixels) and $R_8^{3,\Xi^1}(F;\kappa)$ (90×93 pixels).

Now we focus on the multiscale analysis (scale and detail illustrations) obtained by the Helmholtz FWT and shown in Figures 4.5–4.11.

Since our target frequencies are $10Hz$ to $100Hz$, the representation over $0.5Hz$ yields no specific details. Nevertheless, as it can easily be seen in Figure 4.5 by comparing the section of F and the band-pass filtered sections, the application of this decomposition reduces the low-frequency artifacts attended in the input seismic section.

The low-frequency artifacts, which are created by unwanted internal reflections and their cross-correlation, can be recognized from the band-pass filtered sections in Figure 4.6.

Moreover, the frequency range, at which a given reflection is dominant, is very useful, because by analyzing a given reflection at different resolutions we are able to study the frequency-dependent attenuation (see, e.g., [64]). For example, the high amplitude events in the center of $R_9^{3,\Xi^1}(F;\kappa)$ and $R_8^{3,\Xi^1}(F;\kappa)$ of the decomposition, appearing at about $10Hz$ (Figure 4.7), we associate (optically) with the oil sand traps that are marked in Figure 4.3.

In Figure 4.8 the decomposition over $20Hz$ is presented. The high-amplitude reflectors can easily be identified in the band-pass filtered sections that are also clearly visible in the input section. Additionally, we can better recognize the faults, the salt dome and the deeper anticlinal structure (cf. Figure 4.3) in $R_{10}^{3,\Xi^1}(F;\kappa), R_9^{3,\Xi^1}(F;\kappa)$.

The band-pass filtered sections illustrated in Figure 4.9 provide finer details that are difficult to discern in F.

Figures 4.10 and 4.11 demonstrate a decomposition over $40Hz$ and $50Hz$, respectively. Their detail information sections visualize finer structures of the salt dome as well as of low-amplitude reflectors.

Because $250Hz$ is out of the frequency range, which is significant for the oil and gas industry, the band-pass filtered sections illustrated in Figure 4.12 contain computational artifacts and noise only.

As a result of the interpretation of the developed Helmholtz FWT and the multiscale representations of the synthetic seismic data set ('Marmousi' model), we are led to state the following advantages:

- The Helmholtz FWT enables us to decompose noisy seismic data sets into multiscale low-pass and band-pass filtered series over a selected frequency. This multiscale technique can be applied in the fields of seismic reflection analysis to detect finer structural information.

- The wavelet transform allows the efficient and economical implementation in form of a tree algorithm for fast numerical computation.

- The multiscale representation can further be applied to the seismic data compression by using entropy coding algorithms.

In conclusion, the Helmholtz FWT can be applied by the interpreters in order to get additional information for analyzing seismic attributes.

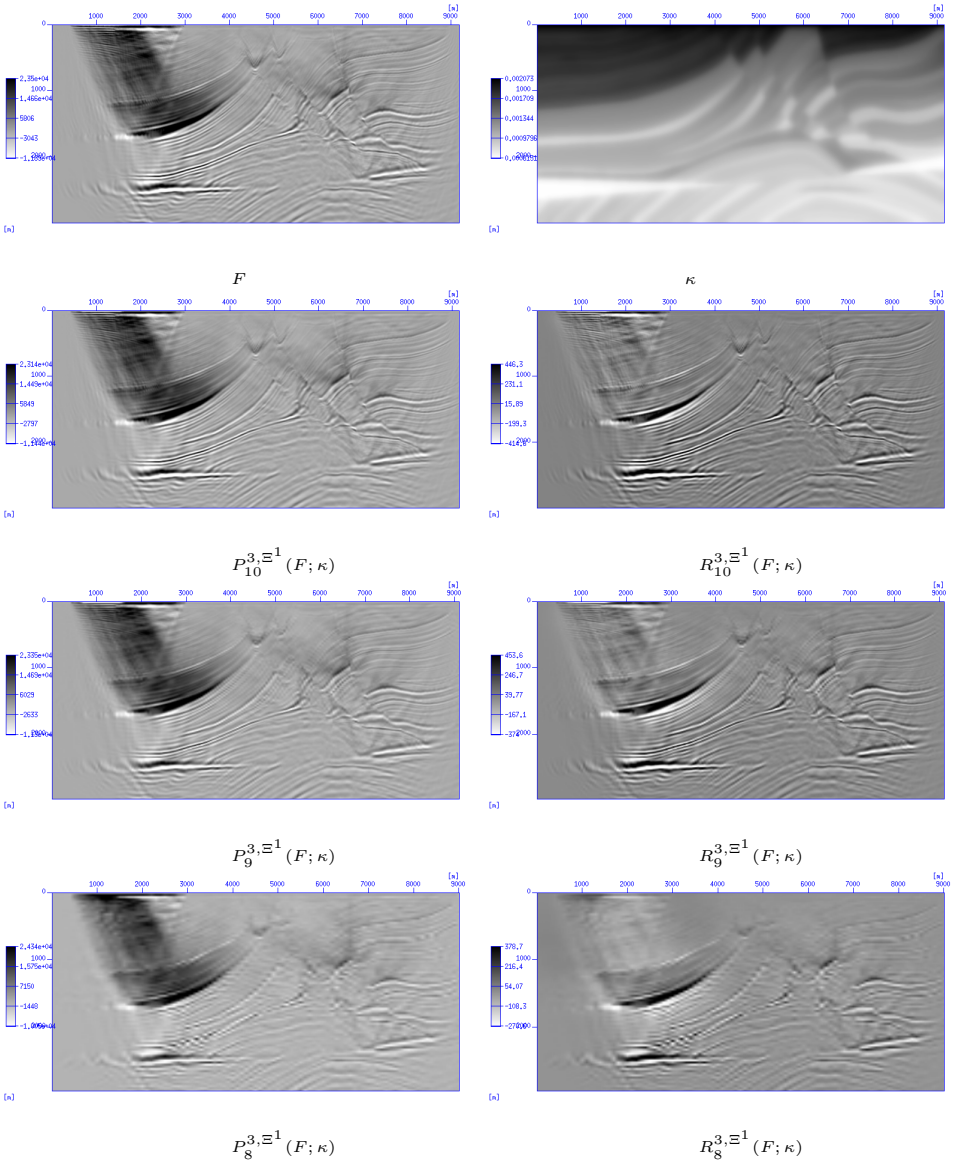

Figure 4.5: Multiscale analysis of the seismic section F (in $[m]$) (Fig. 3.6) for $f = 0.5Hz$.

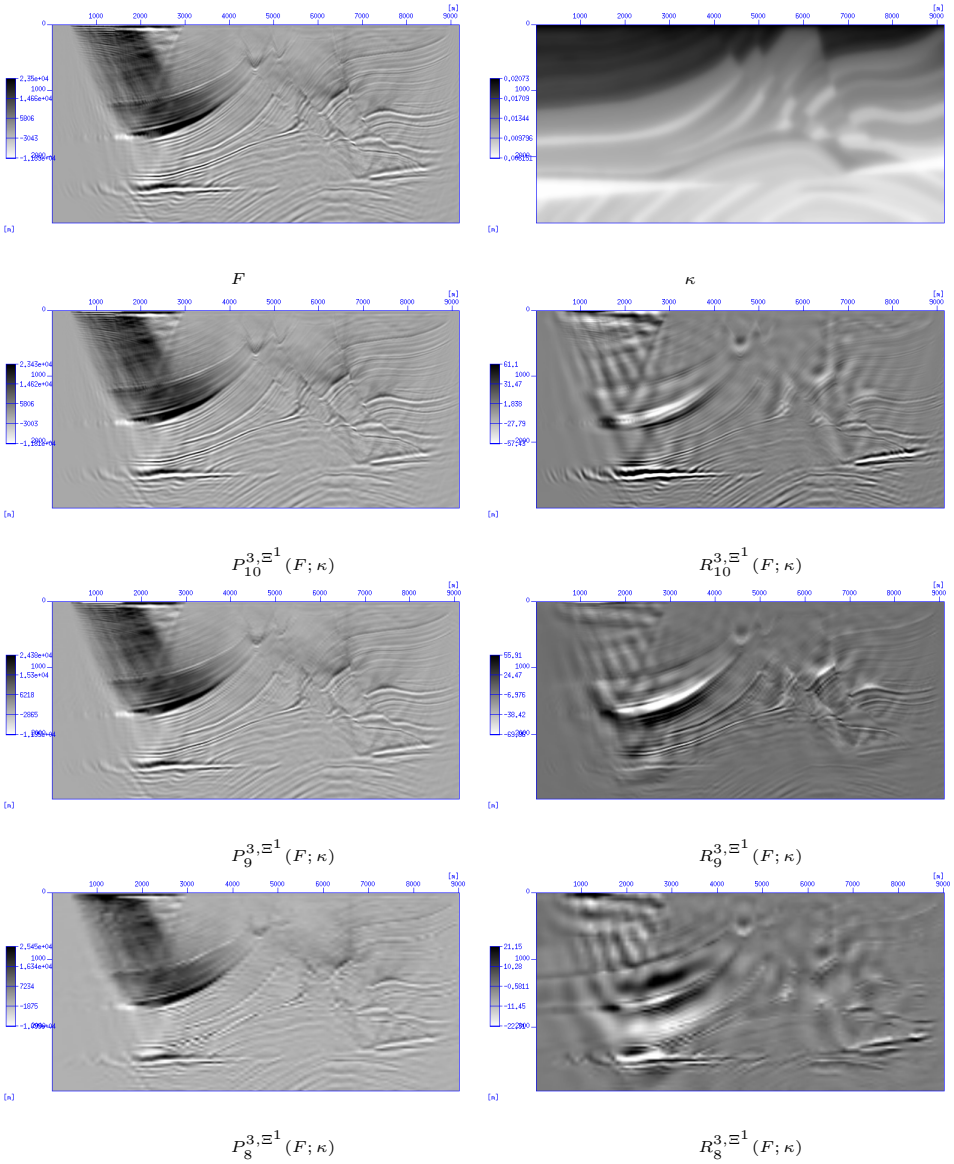

Figure 4.6: Multiscale analysis of the seismic section F (in $[m]$) (Fig. 3.6) for $f = 5Hz$.

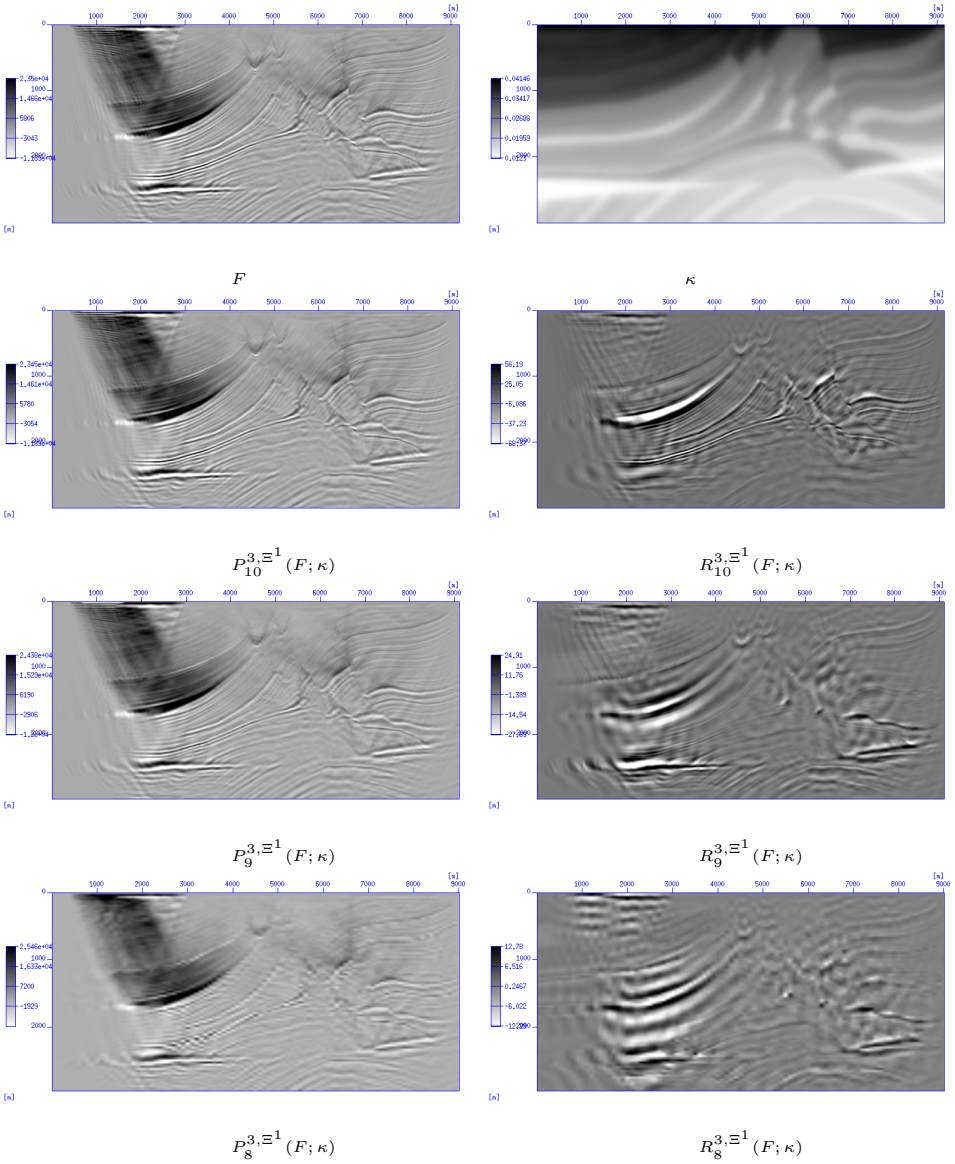

Figure 4.7: Multiscale analysis of the seismic section F (in $[m]$) (Fig. 3.6) for $f = 10Hz$.

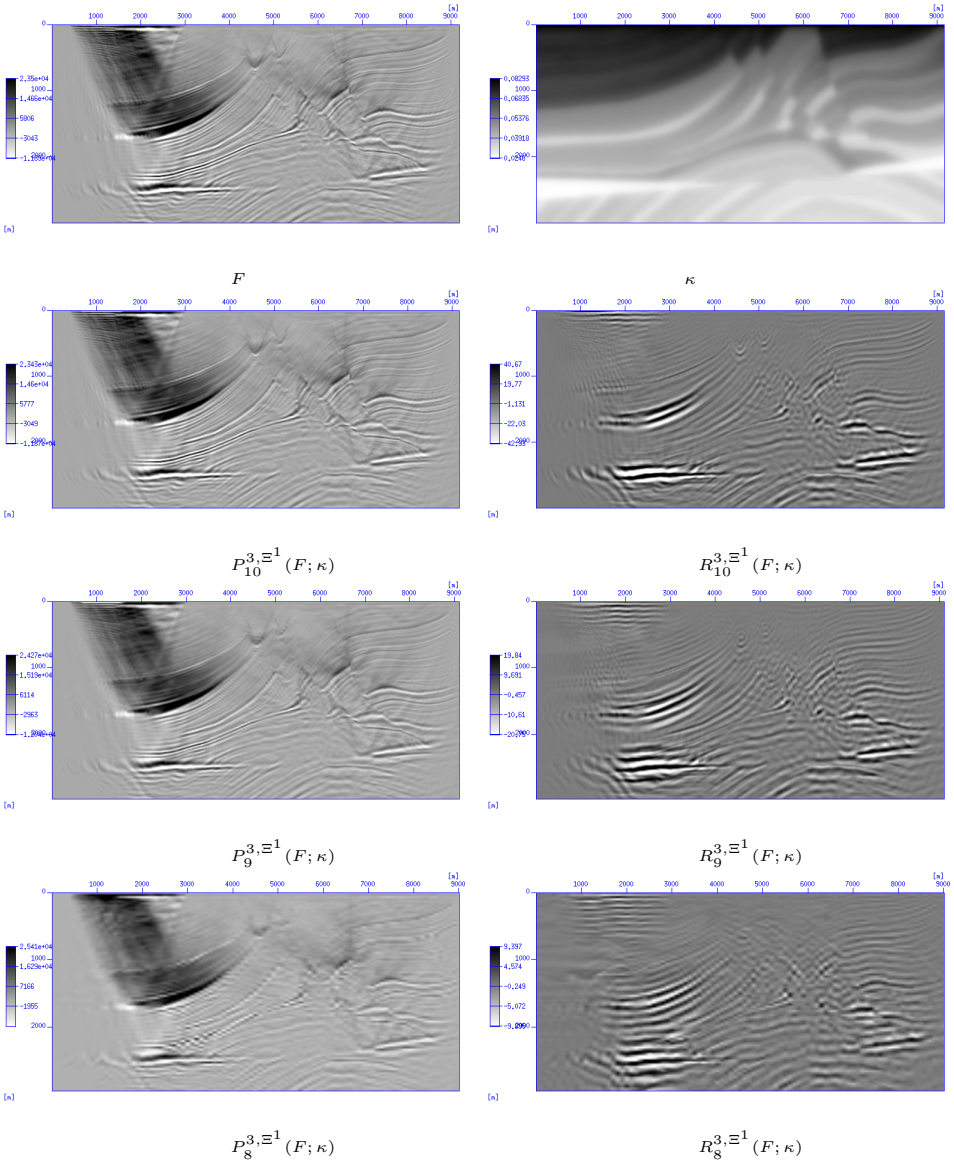

Figure 4.8: Multiscale analysis of the seismic section F (in $[m]$) (Fig. 3.6) for $f = 20Hz$.

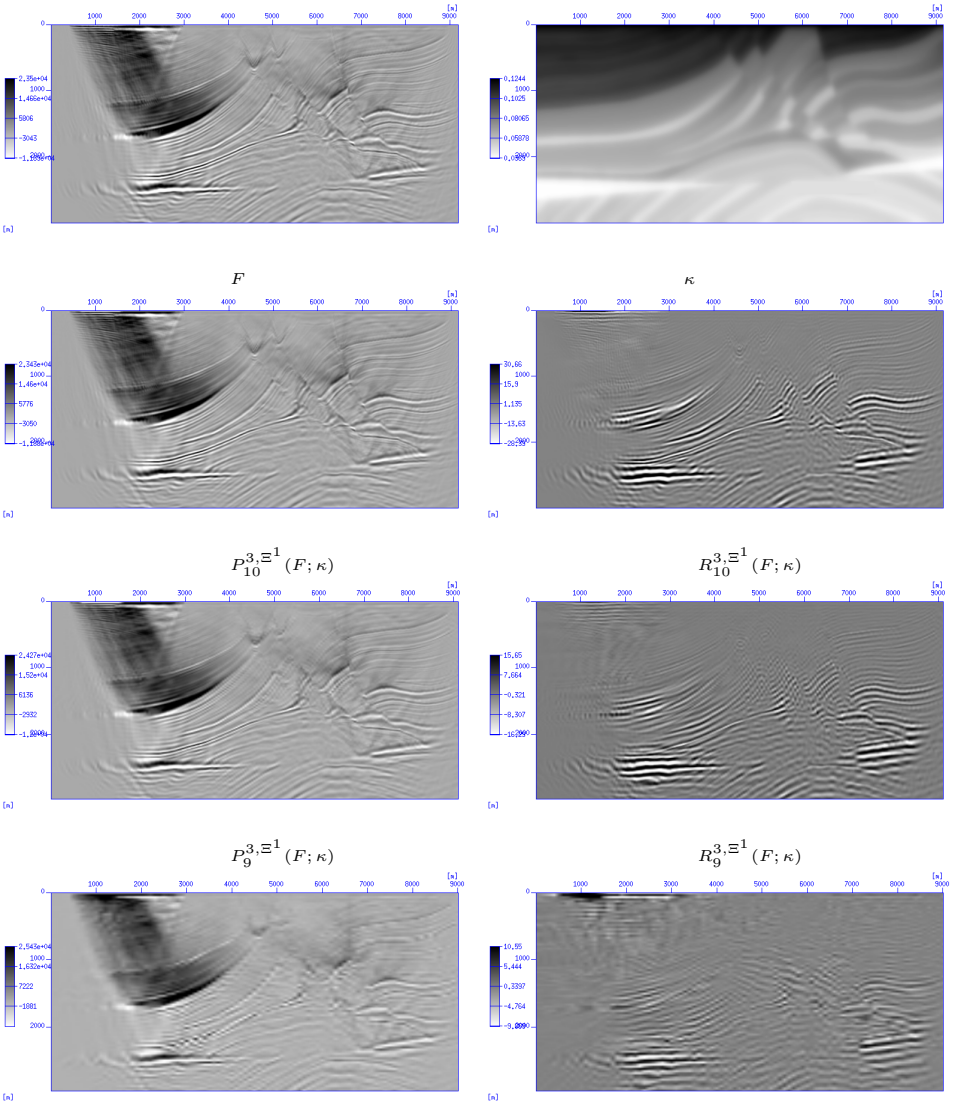

Figure 4.9: Multiscale analysis of the seismic section F (in $[m]$) (Fig. 3.6) for $f = 30Hz$.

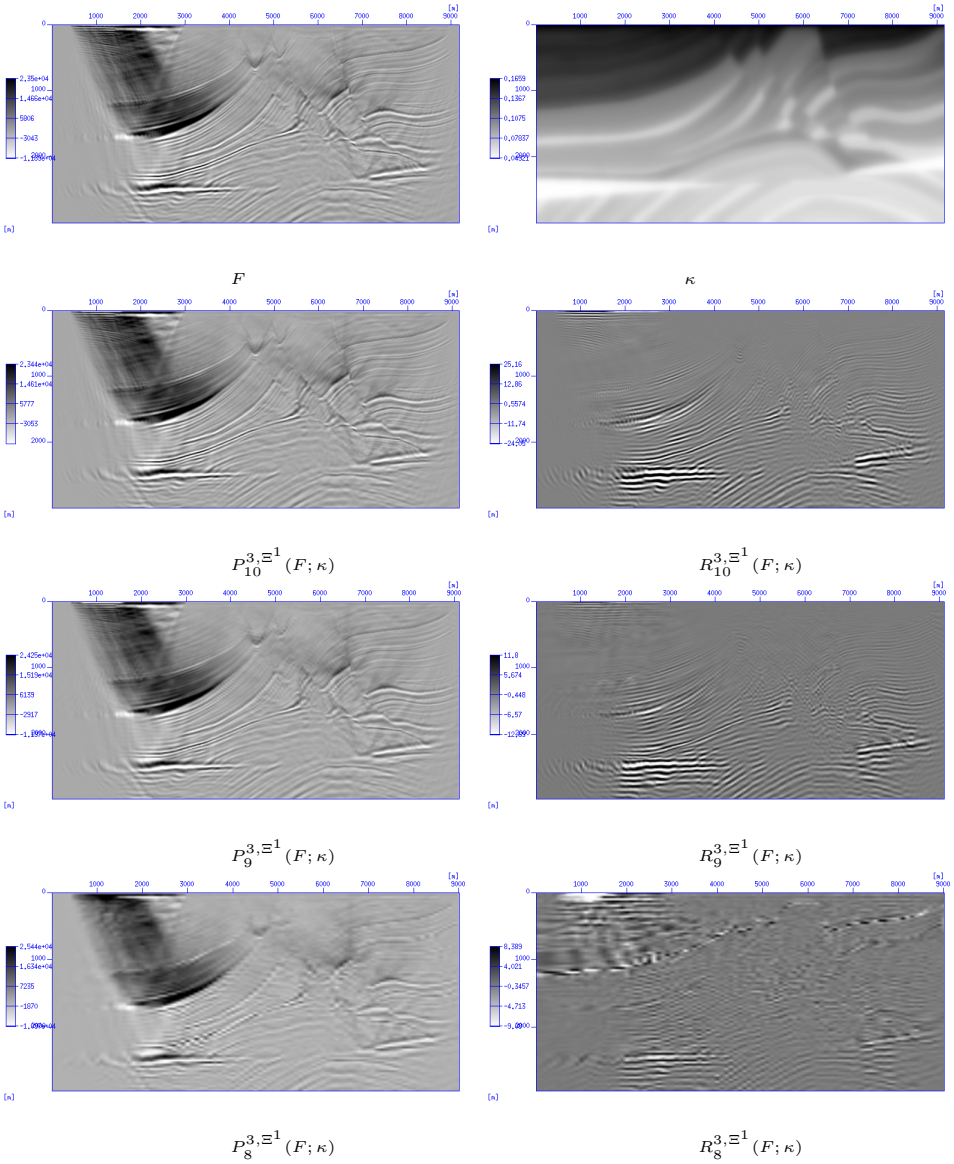

Figure 4.10: Multiscale analysis of the seismic section F (in $[m]$) (Fig. 3.6) for $f = 40Hz$.

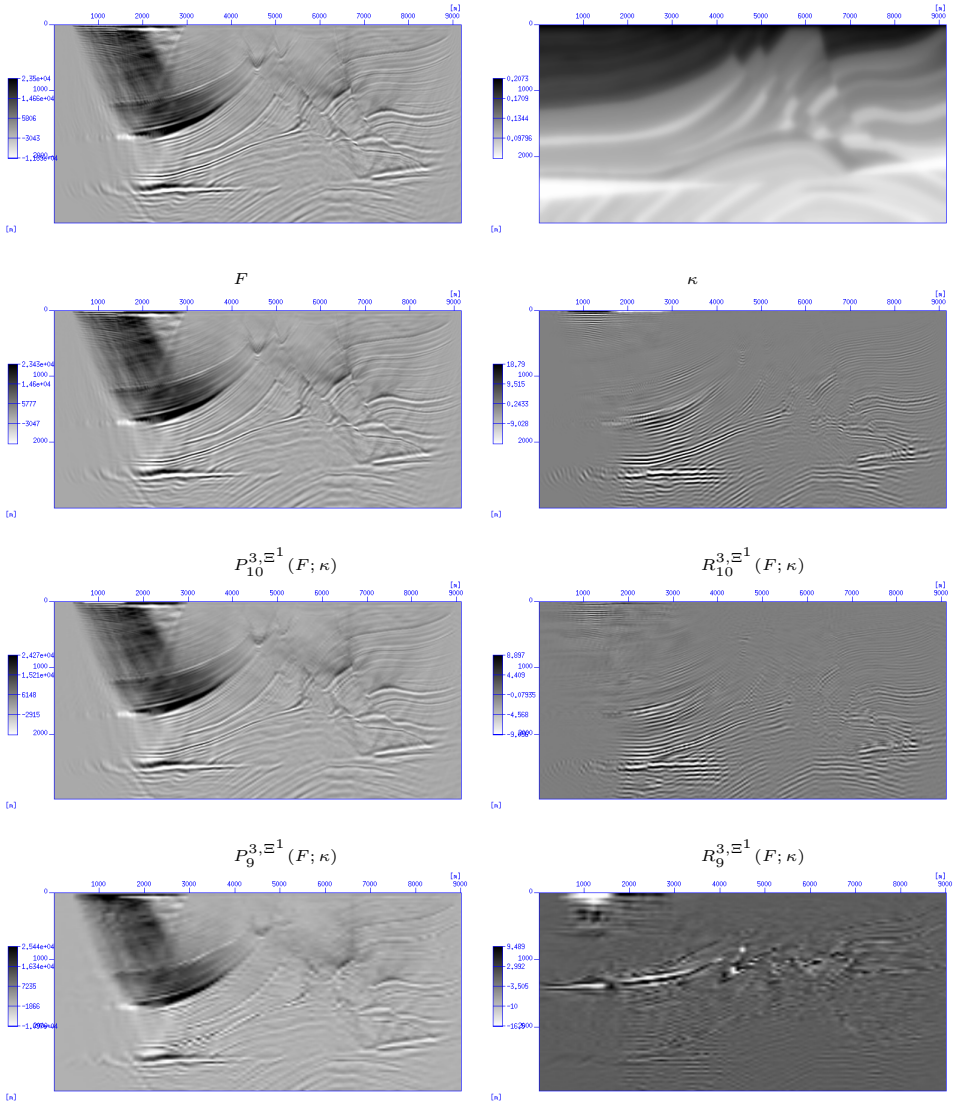

Figure 4.11: Multiscale analysis of the seismic section F (in $[m]$) (Fig. 3.6) for $f = 50Hz$.

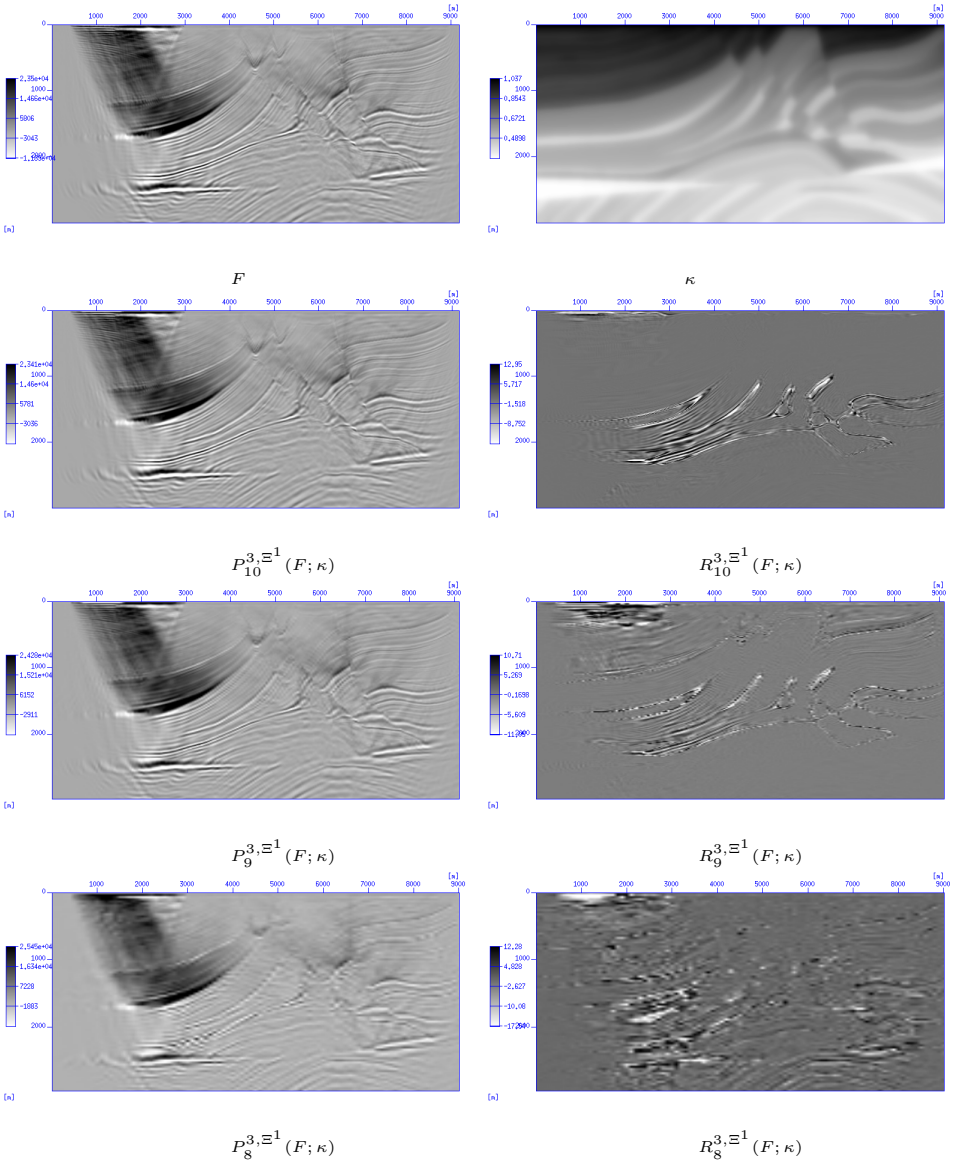

Figure 4.12: Multiscale analysis of the seismic section F (in $[m]$) (Fig. 3.6) for $f = 250Hz$.

Chapter 5

Conclusion and Future Work

The main goal of this work was the construction of an appropriate technique for seismic data postprocessing. Based on the wavelet approximation provided for regular surfaces with smooth boundaries by Freeden, Mayer and Schreiner ([31], [55]), we extended the limit and jump relations of the Helmholtz potential operator to regions with boundaries containing edges and vertices. With respect to these jump and limit relations we constructed a regularization singular integral surface potentials in the Helmholtz theory and allowing a multiscale computation of functions on the surface. For the fast numerical computation we presented a tree algorithm as proposed in [31] for smooth surfaces. We gave several examples of the wavelet decomposition in order to represent a seismic image at different scales for a selected frequency. These decompositions (scale and detail illustration) visualize some structural details specific for a selected frequency in a given seismic data set. In addition, our approach can further be used for data analysis as well as for data compression.

All in all, the purpose of this work is threefold: (*i*) a multiscale approximation by means of wave dependent Helmholtz potentials, (*ii*) to use the space localization properties of the Helmholtz wavelets for pointwise wave reflected seismic data postprocessing, (*iii*) to implement an efficient and economical tree algorithm for fast computation.

For further research the following aspect should be mentioned: The developed Helmholtz wavelets can be used to solve also the boundary value problems of the Helmholtz equation in regions with edges and corners. Therefore, our multiscale technique can be applied to the modeling of wave transmissions in regions of $\mathbb{R}^3$. In order to handle inhomogeneous media, the pertur-

bation theory (e.g., [1], [8], [54], [68]) should be involved. In addition, the computational effort can be drastically reduced by use of the tree algorithm. This is a challenge for future work.

Bibliography

[1] Barbu, L., and Moroşanu, G. *Singularly Perturbed Boundary-Value Problems.* Birkhäuser, 2007.

[2] Baysal, E., Kosloff, D. D., and Sherwood, J. W. C. Reverse Time Migration. *Geophysics 48(11)* (1983).

[3] Baysal, E., Kosloff, D. D., and Sherwood, J. W. C. A Two-Way Nonreflecting Wave Equation. *Geophysics 49(2)* (1984).

[4] Beylkin, G. *Wavelets: Mathematics and Applications.* CRC Press, 1994, ch. On Wavelet-Based Algorithms for Solving Differential Equations.

[5] Beylkin, G., and Vassiliou, A. Wavelet Transforms and Compression of Seismic Data. *Mathematical Geophysics Summer School* (1998).

[6] Biondi, B. L. *Tree-Dimensional Seismic Imaging.* Society of Exploration Geophysicsists, Tulsa, 2006.

[7] Bleistein, N. On the Imaging of Reflectors in the Earth. *Geophysics 52(7)* (1987).

[8] Bleistein, N., Cohen, J. K., and Stockwell, J. W. *Mathematics of Multidimensional Seismic Imaging, Migration, and Inversion.* Springer, New York, Berlin, Heidelberg, 2000.

[9] Bollhöfer, M., Grote, M. J., and Schenk, O. Algebraic Multilevel Preconditioner for the Helmholtz Equation in Heterogeneous Media. *SIAM J. Sci. Comput.* (2008).

[10] Bonomi, E., and Pieroni, E. Energy-Tuned Absorbing Boundary Conditions. In *Proc. 4th SIAM Int. Conf. on Mathematical and Numerical Aspects of Wave Propagation* (1998), Colorado School of Mines.

[11] Bording, R. P., and Liner, C. L. Theory of 2.5-D Reverse Time Migration. In *64th Ann. Internat. Mtg: Soc. of Expl. Geophys* (1994).

[12] Brown, A. R. Interpreter's Corner – Seismic Attributes and Their Classification. *The Leading Edge* (1996).

[13] Brown, A. R. Understanding Seismic Attributes. *Geophysics 66* (2001), 47–48.

[14] Buske, S. Kirchhoff - Migration von Einzelschußdaten. Master's thesis, Institut für Meterologie und Geophysik der Johann Wolfgang Goethe - Universität Frankfurt am Main, 1994.

[15] Candès, E. J., and Demanet, L. The Curvelet Representation of Wave Propagators is Optimally Sparse. *Comm. Pure Appl. Math. 58* (2004).

[16] Candès, E. J., Demanet, L., Donoho, D. L., and Ying, L. Fast Discrete Curvelet Transforms. *Multiscale Model. Simul. 5* (2005).

[17] Chauris, H. Seimic Imaging in the Curvelet Domain and its Implications for the Curvelet Design. In *Annual SEG Meeting and Exposition, Soc. Expl. Geophys.* (2006), vol. 76.

[18] Chauris, H., and Nguyen, T. Towards Interactive Seismic Imaging with Curvelets. In *69th EAGE Conference and Exhibition* (London, 2007).

[19] Claerbout, J. *Basic Earth Imaging.* Standford University, Standford, 2009.

[20] Courant, R., and Hilbert, D. *Methoden der Mathematischen Physik*, vol. I,II. Springer Verlag, 1968.

[21] Daubechies, I. *Ten Lectures on Wavelets.* SIAM, 1992. CBMS-NSF Lecture Notes nr. 61.

[22] Debnath, L. *Wavelet Trasforms and Their Applications.* Birkhäuser, 2002.

[23] Deng, F., and McMechan, G. A. 3-D True Amplitude Prestack Depth Migration. In *SEG Annual Meeting* (San Antonio, 2007).

[24] Douma, H. *A Hybrid Formulation of Map Migration and Wave-Equation-Based Migration Using Curvelets.* PhD thesis, Colorado School of Mines, Center for Wave Phenomena, 2006.

[25] Du, X., and Bancroft, J. C. 2-d Wave Equation Modeling and Migration by a New Finite Difference Scheme Based on Galerkin Method. Tech. rep., CREWES, 2004.

[26] Fairwaether, G., and Mitchel, A. R. A High Accuracy Alternating Direction Method for the Wave Equation. *J. Inst. Maths Applics 1* (1965), 309–316.

[27] Fomel, S. Towards the Seislet Transform. In *SEG Annual Meeting* (New Orleans, 2006).

[28] Freeden, W. On the Approximation of External Gravitational Potential With Closed Systems of Trial Functions. *Bull. Geod. 54* (1980), 1–20.

[29] Freeden, W. *Multiscale Modelling of Spaceborn Geodata.* B. G. Teubner, Stuttgart, Leipzig, 1999.

[30] Freeden, W., Gervens, T., and Schreiner, M. *Constructive Approximation in the Sphere with Applications to Geomathematics.* Oxford Science Publications, Clarendorn, 1998.

[31] Freeden, W., Mayer, C., and Schreiner, M. Tree Algorithms in Wavelet Approximation by Helmholtz Potential Operators. *Numer. Funct. Anal. and Optim.*, 24 (2003), 747–782.

[32] Freeden, W., and Michel, V. *Multiscale Potential Theory (with Application to the Geoscience).* Birkhäuser, Basel, Berlin, Boston, 2004.

[33] Freeden, W., and Schreiner, M. *Spherical Functions of Mathematical Geosciences. A Scalar, Vectorial, and Tensorial Setup.* Springer, Heidelberg, 2009.

[34] Freeden, W., Schreiner, M., and Franke, R. A Survey on Spherical Spline Approximation. *Surv. Math 7* (1996), 29–85.

[35] Gisolf, D., and Verschuur, E. *The Principles of Quantitative Acoustical Imaging.* EAGE Publications, 2010.

[36] Glockner, O. *On Numerical Aspects of Gravitational Field Modeling from SST and SGG by Harmonic Splines and Wavelets with Application to CHAMP Data.* PhD thesis, AG Geomathematics, Kaiserslautern, 2002.

[37] Greengard, L. *The Rapid Evaluation of Potential Fields in Particle Systems.* MIT Press, Cambridge, 1988.

[38] Greengard, L., and Rokhlin, V. Rapid Evaluation of Potential Fields in Three Dimensions. *Vortex Methods* (1988), 121–141.

[39] Greengard, L., and Rokhlin, V. A New Version of the Fast Multipole Method for the Laplace Equation in Three Dimensions. *Acta Numerica 6* (1997), 229–269.

[40] Guitton, A., Valenciano, A., and Bevc, D. Robust Imaging Condition for Shot-Profile Migration. In *SEG Annual Meeting* (New Orleans, 2006).

[41] Haney, M. M., Bartel, L. C., Aldridge, D. F., and Symons, N. P. Insight into the Output of Reverse-Time Migration: What do the Amplitudes Mean? In *SEG Annual Meeting* (Houston, 2005).

[42] Ilyasov, M., Ostermann, I., and A.Punzi. Modeling Deep Geothermal Reservoirs: Recent Advances and Future Problems. In *Handbook of Geomathematics*, W. Freeden, Z. Nashed, and T. Sonar, Eds. Springer, 2010.

[43] Jia, X., and Hu, T. Element-Free Precise Integration Method and its Applications in Seismic Modelling and Imaging. *Geophys. J. Int. 166* (2006).

[44] Kaelin, B., and Guitton, A. Imaging Condition for Reverse Time Migration. In *SEG Annual Meeting* (New Orleans, 2006).

[45] Kaelin, B., and Guitton, A. Illimination Effects in Reverse Time Migration. In *EAGE 69th Conference & Exhibition* (London, UK, 2007).

[46] Keller, W. *Wavelets in Geodesy and Geodynamics.* Walter de Gruyter GmbH & Co. KG, Berlin, 2004.

[47] Kellogg, O. *Foundations of Potential Theory.* Frederick Ungar Publishing Company, New York, 1929.

[48] Kersten, H. Grenz- und Sprungrelationen für Potentiale mit Quadratsummierbarer Flächenbelegung. *Resultate der Mathematik 2* (1979).

[49] Korn, A. *Fünf Abhandlungen zur Potentialtheorie.* Dümmlers Verlangsbuchhandlung, Berlin, 1902.

[50] Lax, P. Symmetrizable Linear Transformations. *Comm. on pure and app. Mathematics 7* (1954), 633–647.

[51] Ljusternik, L. A., and Sobolew, W. I. *Elemente der Funktionalanalysis.* Akademie-Verlag, Berlin, 1968.

[52] Mallat, S. *A Wavelet Tour of Signal Processing: the Sparse Way.* Academic Press, 1998. 3. Auflage 2009.

[53] Martin, G. S., Marfurt, K. J., and Larsen, S. Marmousi-2: An Updated Model for the Investigation of AVO in Structurally Complex Areas. In *SEG Annual Meeting* (2002).

[54] Maslov, V. P. *Asymptotic Methods and Perturbation Theory.* Nauka, Moskva, 1988. in russian.

[55] Mayer, C. *Wavelet Modelling of Ionospheric Currents and Induced Magnetic Fields from Satellite Data.* PhD thesis, TU Kaiserslautern, 2003.

[56] Mikhlin, S. G. *An Advanced Course of Mathematical Physics.* North Holland Publ. Comp., Amsterdam, 1970. translation from russian.

[57] Müller, C. Die Potentiale einfacher und mehrfacher Flächenbelegungen. *Mathematische Annalen 123* (1951), 235–262.

[58] Müller, C. *Foundations of the Mathematical Theory of Electromagnetic Waves.* Springer-Verlag, Berlin, Heidelberg, New York, 1969.

[59] Podvin, P., and Lecomte, I. Finite Difference Computation of Traveltimes in Very Contrasted Velocity Models: a Massively Parallel Approach and its Associated Tools. *Geophys. J. Int. 105* (1991), 271–284.

[60] Popov, M. M. A New Method of Computation of Wave Fields Using Gaussian Beams. *Wave Motion 4* (1982).

[61] Popov, M. M., Semtchenok, N. M., Popov, P. M., and Verdel, A. R. Gaussian Beam Migration of Multi-Valued Zero-Offset Data. In *Days on Diffraction* (St.Petersburg, 2006).

[62] Renaut, R., and Fröhlich, J. A Pseudospectral Chebychev Method for the 2D Wave Equation with Domain Streching and Absorbing Boundary Conditions. *Journal of Computational Physics 124* (1996).

[63] Reynolds, A. C. Absorbing Boudary Conditions for Acoustic Media. In *Numerical Modeling of Sesmic Wave Propagation*, vol. 13 of *Gophysics reprint series*. Society of Exploration Geophysicists, 1990, pp. 471–482.

[64] Rivera-Recillas, D. E., Lozada-Zumaeta, M. M., Ronquillo-Jarilo, G., and Campos-Enriquez, O. Multiresolution Analysis Applied to Interpolation of Seismic Reflection Data. *Geofisica Internacional 44*, 4 (2005), 355–368.

[65] Samarskij, A. A. *Theorie der Differenzenverfahren*. Akad. Verl.-Ges. Geest & Portig, Leipzig, 1984.

[66] Semtchenok, N. M., Popov, M. M., and Verdel, A. R. Gaussian Beam Tomography. In *71st EAGE Conference & Exhibition* (Amsterdam, The Netherlands, 2009).

[67] Smirnov, W. I. *Lehrgang der Höheren Mathematik*. Deutscher Verlag der Wissenschaft, 1962.

[68] Sneider, R., and Trampert, J. *Wavefield Inversion*. Springer Verlag, New York, 1999, ch. Inverse Problems in Geophysics, pp. 119–190.

[69] Symes, W. W. Kinematics of Reverse Time S-G Migration. Tech. rep., Rice University, 2003. TRIP Seminar.

[70] Symes, W. W. Reverse Time Migration with Optimal Checkpointing. *Geophysics 72(5)* (2007).

[71] Takenaka, H., Wang, Y., and Furumura, T. An Efficient Approach of the Pseudospectral Method for Modelling of Geometrically Symmetric Seismic Wavefield. *Earth Planets Space 51* (1999).

[72] Teschke, H. *Über die Darstellung harmonischer und metaharmonischer Funktionen in Gebieten mit nichtglatten Rändern.* PhD thesis, RWTH Aachen, 1978.

[73] Tichonov, A. N., and Samarskij, A. A. *Differentialgleichungen der mathematischen Physik.* Verl. der Wiss., Berlin, 1959.

[74] Vabishevich, P. N. *Computational Methods of the Mathematical Physics. Inverse and Control Problems.* Vuzovskaya kniga, 2009. in russian.

[75] Versteeg, R. The Marmousi Experience: Velocity Model Determination on a Synthetic Complex Data Set. *The Leading Edge* (1994), 927–936.

[76] Vidale, J. Finite-Difference Calculation of Travel Times. *Bulletin of the Seismological Society of America 78*, 6 (1988), 2062–2076.

[77] Walter, W. *Einführung in die Potentialtheorie.* B-I Hochschulskripten, 1971.

[78] Wendland, W. *Lösung der ersten un zweiten Randwertaufgaben des Innen- und Außengebietes für die Potentialgleichung im $\mathbb{R}^3$ durch Randbelegungen.* PhD thesis, Universität Berlin, 1965.

[79] Wendland, W. Die Behandlung von Randwertaufgaben im $\mathbb{R}^3$ mit Hilfe von Einfach- und Doppelschichtpotentialen. *Numerische Mathematik* (1968), 380–404.

[80] Wienholtz, E., Kalf, H., and Kriecherbauer, T. *Elliptische Differentialgleichungen zweiter Ordnung. Eine Einführung mit historischen Bemerkungen.* Springer-Verlag, Berlin, Heidelberg, 2009.

[81] Wloka, J. *Funktionalanalysis und Anwendungen.* Walter de Gruyter, Berlin, New York, 1971.

[82] Wu, R. S., Xie, X. B., and Wu, X. Y. One-Way and One-Return Approximations (de Wolf approximation) for Fast Elastic Wave Modeling in Complex Media. *Advances in Geophysics 48(5)* (2006).

[83] `http://www.litho.ucalgary.ca/atlas/seisexp.gif`.

[84] Xie, X. B., and Wu, R. S. A Depth Migration Method Based on the Full-Wave Reverse Time Calculation and Local One-Way Propagation. In *SEG Annual Meeting* (New Orleans, 2006).

[85] Yilmaz, O. *Seismic Data Analysis: Processing, Inversion, and Interpretation of Seismic Data*. Society of Exploration Geophysicsists, Tulsa, 1987.

[86] Yoon, K., Marfurt, K. J., and Starr, W. Challenges in Reverse Time Migration. In *SEG Annual Meeting* (Denver, Colorado, 2004), vol. 74.

Curriculum Vitae

Maxim A. Ilyasov

11/2007-12/2010 Ph.D. Studies in Mathematics, Geomathematics Group, University of Kaiserslautern/ Fraunhofer ITWM

03/2007-10/2007 ProSAT Program
University of Kaiserslautern/ Fraunhofer ITWM

10/2003-12/2006 Studies in *Mathematics* with minor subject *Informatics*
Duisburg-Essen University
12/2006 Diploma in Mathematics

09/2000-06/2006 Studies in *Applied Mathematics and Informatics* with specialization *Mathematical Cybernetics*
Ulyanovsk State University
06/2006 Diploma in Mathematics, Qualification: Analyst-programmer

Eidesstattliche Erklärung

Hiermit erkäre ich an Eides statt, dass ich die vorliegende Arbeit selbst und nur unter Verwendung der in der Arbeit genannten Hilfen und Literatur angefertigt habe.

Hannover, 6. Juli 2011 Maxim Ilyasov